Ife Journal of Technology

Vol 21, No 2, 2012

Editorial Board

General Information

The Ife Journal of technology is an international journal published by the Faculty of Technology, Obafemi Awolowo University, Ile-Ife, Nigeria.

The journal accepts original manuscripts from anywhere in the world in all engineering and related disciplines as listed below:

i. Agricultural Engineering
ii. Chemical Engineering
iii. Civil Engineering
iv. Computer Science and Technology
v. Electronic and Electrical Engineering
vi. Food Science and Technology
vii. Materials Science and Engineering
viii. Mechanical Engineering
ix. Technology Planning, Development and Management
x. Other engineering and related topics

The journal provides a vehicle for the fast and wide dissemination of results and findings of well-conducted researches in engineering and related fields mainly as research papers (theoretical and experimental), research notes and review articles. The journal also publishes book reviews, news and announcements.

Frequency of Publication
The journal is published twice a year in May and November

Annual Subscription (including postage)

Within Nigeria:	Outside Nigeria
Individuals: N1200.00	Individuals: $50
Institutions: N2500.00	Institutions: $100

Advertisement Rates
Full page (inside): N10,000
Half page (Inside): N5000
Additional for color: N5,000

Correspondence
All correspondence should be addressed to:
The Editor,
Ife Journal of Technology,
Dean's Office
Faculty of Technology,
Obafemi Awolowo University,
Ile-Ife, Nigeria.

IFE JOURNAL OF TECHNOLOGY

Vol. 21, No. 2, 2012

Published by Faculty of Technology, Obafemi Awolowo University,
Ile-Ife, Nigeria

ISSN: 1115-9782

Full Paper

IMPACT OF TREE DENSITY ON SHORT RANGE VHF RADIO WAVE PROPAGATION IN THE MANGROVE SWAMP FOREST

F.O. Agugo
Nigerian Army School of Signals, Apapa, Lagos.

S.A. Adeniran
Department of Electronic and Electrical Engineering, Obafemi Awolowo University, Ile- Ife.
sadenira@oauife.edu.ng

O. Erinle
Department of Electronic and Electrical Engineering, Obafemi Awolowo University, Ile- Ife.

ABSTRACT

Propagation models are developed to suit particular applications and environments. Characterization of a forested radio channel for short range VHF/UHF communication with near ground antennas needs to consider all possible radio wave reflections - tree trunks, ground and tree canopy reflections - in addition to the foliage absorption effects of propagation through tree groves. In the mangrove forest where tree density is usually high, the capacity of tree elements for radio wave scattering at certain propagation parameters cannot be overlooked. This study used an integration of stochastic and empirical modelling to show that forest tree density is the most important parameter in path loss prediction in the mangrove at certain combat communication parameters.

1. INTRODUCTION

Short and medium range military communication/surveillance systems operate on near ground radio channels where radio propagation is highly affected by ecological factors. The new and indeed future wireless systems require that channels be characterized to greater details for optimal performance of wireless communication/surveillance networks. The aim of this study is to provide information on the radio propagation characteristics of the mangrove swamp forest at combat net parameters of near-ground antenna, VHF ranges of 30 - 80 MHz and 150 - 250 MHz and distance range of 50 - 300 metres.

It was obvious from (Meng et al., 2010) that any characterization of a forested radio channel for short range VHF/UHF communication with near ground antennas needed to consider all possible reflections - tree trunks, ground and tree canopy reflections as shown in Fig 1 - in addition to the foliage absorption effects of propagation through tree groves.

A propagation loss model that is based on the summation of the foliage loss (obtained from common foliage loss models) and the effects of radio wave reflections such as ground reflection and tree-canopy reflection was presented in (Meng et al., 2010). It was shown to give better accuracy for near ground VHF communication at short distance, when compared to commonly used Wiessberger, ITU-R and COST235 Models. The theoretical bases of this study are similar to the integration model which was proposed in (Meng et al., 2010) and used in (Agugo and Adeniran, 2011); however, the new insight in this study is the fact that the structure and high tree density of the mangrove forest cannot be taken as smooth flat terrain especially at short ranges and VHF or UHF frequencies (see Fig. 2), hence it cannot be assumed that it would produce only specular reflections as done in (Meng et al., 2010; Agugo and Adeniran, 2011).

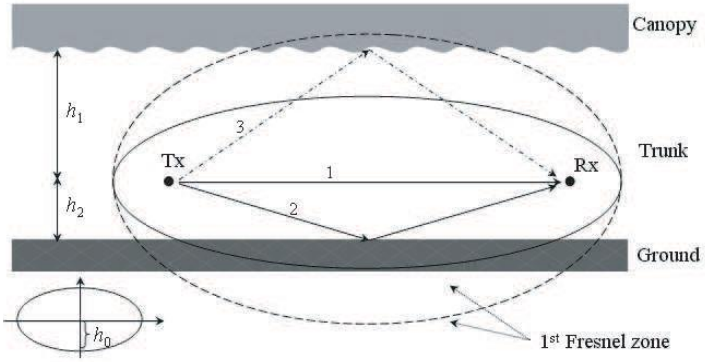

Fig. 1. Ray tracing geometry of direct-1, ground-reflected-2 and tree-canopy-reflected-3 waves (Meng et al., 2010).

Fig. 2: Photographs of Mangrove Swamp Forest.

This new insight is based on the results of the field measurements that were included in (Agugo and Adeniran, 2011),

which gave such interesting indications regarding the mangrove forest.

Essentially, the objective of this study was achieved through the analysis of terrain data and the received signal strength at selected distances from the transmitter of a wireless link that was operated at the combat net parameters of interest. Preliminary information on the forest composition and structure was used to determine significance of each of the dominant propagation mechanisms or phenomena in such channel at short-range, near-ground VHF band. The contribution of each significant mechanism to path loss was evaluated using stochastic geometrical optics approach and relevant standard empirical models. The mathematical formulation that sums the contributions of all the significant propagation mechanisms to obtain the total path loss was used as the characteristic equation or path loss model. This characteristic equation or model elicited the kinds of terrain data required for its quantitative evaluation. Field measurements were be conducted at two mangrove forest sites, first to obtain the primary terrain data required for estimating the quantitative value of path loss using the model, and secondly to obtain the actual values of path loss in the selected sites at the radio parameters of our interest. Measurement sites were selected to ensure difference in forest tree density. Secondary terrain data was obtained from literature as necessary. Graphs of path loss variability with respect to distance and frequency for different tree density values plotted with both the estimated and the measured values was analysed and compared to obtain their general trends and relationship. Estimation error of the model was calculated using statistical deviation method.

2. CONCEPTUAL FRAMEWORK

Generally, the basic propagation phenomena that are often considered in propagation modelling are reflection, refraction, diffraction, absorption and scattering (Zwick et al., 2009). A pictorial overview of these phenomena is shown in Fig 3.

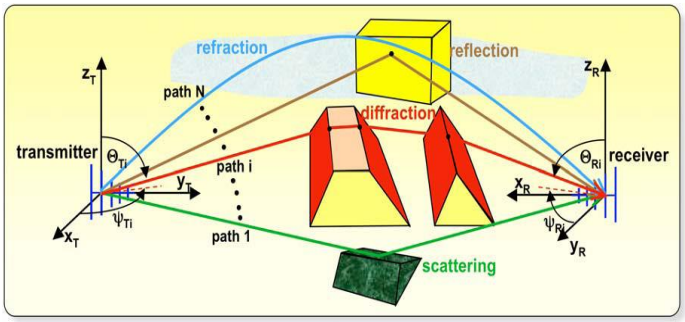

Fig. 3: Radio Propagation Phenomena.

Scattering is a phenomenon in which the direction or polarization of the wave is changed when the wave encounters propagation medium discontinuities in the order of or smaller than the wavelength. Scattered waves are produced by rough surfaces, small objects (e.g. foliage, street signs, etc) or by other irregularities in the channel as shown in Figs. 4 and 5. It results in a disordered or random change in the incident energy distribution. The actual received signal in a radio system is often different from what is predicted by free-space propagation, reflection, and diffraction models alone. Indeed, a wave propagating through a volume containing many individual small objects (e.g. forest), looses energy due to phase shifts and the non-vanishing imaginary part of the objects' total permittivity, as well as scattering off the direction of propagation. However, when an electromagnetic wave impinges on a single object whose size is small compared to the wavelength, a rough surface, or a volume containing many individual small objects such as tree trunks, branches, and leaves in a forest, the energy is spread out in all directions due to scattering, and this may even provide additional radio energy at the receiver (Zwick, 2009).

Hence, a theoretical description of these effects is very complex, and is thus mostly based on approximations. Therefore, losses relating to scattering are often accounted for by using simple empirical formulas.

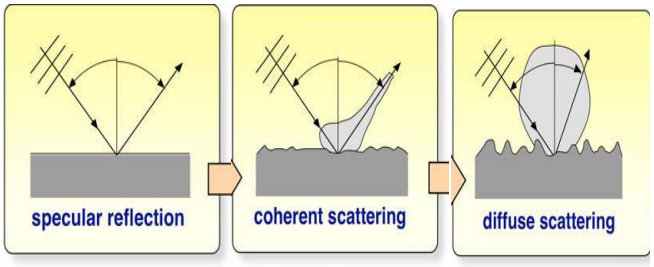

Fig. 4: Illustration of the transition from Specular Reflection to Scattering.

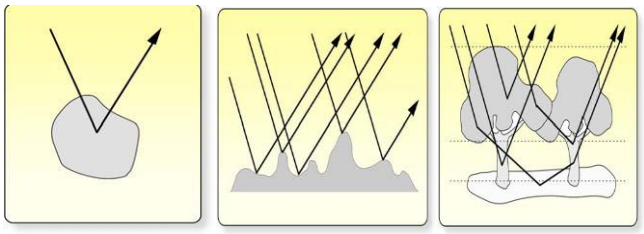

Fig. 5: Illustration of Point, Area and Volume Scattering.

The Blaunstein's model is a stochastic approach to investigate the absorbing and multiple scattering effects that accompany the process of radio wave propagation through forested areas (Blaunstein et al., 2003; Blaunstein and Christodoulou, 2007). This is a combination of probabilistic and deterministic approaches, which describes the random media scattering phenomenon. The geometrical optics approximation is used to account for propagation over a series of trees modelled as absorbing amplitude/phase screens with rough surfaces. A completely stochastic approach would require the propagation designer to obtain the absorption effects of trees using their real physical parameters, such as permittivity and conductivity, as well as the random distribution of their branches and leaves, which would be highly complex. However, it has been shown that it is possible to obtain reasonably accurate estimates of the absorption effects of trees using an appropriate standard empirical model such as the Weissberger's or ITU-R Models (Meng et al, 2010; Agugo and Adeniran, 2011). Hence, complex computations are eliminated without practical loss of accuracy by appropriate integration of empirical and stochastic models.

The Blaunstein's Model is a generalized model that covers wide ranges of frequency and distance. It gives the average total received EM field, I_{total}, in terms of the coherent and the incoherent components, I_{co} and I_{inc} respectively. The beauty of the model is that both I_{co} and I_{inc} are made up of terms some of which are relevant only for certain distance ranges, hence it can be adapted for particular distance ranges to reduce its complexity. In general, it evaluates the total path loss, L_{total}, as

$$L_{total} = -10 \log [\lambda^2 (I_{co} + I_{inc})] \quad (1)$$

The main limitation of Blaunstein's Model is in stochastic computation of absorption effects of trees. Nevertheless, its evaluation of the multiple scattering effects of trees shows high accuracy, and could be adapted especially where a reliable estimate of forest tree density is obtainable.

3. METHODOLOGY

A wave propagating through a volume containing many individual small objects (e.g. forest), looses energy due to phase shifts and the non-vanishing imaginary part of the objects' total permittivity, as well as scattering off the direction of propagation. However, an electromagnetic wave that impinges on a single object whose size is

small compared to the wavelength, a rough surface, or a volume containing many individual small objects such as tree trunks, branches, and leaves in a forest, would have the energy spread out in all directions due to scattering, and this may even provide additional radio energy at the receiver (Zwick et al., 2009). Hence, in addition to the absorptive effect, the multiple scattering effects of the mangrove trees need to be considered in evaluating the path loss in the mangrove forest at the propagation parameters of our interest.

To estimate the path loss resulting from the multiple scattering effects, we consider the array of trees as cylinders with randomly distributed surfaces, all placed on a flat terrain (Fig 6). Assuming that the reflecting properties of the trees are randomly and independently distributed (but are statistically the same), then the values of the reflection coefficient are complex with uniformly distributed phase in the range of [0, 2π], with correlation scales in the horizontal dimension, ℓ_h, and in the vertical dimension, ℓ_v, respectively. Thus, the average value of the reflection coefficients is zero, that is $\langle R(\varphi_s, r_s)\rangle = 0$. The geometry of the problem is shown in Fig. 7, where $A(d_1) = \mathbf{r}_1$ denotes the location of the transmitting antenna at height $h_T = z_1$; $B(d_2) = \mathbf{r}_2$ is the location of the receiving antenna at height $h_R = z_2$. To derive an average measure of field intensity for waves passing through the layer of trees after multiple scattering, we consider each tree as a phase-amplitude cylindrical screen. Figure 6 shows an array of these screens placed at $z = 0$. The trees have an average height, $\bar{h}$, and width, $\bar{w}$. These trees are randomly and independently distributed and they are oriented in arbitrary directions at the plane $z = 0$ with equal probability and with average density ν (per km^2). In near ground propagation where both antennas are placed within the forest environment and are lower than the average tree height, that is $0 < z_2; z_1 < \bar{h}$, then the multi-scattering effects are predominant and must be taken into account. In this case, the range of direct visibility (LOS conditions) between the two terminal antennas is given by $\bar{\rho} = {\gamma_0}^{-1}$, (Blaunstein and Christodoulou, 2007), where γ_0 is given as

$$\gamma_0 = 2\bar{w}\nu/\pi \tag{2}$$

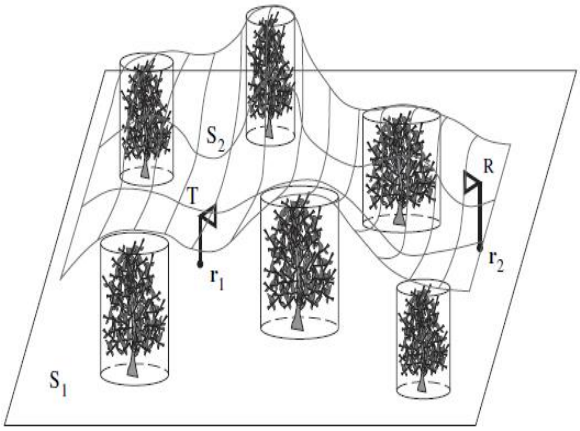

Fig. 6: Modelling of Trees as Cylindrical Screens.

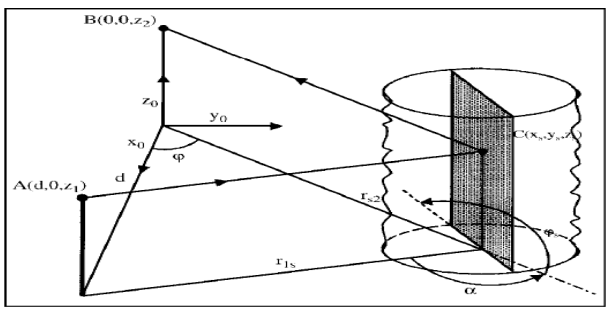

Fig. 7: Geometrical Presentation of the Scattering Model of Trees as Cylindrical Screens.

The 'roughness' of a tree's surface is described by considering it to have non uniform reflection coefficient, and introducing a correlation function for the reflection coefficient R. The correlation function is defined for $\ell_h, \ell_h, \ell_v \ll \bar{\rho}, \bar{w}, \bar{h}$ as

$$K(\mathbf{r}_{2S}, \mathbf{r}_{1S}) = \langle R_{2S} \cdot R^*_{1S}\rangle = R \cdot \exp\left\{-\frac{|\rho_{2S}-\rho_{1S}|}{\ell_h} - \frac{|z_{2S}-z_{1S}|}{\ell_v}\right\} \tag{3}$$

where $\mathbf{r}_{2S}$ and $\mathbf{r}_{1S}$ are points at the surface of an arbitrary tree as shown in Figure 2; R is the absolute value of the reflection coefficient given by Equation 8 for the two kinds of field polarization, $R_{2S} = R(\mathbf{r}_{2S}), R_{1S} = R(\mathbf{r}_{1S})$.

The main equations for the average field intensity are obtained by taking into account the Green's Function representation of wave propagation equation, Kirchhoff's approximation and Twersky's approximation. Green's Function representation of wave propagation describes an arbitrary source as a linear superposition of point sources. This is mathematically expressed as

$$s(\mathrm{r}) = \int \mathrm{d}\mathrm{r}'\, s(\mathrm{r}')\delta(\mathrm{r}-\mathrm{r}'). \tag{4}$$

The scalar wave equation with the source in the right hand side can be presented as

$$\nabla^2\Psi(\mathrm{r}) - k^2\Psi(\mathrm{r}) = s(\mathrm{r}) \tag{5}$$

and the corresponding equation for the Green's function in an unbounded medium is

$$\nabla^2\mathrm{G}(\mathbf{r},\mathbf{r}') - k^2\mathrm{G}(\mathbf{r},\mathbf{r}') = -\delta(\mathbf{r}-\mathbf{r}'). \tag{6}$$

The solution of equation (6) is (Blaunstein and Christodoulou, 2007)

$$\mathrm{G}(\mathrm{r}) = \frac{1}{4\pi}\frac{\exp\{ikr\}}{r} \tag{7}$$

and the corresponding solution of Equation 3.4 is

$$\Psi(\mathbf{r}) = -\int_{\mathrm{V}} \mathrm{d}\mathbf{r}'\mathrm{G}(\mathbf{r},\mathbf{r}')\, s(\mathbf{r}'). \tag{8}$$

Using Equation 3.6, we easily obtain a general solution for the inhomogeneous Equation (5) given by

$$\Psi(\mathbf{r}) = -\int_{\mathrm{V}} \mathrm{d}\mathbf{r}' \left\{\frac{\exp[ik|\mathbf{r}-\mathbf{r}'|]}{4\pi|\mathbf{r}-\mathbf{r}'|}\right\} s(\mathbf{r}'). \tag{9}$$

For the case of wave propagation through the forest layer with randomly distributed trees (screens), the total field at the receiver location $\mathbf{r}_2$ for the scattering problem can be written in the form

$$U(\mathbf{r}_2) = U_i(\mathbf{r}_2) + \int_S \left\{U(\mathbf{r}_s)\frac{\partial G(\mathbf{r}_2,\mathbf{r}_s)}{\partial \mathbf{n}_s} - G(\mathbf{r}_2,\mathbf{r}_s)\frac{\partial U(\mathbf{r}_s)}{\partial \mathbf{n}_s}\right\}\mathrm{d}S \tag{10}$$

where $U_i(\mathbf{r}_2)$ is the incident wave field, $\mathbf{n}_s$ is the vector normal to the terrain surface S at the scattering point r_s; $G(\mathbf{r}_2, \mathbf{r}_s)$ is the Green's function of the semi-space defined in Equations 3.6 and 3.8, which can be rewritten as (Blaunstein and Christodoulou, 2007)

$$\mathrm{G}(\mathbf{r}_2,\mathbf{r}_s) = \frac{1}{4\pi}\left\{\frac{\exp[ik|\mathbf{r}_2-\mathbf{r}_1|]}{|\mathbf{r}_2-\mathbf{r}_1|} \pm \frac{\exp[ik|\mathbf{r}_2-\mathbf{r}_1'|]}{|\mathbf{r}_2-\mathbf{r}_1'|}\right\}. \tag{11}$$

Here $\mathbf{r}_1'$ is the point symmetrical to $\mathbf{r}_1$ relative to the Earth's surface S_1. In integral Equation 9, the random surface S (relief of the terrain with obstructions) is treated as the superposition of an ideal flat ground surface S_1 ($z = 0$) and rough surface S_2 is created by the obstructions (see Figure 6). We construct the Green's function in the form of Equation 11 to satisfy a general electro-dynamic approach; that is, to describe both the vertical (sign "+" in Equation 11) and horizontal (sign "-" in Equation 11) polarizations with their corresponding boundary conditions. The boundary conditions (known as Dirichlet and Neumann's boundary conditions

respectively) are $\nabla G(\mathbf{r},\mathbf{r}')=0$ and $\mathbf{n}\cdot\nabla G(\mathbf{r},\mathbf{r}')=0$. In fact, by introducing the Green's function in Equation 11 with the "+" sign in Equation 10 we satisfy the Dirichlet boundary conditions at the flat (non disturbed) Earth's surface S_1 (z=0). That means, $G_{z=0}$ = 2 and $\frac{\partial U}{\partial \mathbf{n}_s}$= 0. At the same time, using the sign "-" we satisfy the Neumann boundary conditions at the plane z = 0: $G_{z=0}$ = 0 and u = 0. Hence, if the source is described by Equation 11, we can exclude the integration over the non disturbed surface S_1, assuming the surface S_1 is perfectly reflecting. Next, by using the Kirchhoff's approximation (which states that the wave at each point on a quasi smooth surface is a superposition of the incident and the reflected wave fields), we can determine the scattered field $U_r(\mathbf{r}_s)$ from the forested layer as a superposition of an incident wave $U_i(\mathbf{r}_2)$, the reflection coefficient $R(\varphi_s,\mathbf{r}_s)$, and the shadow function $Z(\mathbf{r}_2,\mathbf{r}_1)$. The shadow function equals one, if the point of scatter r_s inside the forested layer can be observed from both points $\mathbf{r}_1$ and $\mathbf{r}_2$ of the transmitter and receiver locations as shown in Figure 6, and equals zero in all other cases. Taking into account all these assumptions, Equation 10 can be rewritten following the method used by (Blaunstein et al., 2003) as

$$U(\mathbf{r}_2)=\mathrm{Z}(\mathbf{r}_2,\mathbf{r}_1)\tilde{G}(\mathbf{r}_2,\mathbf{r}_1)+2\int_{S2}\{\mathrm{Z}(\mathbf{r}_2,\mathbf{r}_s,\mathbf{r}_1)R(\varphi_s,\mathbf{r}_s)\cdot \tilde{G}(\mathbf{r}_2,\mathbf{r}_1)(\mathbf{n}_s\cdot\nabla_s)\}\mathrm{d}S, \quad (12)$$

where $\nabla_s=\left(\frac{\partial}{\partial x},\frac{\partial}{\partial y},\frac{\partial}{\partial z}\right)$, $\varphi_s=\sin^{-1}\left(\mathbf{n}_s\cdot\frac{\mathbf{r}_2-\mathbf{r}_1}{|\mathbf{r}_2-\mathbf{r}_1|}\right)$ (Figure 7) and $\tilde{G}(\mathbf{r}_2,\mathbf{r}_1)$ is the normalized Green's function. The solution of Equation 12 may be presented in operator form through a set of Green's functions expansion as (Blaunstein and Christodoulou, 2007; Blaunstein et al., 2003)

$$U_2=\mathrm{Z}_{21}\tilde{G}_{21}+\left(\mathrm{Z}_{2S}\hat{M}_{2S}R_S\right)\mathrm{Z}_{S1}\tilde{G}_{S1}+\left(\mathrm{Z}_{2S}\hat{M}_{2S}R_S\right)\left(\mathrm{Z}_{SS'}\hat{M}_{SS'}R_{S'}\right)\mathrm{Z}_{S'1}\tilde{G}_{S'1}+\cdots \quad (13)$$

Here, $\hat{M}_{\alpha\beta}$ is an integral-differential operator that describes the expression inside the bracket in Equation 13 and the variables $\mathrm{Z}_{\alpha\beta}$ and $R_{\alpha\beta}$ are the corresponding shadow and reflection coefficient functions denoted by indexes α and β. Noting Twersky's approximation, which states that the contributions of multiple scattered waves are additive and independent (hence does not take into account mutual multiple scattering effects) together with the condition that $\langle R(\varphi_s,d_s)\rangle=0$, it is possible to obtain the coherent part of the total field from Equation 13 by averaging Equation 12 over the reflecting properties of each tree and over all tree positions (Twersky, 1967). Thus,

$$\langle U_2\rangle=\langle \mathrm{Z}_{21}\rangle\tilde{G}_{21}. \quad (14)$$

Z_{21} is the "shadowing" function that describes the probability of existence of some obstructions in the radio path of the two terminal antennas. As the contributions of the multi-scattered waves are independent (Twersky, 1967), the coherent part of the total field intensity could be represented as (after averaging Equation 13) as

$$\langle I_2\rangle=\langle \mathrm{U}_2\cdot\mathrm{U}_2^*\rangle=\langle \mathrm{Z}_{21}\rangle\tilde{G}_{21}\cdot\tilde{G}_{21}^*ⁿ+\langle\left\{D_{2S,2\tilde{S}}+D_{2S',2\tilde{S}'}\cdot D_{SS',\tilde{S}\tilde{S}'}\right\}\cdot\mathrm{Z}_{S1}\cdot\mathrm{Z}_{\tilde{S}1}\cdot\tilde{G}_{S1}\cdot\tilde{G}_{\tilde{S}1}^*\rangle \quad (15)$$

where $D_{SS',\tilde{S}\tilde{S}'}=Z_{SS'}\cdot Z_{\tilde{S}\tilde{S}'}\cdot\hat{M}_{SS'}\cdot K_{S\tilde{S}}$.

For the conditions defined for the correlation function that describes the roughness of the tree surfaces, ℓ_h, ℓ_v, $\ll \bar{\rho},\bar{w},\bar{h}$ and $k\ell_h$, $k\ell_v \gg 1$ for $0<z_1<\bar{h}$, Equation 14 could be integrated over all the variables of the type $\Delta\mathbf{r}_S=\mathbf{r}_{\tilde{S}}-\mathbf{r}_S$ at the surfaces of scattering trees. By manipulating the expression in Equation 14 according to (Blaunstein and Christodoulou, 2007; Blaunstein et al., 2003), we obtain

$$\langle I_2\rangle=\langle \mathrm{Z}_{21}\rangle\left|\tilde{G}_{21}\right|^2+\langle\{Q_{2S1}+Q_{2S'S}\cdot Q_{SS1}+\cdots\}\cdot\mathrm{Z}_{S1}\left|\tilde{G}_{S1}\right|^2\rangle \quad (16)$$

Where $Q_{SS',\tilde{S}\tilde{S}'}=Z_{SS'}\cdot\left|\tilde{G}_{21}\right|^2\cdot\sigma_{S''S'S}$.

The cross-sectional area of scattering has been given as (Blaunstein and Christodoulou, 2007; Blaunstein et al., 2003)

$$\langle\sigma\rangle=\frac{\gamma_0 R}{4\pi}\cdot\sin^2\frac{\alpha}{2}\cdot\frac{k\ell_v}{1+(k\ell_v)^2(\sin\vartheta'-\sin\theta')^2}\cdot\frac{k\ell_h}{1+(k\ell_h)^2} \quad (17)$$

By averaging Equation 15 over all tree (screen) positions – integrating over the surfaces of the screens as well as over their mirror surfaces $(-\bar{h}\le z,z',z'',\ldots\le\bar{h})$. The averaging over the screen orientations for each scatter point affects only the value of σ from Equation 17. At the same time, the averaging over the number and position of all screens affects the "shadow" function Z. This approximation together with that of $\langle R(\varphi_s,r_s)\rangle=0$ (that the mean reflection coefficient round the tree is zero) makes it possible to obtain the coherent part of total field intensity, I_{co}, as (Blaunstein and Christodoulou, 2007; Blaunstein et al., 2003)

$$I_{co}=\frac{e^{-\gamma_0 d}}{16\pi^2 d^2}*\left[2sin\frac{kh_T h_R}{d}\right]^2 \quad (18)$$

For the incoherent part of the total field intensity, the Equation 15 can be presented in operator form as

$$\langle I_{inc}(\boldsymbol{r_2})\rangle=2\{Q+Q^2+Q^3+\cdots\}P(\boldsymbol{r_2},\boldsymbol{r_1}) \quad (19)$$

where the effect of the integral operator on the functions at the right-hand side of Equation 18 can be expressed as

$$Qf(\mathbf{r}_2,\mathbf{r}_1)=\int_V(\mathrm{d}\mathbf{r})P(\mathbf{r}_2,\mathbf{r})\frac{\langle\boldsymbol{\sigma}(\mathbf{r}_2,\mathbf{r},\mathbf{r}_1)\rangle}{|\mathbf{r}_2-\mathbf{r}_1|}f(\mathbf{r},\mathbf{r}_1). \quad (20)$$

The product $\mathrm{d}\mathbf{r}=\mathrm{d}S\cdot\mathrm{d}n$ defines the element of volume V of a plane parallel to the tree layer with width $,2\bar{w}$ over which the integration of the right hand side of Equation 20 takes place. Using the same assumptions that were used in deriving Equation 1 and setting $kz_2\gg1$, $z_2<\bar{h}$, we can integrate Equation 19 over variable z to get

$$(4\pi)^2|\rho_2-\rho_1|\cdot\langle I_{inc}(\boldsymbol{r_2})\rangle=2\{q+q^2+q^3+\cdots\}g(\rho_2-\rho_1) \quad (21)$$

where

$$g(\rho_2-\rho_1)=\frac{\exp\{-\gamma_0|\rho_2-\rho_1|\}}{|\rho_2-\rho_1|} \quad (22)$$

If the integration is over ρ with infinite limits, the operator $\hat{q}$ becomes

$$\hat{q}f(\rho_2,\rho_1)=\frac{v\cdot\bar{w}\cdot R}{4\pi}\int(\mathrm{d}\rho)\left[1-\frac{\rho_2-\rho}{|\rho_2-\rho|}\cdot\frac{\rho-\rho_1}{|\rho-\rho_1|}\right]g(\rho_2-\rho_1)f(\rho-\rho_1). \quad (23)$$

An evaluation of Equation 21, taking into account Equations 22 and 23 and using Laplace's method for $\gamma_0\rho\gg1$ yields the incoherent part of the total field intensity as

$$\langle I_{inc}(\boldsymbol{r_2})\rangle\approx\frac{\gamma_0 R}{(4\pi)^2}\left[\frac{R^3}{4(8)^3}\frac{\exp\{-\gamma_0 d\}}{d}+\frac{R}{32}\left(\frac{\pi}{2\gamma_0}\right)^{1/2}\frac{\exp\{-\gamma_0 d\}}{d^{3/2}}+\frac{1}{2\gamma_0}\frac{\exp\{-\gamma_0 d\}}{d^2}\right] \quad (24)$$

The first two terms in Equation 24 are important only at long distances $d>d_k=\frac{8^3}{\pi\gamma_0 R^2}$, whereas the third term is important at close ranges (Blaunstein and Christodoulou, 2007). Therefore,

$$I_{inc}=R_{HP,VP}*\frac{1}{32\pi^2 d^2}*e^{-\gamma_0 d} \quad (25)$$

provided that $d<\frac{8^3}{\pi\gamma_0 R^2}$.

Hence the path loss due to the multiple scattering effects of the mangrove tree elements, L_{MSE}, may be obtained by applying Equation (1) as

$$L_{MSE} = -10 \log [\lambda^2 (I_{co} + I_{inc})] \quad (26)$$

Similarly, the loss due to the absorptive effects, L_{AE}, is obtained using an appropriate standard empirical forested path loss model. Weissberger's Model is most suitable in the mangrove swamp medium (Meng et al, 2010; Agugo and Adeniran, 2011). Hence the characteristic equation or path loss model (referred hereafter as MIM), would evaluate the total path loss L_{MIM}, as the summation of L_{MSE} and L_{AE}, that is,

$$L_{MIM} = L_{MSE} + L_{AE}, \quad (27)$$

where L_{AE} is obtained using Weisberger's Model.

4. EVALUATION AND ANALYSIS OF RESULTS

In evaluating the path loss using MIM, an estimate of the tree density v, in the area of investigation is required. The value v is used with the average tree width w, to obtain the working average value of γ_0, which is a critical in the MIM model. This estimate of v (which is the number of trees per km^2) was obtained by simple proportion after getting the estimate of the number of trees in an area of 100 m^2, 500 m^2 or 1000 m^2 (whichever was more expedient at each measurement site). The number of trees can be (and indeed was in our case) obtained by physical enumeration. In Ilado-Odo for instance, the number of trees counted within some sampled small strips of forest 10m x 50m dimension ranged between 12 and 13 trees. Thus v could be evaluated as follows:

Average number of tree in the area of 500m^2 = 12.5; therefore, for an area of 1 km^2 (1000000 m^2), $v = \frac{12.5}{500} * 1000000 = 25000$ trees/km^2.

From the study, the tree density v was found to range between 25,000 and 32,000 per km^2, generally increasing from Lagos eastwards. Table 1 shows the values of γ_0 based on various values of the forest parameters estimated for specific mangrove forest areas.

Table 1: Average Values of Tree width and Density across the Nigerian Mangrove Belt

w (m)	v (km^{-2})	γ_0 (km^{-1})	Corresponding Areas
0.7	25,000	11.14	Lagos/Ogun
0.9	27,000	15.50	Ogun/Ondo
1.0	27,000	17.20	Cross Rivers/Akwa-Ibom
1.2	30,000	22.92	Delta/Rivers
1.3	30,000	24.83	Detla/Bayelsa
1.4	32,000	28.52	Bayelsa outskirts
1.5	32,000	30.56	Bayelsa Central

Note: w = Average tree width, v = numbers of tree per km^2, $\gamma_0 = 2\bar{w}v/\pi$.

The average tree width, w, ranges from 0.7 m to 1.5 m. (Note that the proper unit for w should be km, as the dimension of γ_0 is km^{-1}). The absolute reflection coefficient R for wood obtained is 0.4 (Blaunstein, 2004). The plots showing the variability of average path loss relative to distance are in Fig.8. Also, a normalized meshed graph of path loss variability relative to distance and tree density is shown in Fig. 9.

It is observed that the values of path loss at Ilado-Odo are generally lower than those of Nembe. This is in agreement with the prediction results of the MIM, which indicates that path loss should increases with forest tree density. This is despite the more availability of tree canopies at Nembe than Ilado-Odo. Also, there is a general straight line regression with distance. It is also seen that there is essentially negative loss within 50 m of antenna separation, that is, a reduction from the free space attenuation values obtained from Friis' equation. This may be explained by the high contribution of both the coherent and incoherent wave fields since this range may have direct LOS path in addition to volume scattered wave that may produce back scattering effects. The back scattering phenomenon explains why the MIM predicts negative loss at certain propagation and forest parameters.

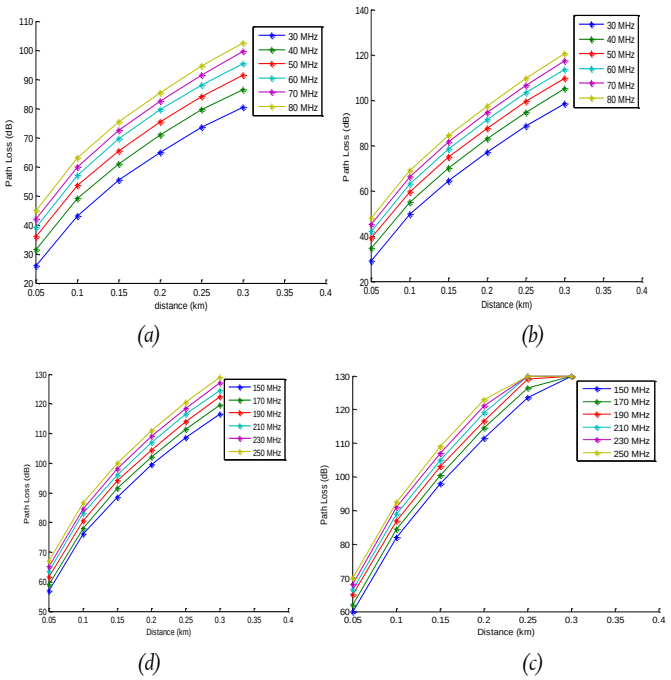

Fig 8: Graphs of average path loss against distance at given frequencies in (a) Ilado-Odo (b) Nembe (c) Ilado-Odo (d) Nembe.

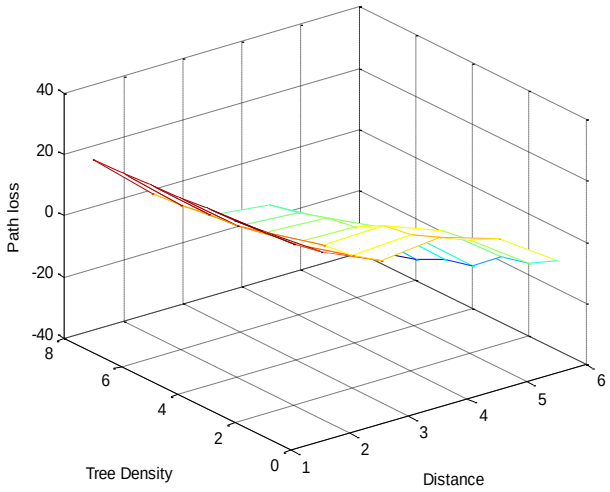

Fig. 9: Mesh Plot Showing Variability of Path loss with Distance and Tree Density (normalized).

4.1. Sensitivity analysis

It is possible to check the sensitivity of the prediction model to errors that may occur in any of the forest parameters required for path loss evaluation using the model. The accuracy of a theoretical prediction depends on the range of variance of each parameter, which describes the terrain features. For instance, a comparison of the values of path loss obtained in Ilado-Odo and Nembe indicates that variations in the values of $\gamma 0$ may have significant effect on LMSE, hence LMIM. From the values, it is seen that the variation of the tree densities within the range can affect the path loss by 10 - 20 dB. This is why, it is very important to know how accurate the various parameters should be, and what would be the effect of an error in any of the parameter i.e. average tree height, $\bar{h}$, width, $\bar{w}$, density v, and reflection coefficient R. For example, the value of R used in all the

predictions was 0.4. Deviations of this value over the range of ±50% (ΔR = 0.2) lead to deviations of the total path loss of less than ±1% (0.5 - 1.0 dB depending on the frequency and distance). Deviations of the parameter γ_0 in the range of ± 50% ($\Delta\gamma_0$ ≈ 5 for Lagos Area or 14 for Bayelsa Area) lead to deviations of the total path loss of in the range of ± 10 - 20% (7.0 - 15.0 dB). It is thus seen that MIM predictions are essentially sensitive only to errors in the value of γ_0. Since γ_0 depends mostly on the estimates of tree density ν per km^2, it can be generally concluded that the accuracy of the MIM largely lies on tree density estimates. Hence, the greatest care needs to be given to obtaining accurate estimates of tree density in the prediction of path loss in mangrove forests.

5. CONCLUSIONS

The combat net equipment/systems typically operate in the VHF and UHF bands, and are likely to be deployed with near ground antenna in areas where the forest structures provide them cover even from aerial view. The most significant contribution of this study was to show the prime importance of forest tree density in the estimation of radio propagation path loss in the mangrove swamp forest. This study has brought out interesting conclusions that would enhance the operation of smart military communication systems. These are:

i. Path loss predictions in the mangrove forest must take due consideration of forest tree density.
ii. The influence of specular ground and tree canopy reflections are negligible.
iii. Path loss variability with distance is approximately linear between 50-300m.
iv. The accuracy of path loss prediction is essentially dependent only on the accuracy tree density estimate.

REFERENCES

Agugo F. and Adeniran S., "Characterization of near-ground radio wave propagation in the mangrove and rain forest areas of Nigeria" Proceedings of 3rd IEEE international conference on adaptive science and technology, 249-255, 2011.

Blaunstein, N., I. Z. Kovacs, and Y. Ben-Shimol, "Prediction of UHF path loss for forest environments," Radio Sci., 38(3): 251-267, 2003.

Blaunstein, N., "Wireless Communication Systems," in Handbook of Engineering and Electromagnetics, Edited by R. Bansal, Chapter 12, Marcel Dekker, New York, pp. 417–481, 2004.

Blaunstein, N. and Christodoulou, C., "Radio Propagation and Adaptive Antennas for Wireless Communication Links: Terrestrial, Atmospheric and Ionospheric", John Wiley & Sons, Inc, 2007.

Meng, Y.S., Lee, Y.H. and Ng, B.C., "Path loss modelling for near ground VHF radio wave propagation through forest with tree canopy effect", *Progress in Electromagnetic research M*, Vol. 12, 2010.

Onuu, M. and Adeosun, A., "Investigation of Propagation Characteristics of UHF waves inAkwa-Ibiom State of Nigeria", Indian Journal of Radio and Space physics, 37:197-203, 2008.

Shoewu, O and Adedipe, A., "Investigation of radio waves propagation models in Nigerian rural and sub-urban areas," American Journal of Scientific and Industrial Research, Science, http://www.scihub.org/AJSIR, 2010.

Twersky, V., "Multiple scattering of electromagnetic waves by arbitrary configurations," Journal of Math. Phys., 8, 569-610, 1967.

Weissberger, M.A., "An initial critical summary of models for predicting the attenuation of radio waves by foliage," *ECAC- TR-81-101*, Electromagnetic Compatibility Analysis Centre, USA, 1981.

Zwick T. Younis, M., Adamiuk, G. and Balduaf, M., "Radio wave propagation fundamentals", Univeersitat Karlruhe (TH) Research University, 2009.

Full Paper

EFFECT OF SELECTED ARTIFICIAL BINDING AGENTS ON THE PELLETABILITY OF ORGANIC FERTILIZER

D.A. Fadare
Mechanical Engineering Department
University of Ibadan, P.M.B. 1, 20002, Ibadan
fadareda@gmail.com

O.A. Bamiro
Mechanical Engineering Department
University of Ibadan, P.M.B. 1, 20002, Ibadan

ABSTRACT

Selection of appropriate binder and its concentration poses great challenge in the application of artificial binding agents for pelletizing of organic fertilizer. In this paper, effects of three (3) artificial binders (kaolin, bentonite and corn starch) at three concentrations (2.5, 10 and 15% by weight) on the mechanical properties (crushing strength, brittle fracture index, axial elastic recovery, durability disintegration time and specific energy requirement) of organic fertilizer pellets were investigated. Cylindrical pellets of 25 mm diameter and 20 mm long were formed using a uniaxial compression machine. The L9 Taguchi orthogonal array design experiment was used to determine the percentage influence of type and concentration of the binders on the variability of the mechanical properties of the pellets. Results showed that the type of binder had the greatest percentage influence of 90.4% (disintegration time), 67.9% (crushing strength), 56.2% (durability), 40.5% (axial elastic recovery), 85.5% (specific energy requirement), while the concentration of the binder showed no significant effect except on the brittle fracture index where the concentration had the highest influence of 36.8%. Corn starch was found to be the best binder with optimal concentrations of 15% for crushing strength, axial elastic recovery, durability and disintegration time, and 10% for brittle fracture index.

Keywords: *Organic fertilizer pellet; binder; mechanical properties; kaolin; bentonite; corn starch*

1. INTRODUCTION

The application of artificial binding agents plays a crucial role in the sustainability of various compaction processes such as: pelletizing, bailing and wafering, briquetting, and tableting. Hence, the choice of appropriate binder and its level of concentration pose great challenges in the use of artificial binding agents in pelletizing of organic fertilizer (Fadare, 2003). Organic fertilizers or compost are produced from controlled decomposition of organic matter. They contains important plant nutrients, which improves the physical, chemical (nutritional) and biological properties of soil and plant growth media (Gould, 2012). The most popular applications of organic fertilizers or compost are as soil amendment and mulch to improve soil health of new and existing installations of plant beds and around trees (Organic Monitor, 2012). The global concern for organic farming is the major driving force for the increase in demand for organic fertilizer and green manure worldwide. Since 1990, the market for organic products has grown from nothing, reaching $55 billion in 2009 (Organic Monitor, 2012). Correspondingly, the total number of organic producers worldwide has increased form 0.2 million in 1999 to about 1.8 million in 2009 (Willer and Kilcher, 2011). Approximately, 37.2 million hectares worldwide are now farmed organically, representing approximately 0.85 percent of total world farmland in 2009 compared with the 11.0 million hectares of organic farmland in 1999 (Willer and Kilcher, 2011). The current global demand potential for organic fertilizer was estimated as 1.06 billion tons annually (Esengun et al., 2007). The use of organic fertilizer or compost is known to be more efficient and environmentally friendly compared to the conventional inorganic fertilizers (Fadare, 2003). Major benefits of using organic fertilizer or compost include: improving soil structure, creating a better plant root environment, supplying significant quantities of organic matter, improving drainage of soil, reducing soil erosion, improving moisture holding capacity of soils, improving and stabilizing soil pH, supplying a variety of nutrients, and supplying the soil with beneficial micro-organisms (Alexander, 2003; Sæbø and Ferrini, 2006; Nevens and Reheul, 2003; Arthur et al., 2011). According to the quantitative analysis of Battelle (2012), the demand for organic fertilizer in the US is about 10 times that of its supply, thus indicating the gross shortage in the supply of organic fertilizer. Despite the high demand for organic fertilizer, its supply has been hindered due to economic factors relating to its "bulkiness" and hence high associated transport and spreading costs compared to that of inorganic fertilizers. In order to overcome this setback, the current trends in composting is towards the compaction of the loose particulates into high density (pelletizing) with main benefits, which includes: reduction in volume, ease of packaging and handling, control of the rate of nutrient release, and improvement in the quality (Weber et al., 2007). Compacting of loose particulates to high density has been widely used with cohesion being achieved through application of pressure and/or temperature with addition of additives such as artificial binders which confer strength to the agglomerates, and as lubricants to reduce friction during the compaction operation. The selection of appropriate binding agent is one of the most critical parameters in pelletizing process. The influence of binding agent on the characteristics of the pellets is both essential in the design and construction of the pelletizing machine and the economic production of the pellets. A comprehensive survey of literature on the effect of binding agent on the pelletability of lignocelluloses agricultural materials has been reported by O'Dogherty (1989). Despite this volume of literature, there is paucity of information on the study of binding agent in the pelletization of organic fertilizer or compost. The energy utilization analysis and energy cost for pelletization of organic fertilizer in Nigeria has been reported by same authors earlier (Fadare et al., 2009; 2010). The work of John et al. (1996) reported the study on the effect of concentration (10 and 20% w/w) of clay as binding agent on the pelletability of composts of poultry droppings and/or sawdust. An increase in pellet's stability/strength was observed with increase in concentration of the binder for compost made from poultry droppings. However, it was also reported that the composts made from sawdust, and the combination of sawdust and poultry manure could not be pelletized satisfactorily under the tested conditions. Other potential

artificial binding agents that have not been fully exploited in pelletizing of compost includes kaolin, bentonite and corn starch. The aim of this paper is to investigate the effect of kaolin, bentonite and corn starch at three concentrations (2.5, 10.0 and 15.0% by weight) on the mechanical properties of pellets of organic fertilizer made from co-composted market refuse and abattoir waste. In view of determining optimum process parameters required for design and operation of commercial scale organic fertilizer pelletizing plant.

2. MATERIALS AND METHODS

2.1. Organic Fertilizer Preparation

Samples of market refuse and abattoir waste generated in a typical municipal market located in Ibadan, south-western, Nigeria, were collected. The market refuse was sorted into two fractions consisting of the biodegradable and non-biodegradable. The biodegradable fraction, which includes food waste, paper, fruits and leaves was shredded in a shredding machine to particle size less than 20 mm. The shredded biodegradable fraction was then co-composted aerobically with the abattoir waste at ratio of 3:1 by wet weight inside open windrow for about 60 days. During the composting period, the windrow was sprinkled with water and turned manually using shovels and garden forks for aeration and circulation of oxygen. Turning of the windrow was done once in every three (3) days for the first fifteen (15) days and thereafter, once every seven (7) days to the end of the composting period. After the composting process, the compost was cured for another 60 days by leaving the windrow unturned and without addition of water. The compost was then dried in a rotary dryer at temperature 60°C for 6 hours. The dried compost was then screened with a sorting machine and milled with a pulverizing machine to particle size of 5.27 µm. The detailed composting process and the determination of the physico-mechanical and chemical properties of the compost have been reported earlier (Fadare, 2003).

2.2. Artificial Binding Agents

Corn (*Zea mais*) starch was obtained from the Department of Industrial Pharmacy, University of Ibadan, Nigeria, while kaolin and bentonite samples were supplied by Raw Material Research and Development Council (RMRDC) Abuja, Nigeria. Samples of 1,000 g compost with corresponding weights of binding agents at varying concentrations of 2.5, 10.0 and 15.0% by weight were measured. The binding agents were dispersed in 200 mL of distilled water. Corn starch dispersion was heated in a water bath at temperature of 95°C for 20 min to form starch gel. The compost and the binding agents were mixed manually.

2.3. Experimental Design

A 3-level (L_9) Taguchi Orthogonal Array experimental design (WinRobust, 1995) was used to determine the main effects of the factors (type and concentration of the binding agent) on the properties of the pellets and to determine the optimum combination of the levels of the variables that give favourable properties (crushing strength, brittle fracture index, axial elastic recovery, durability disintegration time and specific energy requirement) of the pellets. The two (2) factors at three (3) levels of the experimental design are shown in Table 1. The L_9 Taguchi array experimental design matrix is shown in Table 2. Factors (3) and (4) of the array were assigned as error to account for the uncertainties due to interactions between variables, measurement error and uncontrolled factors. A total of nine (9) experiments were conducted for different combinations of factor and levels.

Table 1: Factor and level with code used the experimental design

Factor	Level		
	(1)	(2)	(3)
Type of binder	Kaolin	Corn starch	Bentonite
Concentration of binder (%)	2.5	10.0	15.0

Table 2: The L_9 Taguchi array experimental design matrix

Exp. No.	Type of binder (1)	Conc. of binder (2)	Error (3)	Error (4)
1	1	1	1	1
2	1	2	2	2
3	1	3	3	3
4	2	1	2	3
5	2	2	3	1
6	2	3	1	2
7	3	1	3	2
8	3	2	1	3
9	3	3	2	1

2.4. Compression Tests

Compression tests were conducted on a laboratory hydraulic compression rig (AB specimen mount press). Cylindrical pellets with 25 mm diameter and 25 mm long were formed using closed end cylindrical die assembly. Pellets with 3 mm hole in the centre were formed using a lower punch with a 3 mm pin fixed in the centre and the upper punch with a corresponding hole drilled at the centre. 18 g of each sample were compressed at constant compression speed (0.005 ms^{-1}) to a maximum pressure of 79.0 MPa. The maximum pressure was held for 3 minutes before ejecting the pellets. During each test, initial length of pellet before compression (L), displacement (S) and applied pressure (P) were measured. The experimental setup and dimensions of the die assembly are shown in Figures 1 and 2, respectively. Prior to each test the inside of the die assembly was lubricated with soluble oil to facilitate the ejection of the pellets. The compression ratio (r) was calculated (Faborode and O'Callaghan, 1986) as:

$$r = \frac{L}{L - S} \tag{1}$$

Where L is initial length of pellet (mm) and S is displacement (mm).

The compression curve for each experiment was obtained as the plot of applied pressure (P) against compression ratio (r).

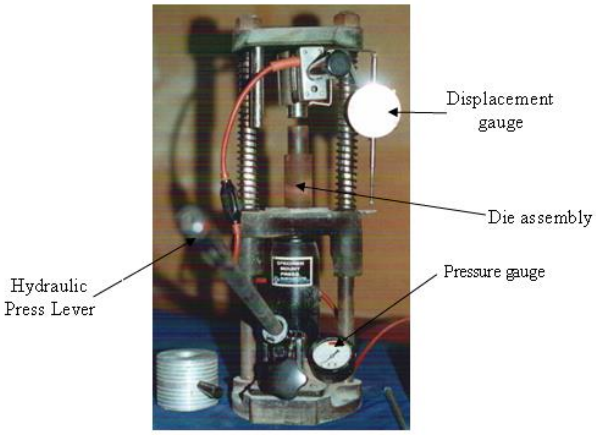

Fig. 1: Experimental setup

2.5. Determination of specific compression energy

The compression curves were modelled using three common mathematical models: exponential model (Equation 2) proposed by Ajayi and Lawal (1995); power model (Equation 3) proposed by O'Dogherty and Wheeler (1982); and the modified exponential model (Equation 4) proposed by Faborode and O'Callaghan (1995):

$$P = Ae^{Br} \tag{2}$$

$$P = Ar^{B} \tag{3}$$

$$P = \frac{A}{B}\left[e^{B(r-1)} - 1\right] \tag{4}$$

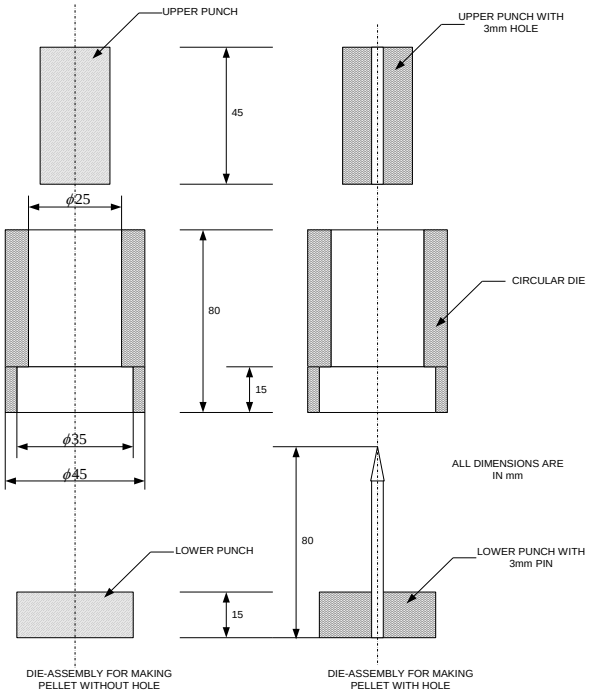

Fig. 2: Dimensions of the die assembly

where, P is applied pressure, r compression ratio, and A and B are empirical constants.

A curve fitting program using unconstrained least square procedure of damped Taylor's series (Spath, 1967) was developed with FORTRAN 90 to determine the model parameters based on Equations 2 - 4. The model predictive performance was evaluated based on the coefficient of determination (r^2). The empirical constants A and B, and the corresponding r^2 for each model were evaluated.

The compression energy (E) requirement for pelletization was determined as the area under the compression curve given by the model with the highest value of coefficient of determination. For the exponential model (Equation 2), the area under the curve was expressed in the general form as:

$$E = \int_{r=0}^{\max r} A\left[\exp^{Br}\right]dr \tag{5}$$

Which upon integration gives:

$$E = \frac{A}{B}\exp(Br)_{\max r} - \frac{A}{B}\exp(Br)_{r=0} \tag{6}$$

2.6. Determination Of Mechanical Properties Of Pellets

The compressive force required to diametrically fracture the pellet was determined by using a tensometer (Type "W", Monsanto, U.K.) and the crushing strength and the brittle fracture index were calculated (Odeku and Itiola, 2002) as:

$$T_D = \frac{2N}{\pi dH} \tag{7}$$

$$T_{D0} = \frac{2N_0}{\pi dH} \tag{8}$$

$$BFI = \frac{T_D - T_{D0}}{2T_{D0}} \tag{9}$$

Where T_D is crushing strength of the pellets without hole (Nm^{-2}); T_{D0} is crushing strength of the pellets with hole (Nm^{-2}); N is compressive force required to diametrically crack/fracture the pellet without hole (N); N_0 is compressive force required to diametrically crack/fracture the pellet with hole (N); d is the diameter of the pellet (m); H is the length of the pellet (m); and BFI is brittle fracture index of pellets.

The axial elastic recovery was calculated using the expression (O'Dogherty and Wheeler, 1982):

$$ER_a = \frac{L_2 - L_1}{L_1} X100\% \tag{10}$$

Where ER_a is axial elastic recovery (%); L_1 is the initial length of pellet before ejection from the die (mm); L_2 is the final length of pellet after ejection (mm).

The durability of the pellets was determined using a laboratory durability tester at the speed of 60 rpm for 5 minute in accordance with the ASAE standards (ASAE, 1998). The initial weights of the pellets before and after the test were measured. The durability of the pellets was calculated as the percentage of the final weight to the initial weight of pellets:

$$\eta = \frac{W_f}{W_i} \times 100\% \tag{11}$$

Where η is durability of pellets (%); W_i is initial weight of pellets before test (kg); W_f is final weight of pellets after test (kg).

The disintegration time (hr) of the pellets was determined as described by Adebayo and Itiola (1998) and Odeku and Itiola (1994) as the time required for the pellets to disintegrate completely into the original particle when in contact or immersed in water.

All measured properties of the pellets were replicated four times.

3. RESULTS AND DISCUSSION

The empirical constants A and B, and the corresponding r^2 of the three compression models investigated are shown in Table 3. The exponential and power law models (Equations 2 and 3) gave consistently high values of r^2 with respective values ranging from 0.9827 - 0.9989 and 0.9634 - 0.9997, while the modified exponential model gave the least with values ranging from 0.7761 - 0.8911. For ease of application, the exponential model (Equation 2) was chosen as the empirical model for the compression curve. Figure 3 shows the exponential compression models for kaolin, bentonite and corn starch at 10.0% concentration, while the exponential compression models for 2.5, 10.0 and 15.0% concentrations of Kaolin are shown in Figure 4.

Samples of pellet formed with hole and without hole with 2.5% concentration of corn starch are shown in Figure 5. The mean values of crushing strength, brittle fracture index, axial elastic recovery, durability, disintegration time and specific energy requirement for compression of the pellets for the different experiments are given in Table 4. The variation in the mechanical properties of the pellets for the different types and concentrations of binding agent are shown in Figures 6 (a-f).

3.1. Effect Of Binder On Pellets Crushing Strength

The variation in the crushing strength of the pellets is shown in Figure 6(a). It was observed that, the crushing strength increased rapidly as the concentration increased for bentonite and kaolin, while for corn starch, crushing strength increased slightly with increase in concentration. For all concentrations investigated, the crushing strength for corn starch was consistently higher than bentonite and kaolin. The order of magnitude was corn starch › bentonite › kaolin.

Except at lower concentration (2.5%) where the crushing strength for kaolin was higher than that of bentonite. The results could be attributed to the smaller particle size and higher fluidity of corn starch compared to bentonite and kaolin. Corn starch tended to flow easily within the crevice of the particulate to form a stronger bond. Hence, when the crevice is saturated, increase in concentration tends to have no effect on the binding strength for corn starch. Whereas, unsaturation due to low fluidity of bentonite and kaolin resulted in increase in crushing strength with increased concentration. Crushing strength is the measure of the binding strength and the resistance of the pellet to impact force, thus indicating ability of the pellet to retain its shape and size during handling. Hence, high crushing strength is recommended for pellet.

Table 3: Compression curve model parameters

Exp.	Exponential law model (Equation 2)			Power law model (Equation 3)			Modified exponential model (Equation. 4)		
No.	A	b	R^2	A	b	R^2	Ax(E-20)	Bx(E-08)	R^2
1	0.0216	3.6979	0.9912	0.3761	6.5203	0.9826	0.0149	7.5444	0.7761
2	0.0094	4.1990	0.9989	0.2266	7.4863	0.9997	0.6352	4.8997	0.7691
3	0.0172	3.9166	0.9945	0.3673	6.8464	0.9871	0.0100	6.1628	0.7656
4	0.1239	2.9015	0.9889	1.4131	4.8118	0.9736	0.0102	6.2243	0.8482
5	0.1499	2.9074	0.9827	1.9300	4.5898	0.9634	0.1306	2.2134	0.8593
6	0.1611	2.9348	0.9948	2.1500	4.5942	0.9834	4.2856	1.2643	0.8911
7	0.0701	3.376	0.9976	1.2222	5.5370	0.9975	4.5698	1.3059	0.8724
8	0.0711	3.3302	0.9979	1.1853	5.4444	0.9906	9.7704	1.9128	0.8538
9	0.101	3.1777	0.9847	1.5714	5.0824	0.9761	5.0512	1.3732	0.8686

Table 4: The measured mechanical properties of pellets

Exp	Response (Mechanical property)					
No.	Crushing strength T_D (kNm^{-2})	Brittle fracture index	Axial Elastic recovery (%)	Durability (%)	Disintegration time (hr)	Specific compression energy (MJ/ton)
1	49.49	4.75	4.12	23.50	1.20	469.97
2	123.18	0.42	4.06	64.20	1.40	489.95
3	151.13	0.34	3.98	75.60	1.50	547.21
4	348.95	0.09	3.45	98.50	27.70	689.06
5	387.56	0.04	2.14	99.50	31.50	842.02
6	406.74	0.06	2.12	99.60	48.80	947.91
7	10.65	1.83	5.02	5.30	0.90	875.41
8	172.81	0.49	3.91	53.10	1.60	820.79
9	329.25	0.97	2.17	74.30	2.40	898.21

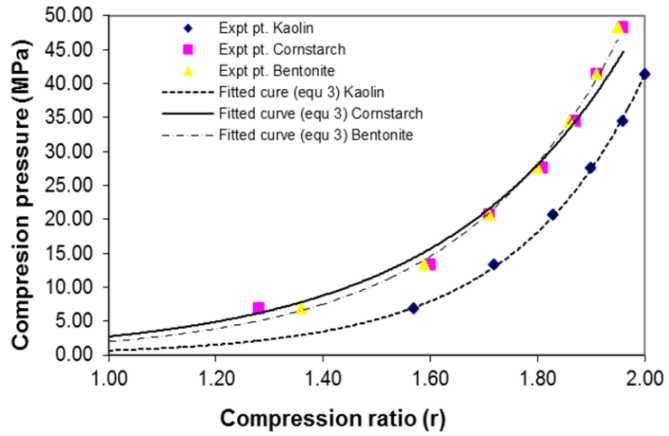

Fig. 3: Exponential compression models for kaolin, bentonite and corn starch at 10% concentration.

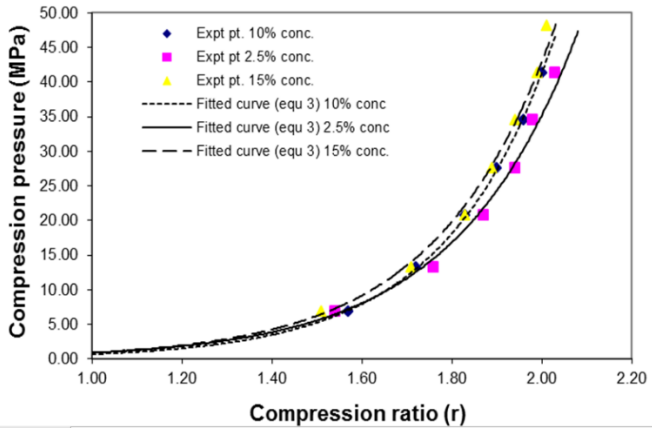

Fig.4: Exponential compression models for 2.5, 10.0 and 15.0% concentrations of Kaolin

This result suggests corn starch as a favourable binder from the point of view of binding strength. Similar increase in crushing strength with increase in concentration of binding agents has been commonly reported by many investigators (Ajayi and Lawal, 1995; Chaplin, 1975; Wealti and Dobie, 1973; Dobie and Walker, 1977).

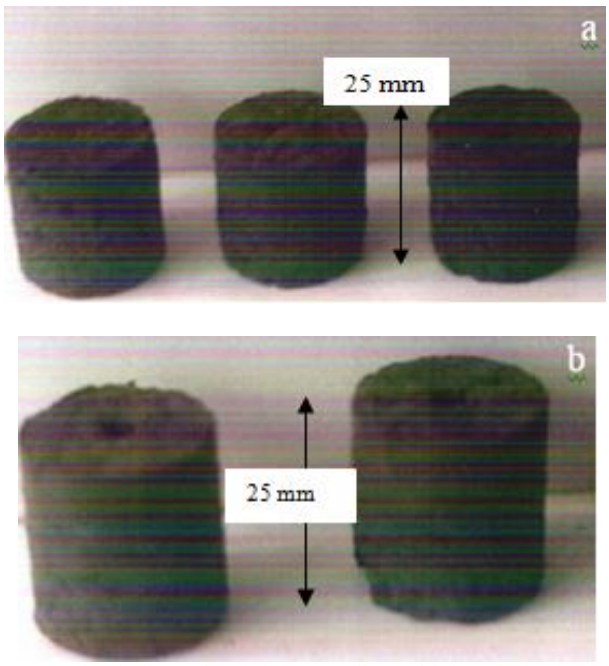

Fig. 5: Samples of pellets without hole (a) and pellets with hole (b) formed with 2.5% concentration of corn starch

3.2. Effect Of Binder On Pellets Brittle Fracture Index

Figure 6(b) shows the influence of the binders on the brittle fracture index of the pellets. The results showed that for kaolin and bentonite the brittle fracture index decreased initially with increased in concentration from 2.5 – 10.0%. With further increase in concentration above 10.0% the brittle fracture index increased for bentonite, while the brittle fracture index decreased slightly for kaolin. For corn starch the brittle fracture index was lower and remained constant as the concentration increased. The brittle fracture index is the measure of the binding efficacy of the binder at inter-particulate junctions of the particles, which facilitates plastic

deformation for the relief of localized stresses and hence limits the lamination tendency in pellets. Hence, a lower brittle fracture index is normally preferred in selection of appropriate binder. From this point of view, corn starch appeared to be more favoured compared to bentonite and kaolin. Odeku and Itiola (1998 and 2002) reported reduction in brittle fracture index with increase in concentration of different binders used for tableting of pharmaceutical products.

3.3. Effect Of Binder On Pellets Axial Elastic Recovery

Figure 6(c) shows the effect of the binders on the axial elastic recovery of the pellets. It can be seen that the axial elastic recovery decreased generally with increase in concentrations for corn starch. For kaolin, the axial elastic recovery remained fairly unchanged, while for bentonite, axial elastic recovery decreased initially with increase in concentration from 2.5–10.0% and remained unchanged with further increase in concentration above 10.0%. Generally, as the crushing strength increases with concentration of binder, the elastic recovery tended to reduce. Elastic recovery is the measure of the tendency of pellets to relax or increase in dimensions after the release of the applied load. Hence, lower elastic recovery is preferred in the selection of binder. In this case, corn starch appeared to be the most preferred binder. Axial recovery ranging up to 85% of initial length and insignificant radial recovery ranging between 2.8 to 4.6%, which tends to reduce with increase in binder concenstration has been reported for compression of sawdust (Ajayi and Lawal, 1995).

3.4. Effect of Binder On Pellets Durability

Figure 6(d) shows the variation in the durability of the pellets. It was observed that the durability increased linearly as the concentration increased for bentonite and kaolin. For corn starch the durability was higher and remained unchanged with increase in concentration. The pellets stability or durability is the measure of its resistance against abrasive wears and impact during handling. It is the ability of the pellet to retain its shape and size form without disintegrating during handling. Hence, high value of durability is generally preferred in the selection of binder. In this case, corn starch appeared to be the most preferred binder. A general increase in the durability has been reported with the use of binding agents (Ajayi and Lawal, 1995; Chaplin, 1975).

3.5. Effect of Binder on Pellets Disintegration Time

The effect of the binding agent on disintegration time is shown in Figure 6(e). For corn starch, the disintegration time increased slightly with increase in concentration from 2.5-10.0% and increased rapidly with concentration above 10.0%. The disintegration time for kaolin and bentonite showed similar trend, with lower values compared to corn starch and fairly constant with increase in concentration. Disintegration time of 5.1, 1.7 and 10.4 min have been reported for paracetamol tablets with 4.0% concentration of Khaya gum, PVP and gelatin respectively (Odeku and Itiola, 2002; 2003). Similar values of 1.1 and 4.5 min have been reported for tablets formed with 10% concentration of yam starch and corn starch respectively (Odeku and Itiola., 1998).

3.6. Effect Of Binder On Specific Compression Energy

Figure 6(f) shows the variation in specific compression energy with concentration of the binders. It can be observed that for range of concentrations used, kaolin required the least energy input. At lower concentrations, less than 10%, bentonite required the highest energy input and the ranking of the value of compression energy was in the order: bentonite › corn starch › kaolin, while at concentration above 10% corn starch required the highest energy in order: corn starch › bentonite › kaolin. The energy requirement for pelletization generally ranged between 469.97 - 947.9 kJ/ton. For compressing grass and lucerne, Shepperson and Marchant (1978) observed a high range of specific energy requirements of 120 - 220 MJ/ton and for wafering of straw a range of 90 - 180 MJ/t was reported by Chaplin (1975). The observed values for the compression of the compost were generally lower than other published works. In terms of energy efficiency, kaolin with the least energy requirement is considered the best binder.

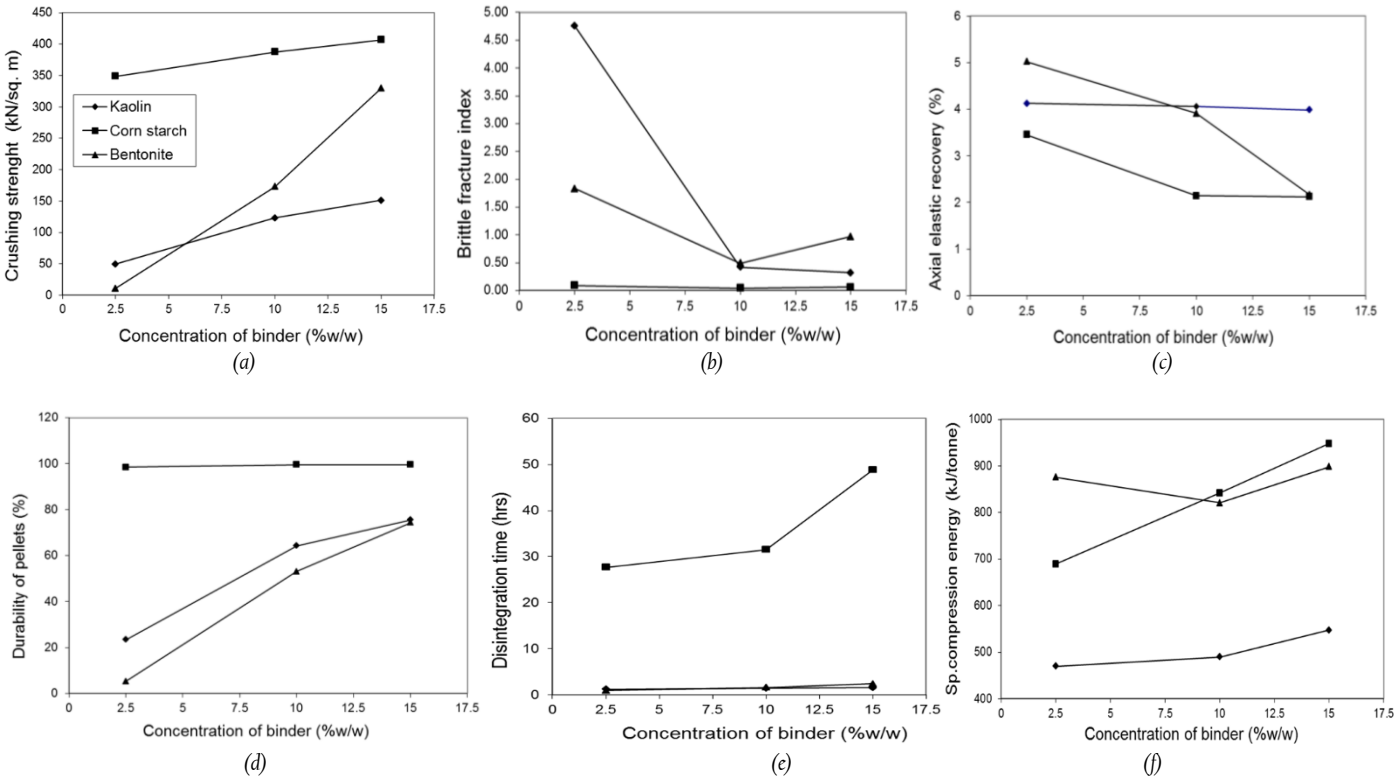

Fig. 6: Effect of binding agents on the properties of pellets: (a) crushing strength; (b) brittle fracture; (c) axial elastic recovery; (d) durability; (e) disintegration time and (f) specific compression energy requirement

3.7. Determination of Optimum Process Parameters

The optimum process conditions that gave the highest favourable magnitude of the properties are summarised in Table 6. The 90% confidence intervals for the predicted properties were 23.5, 16.5, 6.1, 18.8 and 5.3 for crushing strength, brittle fracture index, elastic recovery, durability and disintegration time respectively. Figure 5 shows the order of magnitude of influence of each factor on the properties. It showed that the type of binding agent had the greatest magnitude influence of 90.4% (Disintegration time), 67.9% (Crushing strength), 56.2% (Durability), 40.5% (Axial elastic recovery), and 85.5% (specific energy requirement),

3.8. Analysis of Variance (ANOVA)

The analysis of variance (ANOVA) of the factors on the properties of the pellets is shown in Table 5. The main effect plots of the factors on the pellet's mechanical properties are shown in Figure 6. It can be seen that variation in type and concentration of the binder agents had different effect on properties of the pellets. The relationships between the process variables (type and concentration of binder) and the mechanical properties of the pellet were modelled with the additive model (Phadke, 1989):

$$\Pr op = \overline{T}_i + \overline{C}_i - \overline{Q}, \quad i = 1\text{-}3 \tag{12}$$

Where, Prop is the predicted mechanical property, $\overline{T}_i$ is the mean of all the experimental data with type of binder at level i, $\overline{C}_i$ is the mean of all the experimental data with concentration of binder at level i, and $\overline{Q}$ is the overall mean of all the experimental data.

4. CONCLUSIONS

The effect of three artificial binders (kaolin, bentonite and corn starch) at three concentrations (2.5, 10 and 15% by weight) on the mechanical properties (crushing strength, brittle fracture index, axial elastic recovery, durability and disintegration time) of the organic fertilizer pellets have been investigated using L9 Taguchi orthogonal array. Based on the analysis of results obtained in the study, it can be the concluded that the type of binding agent has the greatest magnitude influence of 90.4% for disintegration time, 67.9% for crushing strength, 56.2% for durability, 40.5% for axial elastic recovery, and 85.5% for specific energy requirement. The order of magnitude of influence for crushing strength, axial elastic recovery durability and specific energy requirement was Type of binder › Concentration of binder › Error. For disintegration time the order was Type of binder › Error › Concentration of binder, while for brittle fracture index the concentration of binder has the highest magnitude of influence of 36.8% in the order Concentration of binder › Error › Type of binder. Corn starch was found to be the best binder for optimal properties of the pellets with optimal concentrations of 15% for crushing strength, axial elastic recovery, durability and disintegration time, and 10% for brittle fracture index. The trends observed suggest need for further works to confirm correlations.

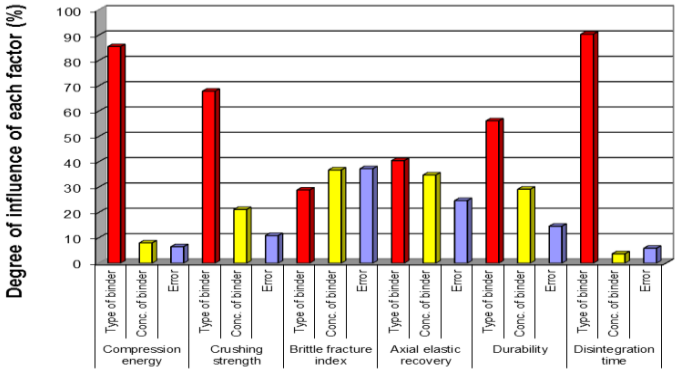

Fig. 7: Degree of influence of each factor on the mechanical properties of the pellets

Table 6: Optimum process conditions

Property	Optimum factor	
	Type of binder	Concentration of binder (%)
Crushing strength	Cornstarch	15
Brittle fracture index	Cornstarch	10
Elastic recovery	Cornstarch	15
Durability	Cornstarch	15
Disintegration time	Cornstarch	15
Specific compression energy	Kaolin	2.5

Table 5: Analysis of variance (ANOVA) for the properties of the pellets

Mechanical properties	Factors	SS	DOF	MS	F	P	DF (%)
Crushing strength	Type of binder	122751.8	2	61375.9	12.5		67.9
	Conc. of binder	38364.6	2	19182.3	3.9		21.2
	Error	19640.6	4	4910.1			10.9
Brittle fracture index	Type of binder	4.8	2	2.4	-		28.9
	Conc. of binder	6.8	2	3.4	-		36.8
	Error	6.9	4	1.7			37.3
Axial elastic recovery	Type of binder	3.6	2	1.8	3.3		40.5
	Conc. of binder	3.1	2	1.6	2.9		34.8
	Error	2.2	4	0.5			24.7
Durability	Type of binder	5129.4	2	2564.7	7.7		56.2
	Conc. of binder	2668.1	2	1334.0	4.0		29.2
	Error	1331.4	4	332.9			14.6
Disintegration time	Type of binder	2380.6	2	1190.3	30.4		90.4
	Conc. of binder	97.5	2	48.8	-		3.7
	Error	156.63	4	39.2			5.9

Key: SS- Sun of squares; DOF- Degree of freedom; MS- Mean square; F- ; P- Probability; DF(%)- Percentage degreed of influence of each factor

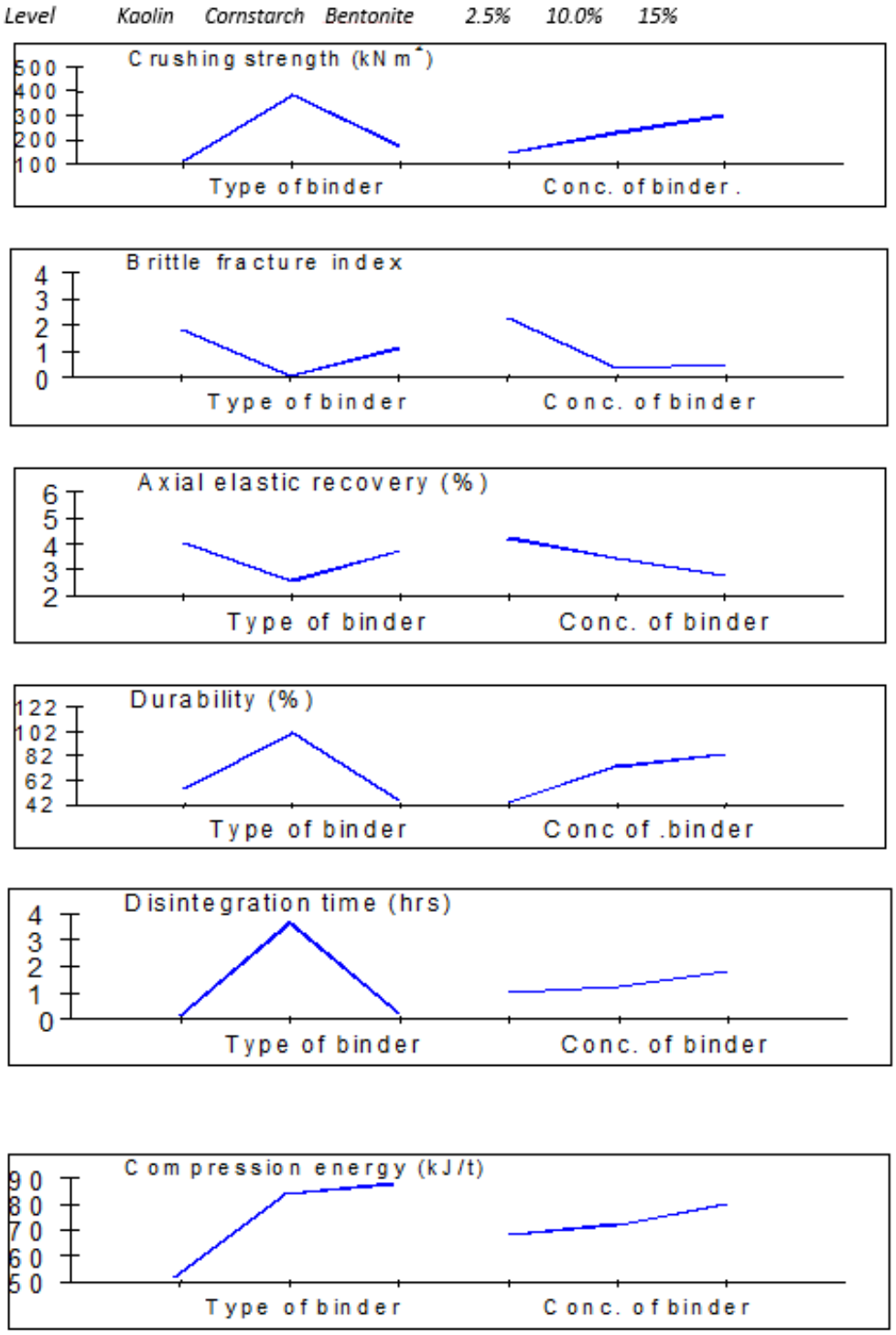

Fig. 8: Main effects plot of each factor on mechanical properties of the pellets

REFERENCES

Adebayo, A.S. and Itiola, O.A., "Evaluation of breadfruit and cocoyam starches as exodisintegrants in a paracetamol tablet formulation". Pharm. Pharmacol. Commun., 4: 385-389, 1998.

Ajayi, O.A. and Lawal, C.T., "Some quality indicators of sawdust/palm oil sludge briquettes", Journal of Agricultural. Engineering Technology, 3: 55-65. 1995.

Alexander, R., "Compost Marketing Guide", Alexander Associates, Inc., United States, 2003.

Arthur, E., Cornelis, W.M., Vermang, J. and De Rocker, E., "Effect of compost on erodibility of loamy sand under simulated rainfall", CATENA, 85(1): 67-72, 2011.

ASAE Standards, "America Society Agricultural Engineering Standards", St. Joseph, Mich. 45th Ed., 1998.

Battelle, "Compost supply and demand", A report of Environmental Services Industry, United State, 2012. Available at: http://www.faqs.org/abstracts/Environmental-services-industry/Compost-supply-and-demand-Using-compost-to-treat-wastewater-effluent.html#ixzz1Riza2FxM , Accessed January 2012.

Chaplin, R.V., Straw wafering tests. Department Note DN/FC/614/1390, National Institute of Agricultural Engineering, Silsoe, 1975.

Dobie, J.B. and Walker, H.G., "Effects of NaOH and NH_3 on cubality and digestibility of rice straw", Transactions of American Society of Agricultural Engineers, 20(6): 1018–1021, 1977.

Esengun, K., Erdal, G., Gunduz, O. and Erdal, H., "An economic analysis and energy use in stake-tomato production in Tokat province of Turkey", Renewable Energy,32: 1873-1881, 2007.

Faborode, M.O. and O'Callaghan, J.R., "Theoretical analysis of the compression of fibrous agricultural materials", Journal of Agricultural Engineering Research. 35: 175 – 191, 1986.

Fadare, D.A., "Development of an organo-mineral fertilizer processing plant", A Ph.D. Thesis of Department of Mechanical Engineering, University of Ibadan, Ibadan, Nigeria, Pp. 343, 2003.

Fadare, D.A., Bamiro, O.A. and Oni, A.O., "Energy analysis of an organic fertilizer plant in Ibadan, Nigeria", Journal of Research in Engineering, 6(2): 112-120, 2009.

Fadare, D.A., Bamiro, O.A., and Oni, A.O., "Energy and cost analysis of organic fertilizer production in Nigeria", The International Journal of Energy, 35(1): 332-340, 2010.

Gould, M.C., "Current practices and market demand potential for compost produced by small to medum sized farms in Michigan: a market research report", Extension Educator-Nutrient Management, Michigan State University Extension, 2012. Available at: www.newag.msu.edu/LinkClick.aspx?fileticket=W5nhJooXJm4%3D&tabid=37, Accessed January 2012.

John, N.M., Adeoye, G.O., Sridhar, M.K.C., "Compost pelletization eases end use in Nigeria", Biocycle, June 1996 p. 55-56, 1996.

Nevens, F. and Reheul, D., "The application of vegetable, fruit and garden waste (VFG) compost in addition to cattle slurry in a silage maize monoculture: nitrogen availability and use", European Journal of Agronomy, 19(2): 189-203, 2003.

O'Dogherty, M.J., "A review of the mechanical behaviour of straw when compressed to high densities", J. Agric. Engng. Res., 44: 241-265, 1989.

O'Dogherty, M.J. and Wheeler, J.A., "The effect of die, mode of loading and chopping on the compression of straw to high densities in closed cylindrical dies", Divisional Note DN/1103, National Institute of Agricultural Engineering, Silsoe, 1982.

Odeku, O.A. and Itiola, O.A., "Characterization of Khaya gum as a binder in a paracetamol tablet formulation", Drug Development and Industrial Pharmacy. 28(3): 329 – 337, 2002.

Odeku, O.A. and Itiola, O.A., "Evaluation of Khaya gum as a binder in a paracetamol tablet formulation", Pharm. Pharmacol. Commun. 4:183– 188, 1998.

Odeku, O.A. and Itiola, O.A., "Evaluation of the binding properties of khaya gum", A paper presented at the National Symposium on Pharmaceutical Technology, University of Ibadan. June 6–10, 1994.

Organic Monitor, "Quality of organic compost", United State, 2012. Available at: www.organicmonitor.com, Accessed January 2012.

Phadke, M.S. "Quality engineering using robust design", Prentice-Hall Int. Inc., US, pp 334, 1989.

Sæbø, A. and Ferrini, F., "The use of compost in urban green areas – A review for practical application", Urban Forestry Camp; Urban Greening, 4(3–4): 159-169, 2006.

Shepperson, G. and Marchant, W.T.B. "Production of grass and alfalfa cobs using an experimental ring die press", Proceedings of 2nd International Green Crop Drying Conference, Saskatoon, pp. 264–270, 1978.

Wealti, H. and Dobie, J.B., "Cubability of rice straw as affected by various binders", Transactions of American Society of Agricultural Engineers, 16(2): 380–383, 1973.

Weber, J., Karczewska, A., Drozd, J., Licznar M., Licznar S., Jamroz E. and Kocowicz A., "Agricultural and ecological aspects of a sandy soil as affected by the application of municipal solid waste composts", Soil Biology and Biochemistry, 39(6): 1294-1302, 2007.

Willer, H. and Kilcher, L., "The world of organic agriculture: statistics and emerging trends". Bonn; FiBL, Frick: IFOAM, 2011. Available at: www.organic-world.net. Accessed January 2012.

WinRobust "WinRobust version 1.02: User guide", 1995.

Full Paper

STUDIES ON THE THREE-STAGE DILUTE HYDROCHLORIC ACID OVEN LEACHING OF A LOW GRADE IRON ORE

J.O. Ajao
Department of Materials Science and Engineering
Obafemi Awolowo University, Ile-Ife.

A.A. Adeleke
Department of Materials Science and Engineering
Obafemi Awolowo University, Ile-Ife.
ade.adeleke0610@yahoo.com

K.E. Oluwabunmi
Department of Materials Science and Engineering
Obafemi Awolowo University, Ile-Ife.

ABSTRACT

Iron ore for use in the blast furnace are required to contain at least 63% Fe. The -63 µm fraction of Itakpe iron ore having 34.70% Fe was leached with dilute hydrochloric acid in single and multiple stages (with intermediate water washing) in the sequences H_2O-HCl-H_2O and HCl-H_2O-H_2O. The ore as-received and as-leached were also subjected to X-ray fluorescence analysis, while the efficiency of the concentration process was evaluated semi-quantitatively and quantitatively by weight loss % and changes in the chemical compositions obtained. The results obtained showed that the three-stage leaching of the iron ore in the sequence H_2O-HCl-H_2O at 0.375M dilute hydrochloric acid concentration produced the highest weight loss and yielded iron ore concentrate with 64.5% Fe, indicating a 85.9% upgrading of the Fe content. Similarly, the Si, Al, Ti, Ca, Na, Mg, K and P were reduced by 66.7, 75.8, 40, 96.6, 89.7, 90.1, 89.1 and 94.7 percents, respectively. The Fe content of the concentrate exceeds the 63% specification for the blast furnace use and is only 2.5% below the 67% required for Midrex direct reduction process. The very high reductions in the alkali oxides, phosphorous/sulphur are significant because of their negative roles in iron and steel making.

Keywords: *iron ore, leached, dilute acid, stages, concentrate*

1. INTRODUCTION

Iron is one of the largest eight elements in the earth's crust and is the fourth most abundant element at about 5% by weight. The main ores of iron include magnetite, hematite, limonite, goethite, siderite, pyrite and ilmenite (Silver, 1993). Nigeria has several deposits of iron ore found in Itakpe, Agbaja, Ajabanoko, Koton Karfe and Toto Muro. The Itakpe iron ore has a proven reserve of about 200 million tons and has been designated to supply sinter grade concentrates of 63% to 64% Fe for the blast furnace ironmaking at Ajaokuta The deposit extends approximately 3,000 m in length and includes about 25 layers of ferruginous quartzite. The deposit with an average iron content of approximately 35% is a banded iron formation containing a mixture of magnetite and hematite with ratio varying throughout the deposit (Adepoju and Olaleye, 2001; Umunakwe, 1985).

Elements such as phosphorous (P) and potassium (K), within the lower quality iron ore have detrimental effect on steelmaking process. The quality of iron ores have been improved by methods such as washing, heavy media separation, jigging, drying, flotation, magnetic and electrostatic concentration (Wills, 1992). Leaching is a widely used extractive metallurgy technique which converts metals into soluble salts in aqueous media. There are a variety of leaching processes, usually classified by the types of reagents used in the operation. The reagents required depend on the ores or pretreated material to be processed. Baba *et al* (2005) and (2007) studied the leaching dissolution of Itakpe iron ore using sulphuric and hydrochloric acids. The ore dissolution rate was found to be significantly influenced by temperature and acid concentration and only moderately by stirring speed and particle size. Model to predict the concentration of phosphorus removed relative to the initial and final pH of the leaching solution during leaching of iron oxide ore in sulphuric acid solution also has been derived (Nwoye *et al*, 2008). Adeleke (2011) developed a multistage leaching method with intermediate water leaching at the normal atmospheric pressure for the economic demineralization of selected coals.

The aim of this study is to determine the response of the low grade Itakpe iron ore to multistage leaching with dilute hydrochloric acid at the normal atmospheric pressure.

2. EXPERIMENTAL PROCEDURE

2.1. Materials

2.1.1. Iron ore sample preparation

About 5 kg of Itakpe iron ore was obtained from the bulk sample at the National Iron Ore and Mining Project, Itakpe, Kogi State, Nigeria. The ore was broken into sizes that could be fed into the jaw crusher using a sledge hammer. The sample was crushed in a laboratory dodge crusher and afterward ground in a laboratory ball mill model number Lf-b-32. Representative sample was then taken and air dried for about 48 hours.

2.2. Methods

2.2.1. Sieve analysis

About 150 g of the ore was placed in the uppermost sieve in a nest of sieves with standard apertures of 425, 300, 212, 150 and 63 µm. The loaded nest of sieves was then allowed to vibrate for about 15 minutes. Afterward, the sieves were taken apart and the amount of material retained on each sieve was weighed (Adepoju and Olaleye, 2001). The -63 µm fraction size that constituted the largest proportion of the Itakpe ore was selected for this study.

2.2.2. Single and multistage leaching

Firstly, a 6M dilute solution of hydrochloric acid was prepared by adding 100 ml of distilled water into 100 ml of the 12M BDH

Laboratories Limited concentrated hydrochloric acid solution. Afterwards, dilute solutions of 0.75, 1, 1.25 and 1.5M were prepared by serial dilution. For the single stage leaching, about 1 g sample of -63 µm size fraction was weighed and transferred into a 250 ml beaker containing 30 ml of 0.75M hydrochloric acid. The reaction mixture was stirred for 5 minutes and then covered with an aluminium foil. The mixture was then placed in the Gallenkamp 7B 16590 oven and heated for 1 hour at about 80°C. After heating, the solution was cooled in the oven for another 1 hour and then filtered into a conical flask using a Whatman filter paper. The residue was collected and oven dried at about 80°C and then re-weighed. The difference in weight was noted for determining the fraction of the iron ore that had been dissolved. The same procedure described was repeated for 0.0625, 0.125, 0.25, 0.375, 0.50 and 1M hydrochloric acid. The procedure was again repeated with 0.375M solution but for 45, 75, 90 and 105 minutes contact times. The latter test was further repeated but at 45, 65, 75, 85 and 95° C temperatures for 75 minutes.

For the three-stage step leaching, about 1 g of the -63µm size fraction was leached in 95° C for 75 minutes with 30 ml 0.375 M dilute hydrochloric acid and the residue filtered and dried as described in the single stage leaching. The procedure was repeated on the residue obtained from the first stage but with water. The latter water cleaning procedure was finally repeated as the third stage of the HCl-H_2O-H_2O sequence. The three stage leaching was further repeated but in the sequence H_2O-HCl-H_2O. The procedure described for the H_2O-HCl-H_2O and HCl-H_2O-H_2O sequences were further repeated but with 1.2 and 2.4 g of the iron ore to make 40 and 80 g/litre pulps.

The final residue of the two three stages routes that gave the highest percentage dissolution of gangue minerals was taken for X-ray fluorescence analysis and photomicrography under the light transmission microscope.

2.2.3. *X-ray fluorescence analysis*

About 0.5 g of the leached sample was pressed to obtain cylindrical pellets by the X-ray fluorescence spectrometer machine model HERZOG PW1606. Then, the pellets was mounted on the sample holder and each sample was irradiated for 20 minutes at a fixed tube operating condition of 25KV and 6MA.afterwards the results were displayed on the desktop computer which was connected to the X-ray fluorescence spectrometer.

3. RESULTS AND DISCUSSION

3.1. Results

The results of the XRF analyses carried out on the iron ore as-received and as-leached XRF are presented in Table 1, while Fig.1 shows the X-ray diffraction results on the as-received iron ore sample:

Table 1: Chemical Composition of Itakpe iron ore as-received (ar) and as-leached (al) by X-ray fluorescence analysis

Elements	-63 µm Itakpe iron ore (ar)	-63 µm Itakpe iron ore (al)	% Increase/ Decrease
Iron (Fe)	34.70	64.5	85.9
Silicon (Si)	20.10	6.70	-66.7
Aluminium (Al)	1.65	0.40	-75.8
Titanium (Ti)	0.10	0.06	-40
Calcium (Ca)	0.87	0.03	-96.6
Sodium (Na)	0.39	0.04	-89.7
Magnesium (Mg)	0.22	0.02	-90.1
Potassium (K)	0.55	0.06	-89.1
Phosporous (P)	0.95	0.05	-94.7
Sulphur (S)	0.03	Nd	-100

3.2. Discussion

The results obtained showed that an initial increase in leaching rate of Itakpe iron ore occurred with increasing molar concentrations of hydrochloric acid, the maximum being determined as – at 0.375M. The weight losses obtained might have been due to the dissolution of gangue mineral oxides in the ore. It is known that sodium oxide reacts exothermically with cold water to produce sodium hydroxide solution. As a strong base, sodium oxide also reacts with acids. For example, it reacts with dilute hydrochloric acid to produce sodium chloride solution. Also, magnesium oxide reacts with warm dilute hydrochloric acid to give magnesium chloride solution. Aluminium oxide is amphoteric and thus reacts as both a base and an acid. Aluminium oxide does not dissolve in water. The oxide ions it contains are held too strongly in the solid lattice to react with water (Hughes, 2012).

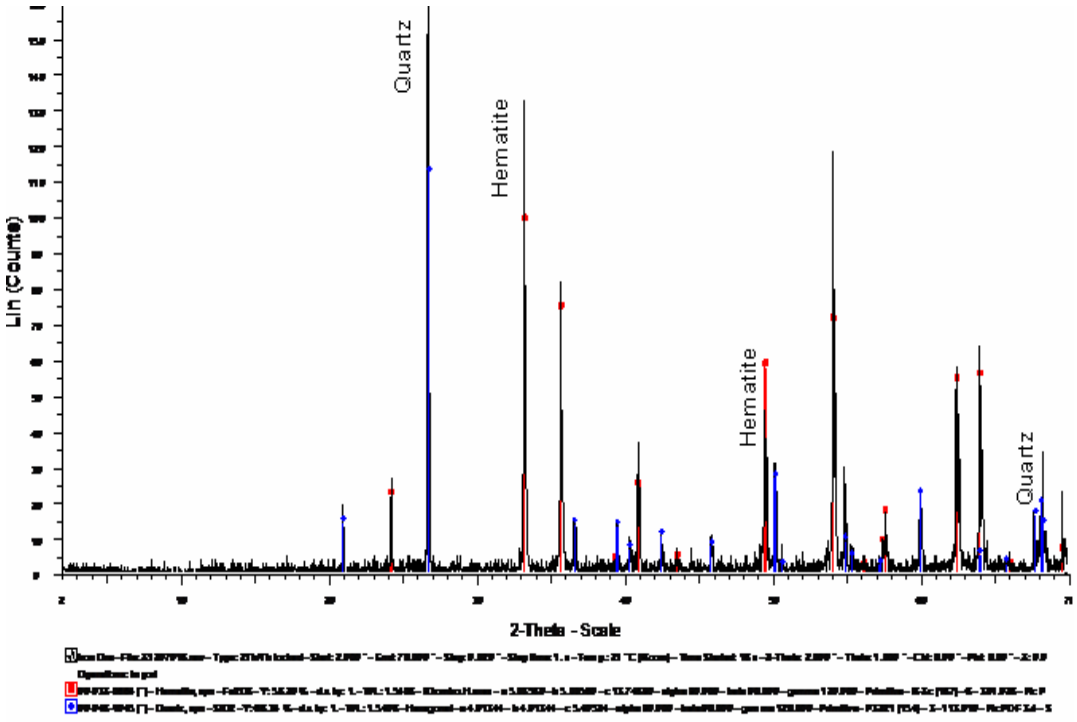

Fig.1: X-ray diffractogram of the iron ore as-received

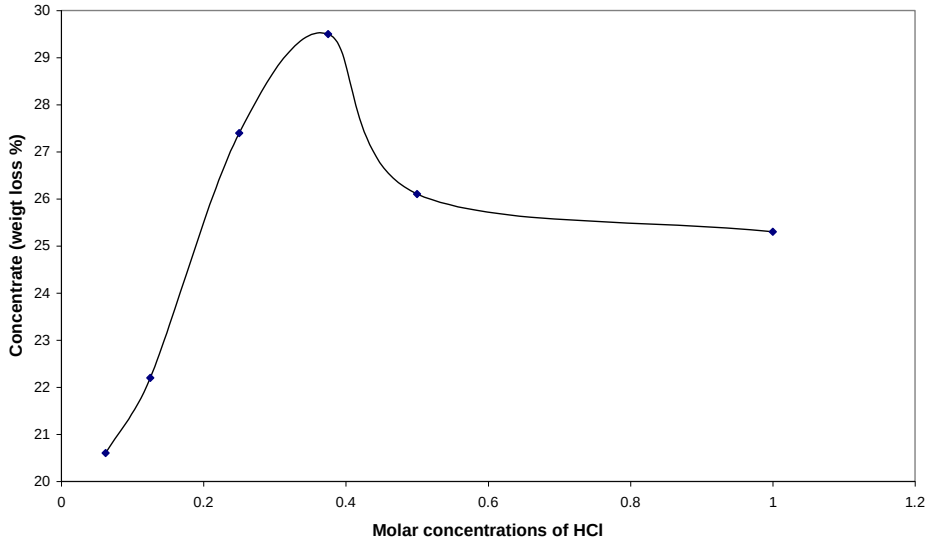

Fig. 2: Effect of HCI molar concentration on the one stage leaching rate of -63µm Itakpe iron ore sample

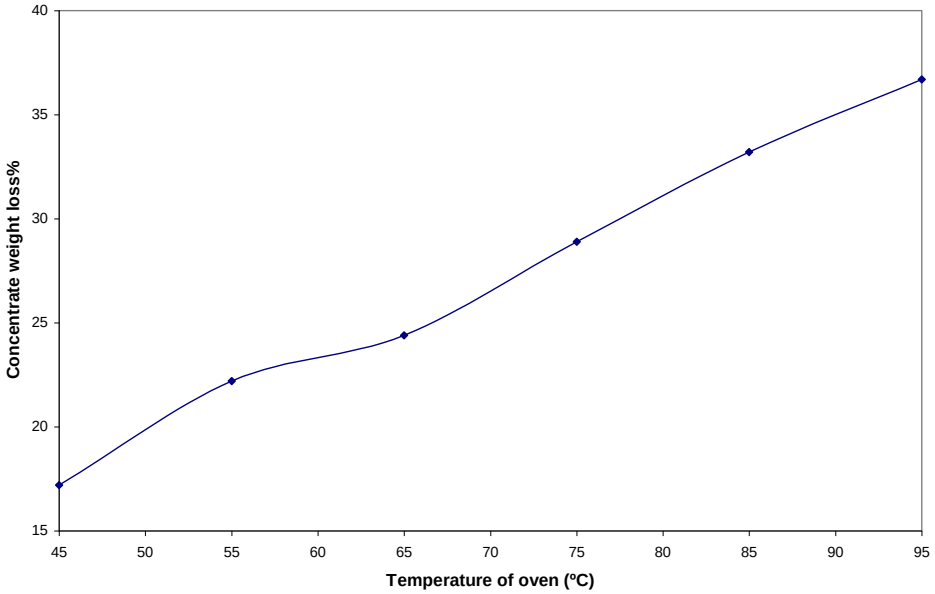

Fig 3: Effect of temperature on the one stage leaching rate of -63µm Itakpe iron ore sample

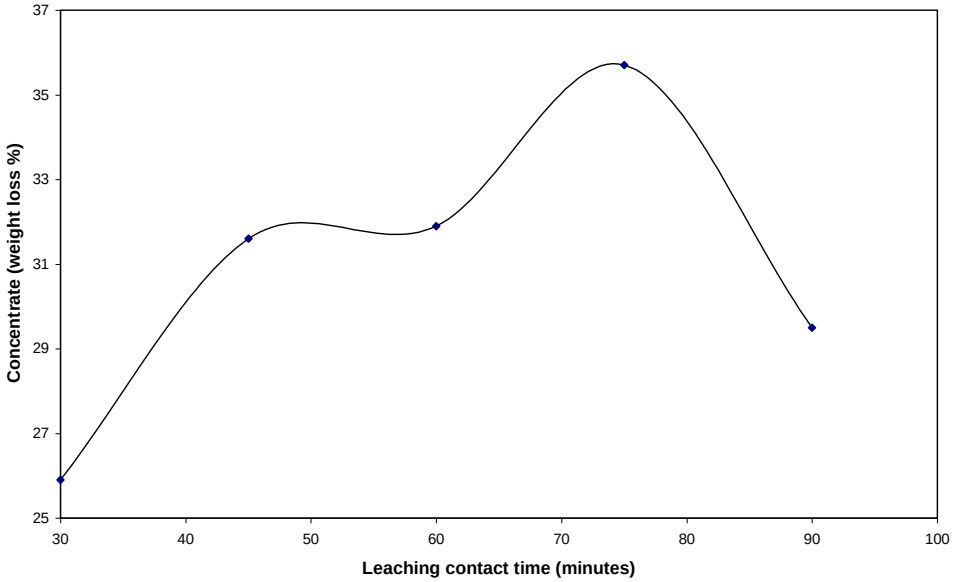

Fig 4: Effects of contact time on the one stage leaching rate of -63µm Itakpe iron ore sample

Since alumina contains oxide ions, it reacts with acids in the same way as sodium or magnesium oxide. For example, aluminium oxide reacts with hot dilute hydrochloric acid to produce aluminium chloride solution (Hughes, 2012). Phosphorus (V) oxide reacts violently with water to give a solution containing a mixture of acids. On the other hand, silicon dioxide has no basic properties and so it does not react with acids. Instead, it is very weakly acidic, reacting with strong bases. In addition, silicon dioxide does not react with water, because of the difficulty of breaking up the giant covalent structure. The decrease in leaching rate beyond the 0.375M hydrochloric acid concentration might be due to the precipitation of dissolved oxides at high concentrations of the acid leachant. An average ash oxides increase of +29.38% has been reported in the autoclave alkali leaching of a -75µm Illinois no. 5 coal sample under air/oxygen pressure at 150ºC with 0.2 M sodium carbonate in 1 hour. This result shows that very high concentrations of a leaching reagent may cause an increase in ash gangue content. (Chuang *et al*. 1983). Formation of potassium aluminosilicates has been shown to cause increased ash gangue content of Indian Makun coal on leaching it at 150ºC with potassium hydroxide (Mukherjee and Borthakur, 2003).

The results obtained further showed that the leaching rate of the Itakpe iron ore increased almost linearly with increasing oven temperature (Fig. 3). These results thus indicate that increasing temperature favours the dissolution reactions of the gangue oxides in the ore. The general increase in weight loss % with increasing temperature is due to the fact that at higher temperatures, rates of reactions are faster. Chemical equilibrium is therefore more likely to be closely attained in the entire macro-system than at lower temperatures (Ghosh and Ray, 1982). Also, when the temperature of the leaching reaction was increased, more heat was supplied to the heterogeneous system consisting of particles of the iron ore and the reagents. Since heat is a form of energy, part of the energy supplied caused an increase in the kinetic energy of the reagent molecules and this will increase their collision rates with the iron ore particles. Temperature has been described as being analogous to concentration when applying the Le Chatelier's principle to heat effect on a chemical reaction.

The results obtained also showed that leaching dissolution rate of the gangue oxides in the ore increase linearly with contact time at first and later non-linearly to reach a maximum at 75 minutes. The decrease in leaching rate beyond 75 minutes indicates that precipitations of dissolved gangue oxides might have occurred on prolonged heating of the leached solution. The leaching of calcium hydroxide was reported to be affected by leach contact time (Wang *et al*, 1996).

For the three-stage leaching, weight loss percents of 13.6, 14, 5.2 and 20.1, 4, 2.2 were obtained for the H_2O-HCl-H_2O and HCl-H_2O-H_2O leaching sequences for the three consecutive stages, giving total weight loss percents of 32.8 and 26.3, respectively;. The results obtained showed that though the first stage acid leaching at 33.3 g/litre produced a higher leaching rate than the first stage water leaching; the subsequent leaching of the product of the latter yielded much higher leaching rates than the product of the former. Leaching at higher pulp densities of 40 and 80 g/litre gave lower weight loss percents of 25.2, 21.3 and 24.6, 17.5 for the H_2O-HCl-H_2O and HCl-H_2O-H_2O leaching sequences, respectively. The results obtained further confirmed the leaching sequence H_2O-HCl-H_2O as better and also showed that the increase in pulp density from 33.3 to 80 g/litre only decreased the weight loss percent by 8.2 in the H_2O-HCl-H_2O leaching sequence. The results obtained thus strongly suggest that dilute hydrochloric acid leaching is an economic mean of upgrading the Itakpe iron ore for ironmaking. The analysis conducted on the H_2O-HCl-H_2O leaching sequence product at the 33.3% pulp density showed that the iron (Fe) content was increased to 64.5% implying an 85.9% upgrade, while the contents of Si, Al, Ti, Ca, Na, Mg, K and P were reduced by 66.7, 75.8, 40, 96.6, 89.7, 90.1, 89.1 and 94.7, respectively. The content of sulphur in the concentrate could also not be detected, implying an almost 100% sulphur removal from the ore. The increase of the Fe content to 64.5% makes the Itakpe iron ore suitable for the blast furnace ironmaking process (Raw Materials Specification, 1994), while the great reductions in the alumina and alkali oxide contents will improve the efficiency and productivity of the ironmaking process (Loison *et al*, 1989, Malzbender, 2003, Han and Meng, 1987).

4. CONCLUSIONS

The -63 µm fraction of Itakpe iron ore that constitutes the highest percentage of the ore has been successfully leached in three stages at atmospheric pressure, 0.375M sulphuric acid concentration and in H_2O-HCl-H_2O three-stage leaching sequence to obtain a concentrate assaying 64.5% Fe at 33.3 g/litre pulp density. The quantity of the deleterious alkali oxides and alumina were also greatly reduced making the concentrate obtained suitable for efficient ironmaking by the blast furnace route

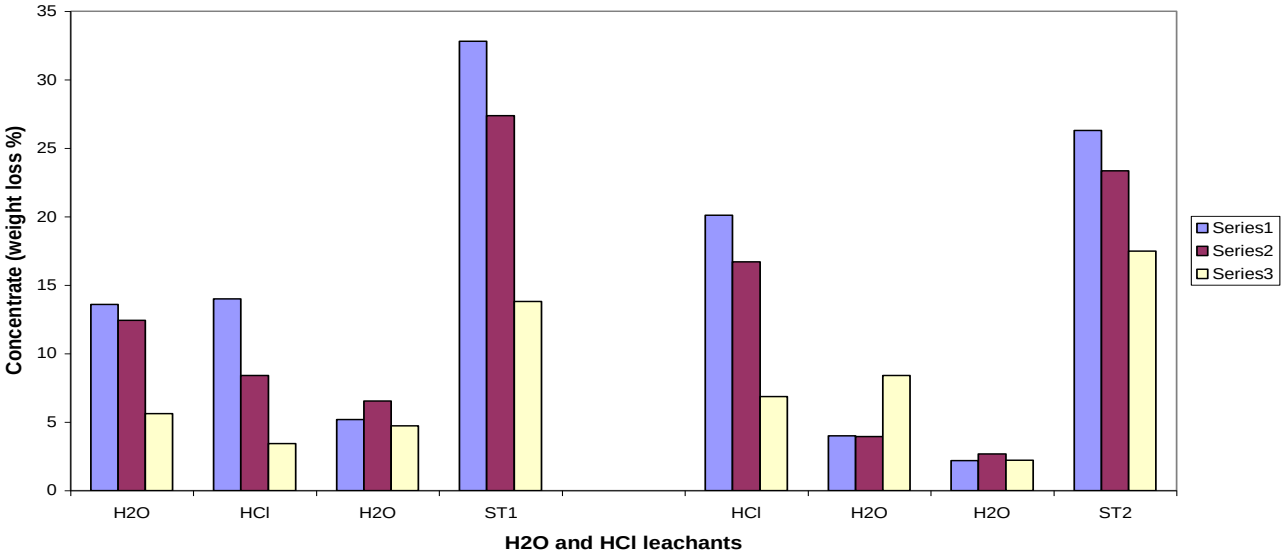

Fig. 5: Effects of leaching sequences H2O-HCl-H2O and HCl-H2O-H2O and solid-liquid ratios 33.3, 40 and 80 g/l on the three-stage leaching and total weight losses % (ST1 and ST2) for -63 µm Itakpe iron ore

REFERENCES

Adeleke, A.A., Development of a process route to upgrade selected coals for iron and steelmaking, Ph,D. Thesis, Department of Materials Science and Engineering, Obafemi Awolowo University, Ile-Ife, Nigeria, 2011.

Adepoju, S.O. and Olaleye, B.M., Gravity concentration of silica sand from Itakpe iron-ore tailings by tabling operation. *Nigerian Journal of Engineering Management* 2(2):51-55, 2001.

Baba, A., Adekola, F.A., and Lawal, A.J., Investigation of Chemical and Microbial Leaching of Iron ore in sulphuric acid. *Journal of Applied Science and Environmental Management*, 11(1):39 – 44, 2007.

Baba, A., Adekola, F.A., Folashade, A.O., Quantitative leaching of a Nigerian iron ore in hydrochloric acid. *Journal of Applied Science and Environmental Management* 9(3):15 – 20, 2005.

Chuang, K.C., Markuszewski, R. and Wheelock, T.D., Desulphurization of coal by oxidation in alkaline solutions. *Fuel Processing Technology*, 7:43-57, 1983.

Ghosh, A. and Ray, H.S., Principles of Extractive Metallurgy. John Wiley & Sons, New York, 1991.

Han, O. and Meng, O., Leaching of pyrite ore in hydrogen peroxide and sulphuric acid. *Hydrometallurgy*, 46:71–83, 1997.

Hughes, P., Oxides and hydroxides. http://www.rod.beavon.clara.net/oxides.htm, 29th February, 2012.

Loison, R., Foch, P, and Boyer, A., Coke quality and Production. Butterworths, 2nd Edition, London, 1989.

Malzbender, J., Comment on hardness definitions. Journal of the European Ceramics Society 23: 1355, 2003.

Mukherjee, S. and Borthakur, P.C., Demineralization of sub-bituminous high sulphur coal using mineral acids. *Fuel Processing Technology* 85(2):157-164, 2004.

Nwoye, C.I., Amara, G.N., and Onyemaobi, O.O. Model for Evaluating Dissolved Iron during Leaching of Iron Oxide Ore in Sulphuric Acid Solution. *International Journal of Natural Sciences* 4(2):209-211, 2008.

Raw Materials and products specifications. For Federal Government Steel Companies, Nigeria, p. 6, 1994.

Silver, J., Chemistry of iron. Blackie Academic and Professional Inc., New York, 1993.

Umunakwe P.U., Developing a new mine: The Itakpe case, Proceedings of the Annual Conference of Nigeria Mining and Geosciences Society, Jos, Nigeria, 1985.

Wang, J., Zhan-Guo, Z., Kobayashi, Y. and Tomita, A. Chemistry of $Ca(OH)_2$ leaching on mineral matter removal from coal, 1996. (http://pubs.acs.org/doi/abs/10.1021/ef9501307, 22nd September 2010).

Wills, B.A. Mineral Processing Technology. 5th Edition, Pergamon Press, New York, 1992.

Full Paper

STATISTICAL APPROACH TO ALCOHOLYSIS OPTIMIZATION OF SORREL (*HIBISCUS SABDARIFFA*) SEED OIL TO BIODIESEL AND EMISSION ASSESSMENT OF ITS BLENDS

E. Betiku
Biochemical Engineering Laboratory,
Department of Chemical Engineering, Obafemi Awolowo University,
Ile-Ife 220005, Osun State, Nigeria.
ebetiku@oauife.edu.ng

T.F. Adepoju
Biochemical Engineering Laboratory,
Department of Chemical Engineering, Obafemi Awolowo University,
Ile-Ife 220005, Osun State, Nigeria.

B.O. Solomon
National Biotechnology Development Agency,
16, Dunukofia Street, Area 11, Garki,
P.M. B. 5118 Wuse, Abuja, Nigeria.

ABSTRACT

In an effort to optimize the reaction conditions of biodiesel production from Sorrel seed oil, Response Surface Methodology (RSM) was applied and the effects of reaction temperature, catalyst amount, reaction time and methanol/oil molar ratio, and their reciprocal interactions were ascertained. A total of 30 experimental runs were designed by Central Composite Rotatable Design (CCRD) and carried out. A quadratic polynomial was obtained for predicting the transesterification process and the ANOVA test showed the model to be significant ($p<0.05$). The validity of the predicted model was established by carrying out three independent replicate experiments. The actual maximum Sorrel oil methyl ester (SOME) yield obtained was 99.23% (w/w) at methanol/oil molar ratio of 6.21, catalyst amount of 1.03 wt%, reaction temperature of 51 °C and reaction time of 63 min. The fuel properties of the SOME were found to be within the ASTM D6751 and DIN EN 14214 biodiesel standards. The fatty acid profile of the SOME revealed the dominant fatty acids were oleic (58.34%), palmitic (18.28%) and linoleic (21.19%). Emission assessment revealed 70% reduction of CO at B80 and 80% reduction of NO concentration at B40.

Keywords: *Biodiesel, Sorrel oil, Transesterification, Optimization, Response surface methodology*

1. INTRODUCTION

Fatty acid methyl esters (Biodiesel), which is considered as a substitute of convectional diesel is gaining ground as a biodegradable, non-toxic and environment-friendly fuel to neat diesel (Knothe et al., 2005; Demirbas, 2008). It is produced through a chemical process known as "transesterification or alcoholysis" in which there is displacement of alcohol from an ester under acidic or basic catalytic conditions producing free glycerol and the fatty acid esters of the respective alcohol (Knothe et al., 2007). Biodiesel is derived from renewable feedstock like vegetable oils or animal fats. Both edible and non-edible oils have been successfully employed in biodiesel production. In Nigeria, convectional diesel is produced mainly from crude oil; however, there are alternative oil-yielding crops which can be utilized as feedstocks, such as palm oil, *Moringa* oil, shea butter, *Jatropha* and coconut. Sorrel seed oil, a new competitor is emerging as a promising feedstock.

The Sorrel seeds are hard-pressed for oil and the residual cake is cooked, seasoned with *kambo*, a local condiment. Also in some parts of Africa, the bitter seeds are roasted and grounded into powder and is used in oily soup and sauces as a meal for human consumption (Ismail et al., 2008). The seeds are also used for their oil in china while in Malaysia the seeds are used to produce scrubs and soaps. Roasted Sorrel seeds have been used as coffee replacement that is said to have aphrodisiac properties (Duke, 1984). According to Omobuwajo et al. (2000), in northern Nigeria, the seeds are fermented into a condiment known as *Mungza ntusa*. In Sudan, the seeds are used for edible oil manufacture and the by-products of this process are used for poultry feeding (Al-Wandawi et al., 1984). However, in a commercial sense, this oil is not in current widespread use in Nigeria, having relatively few competing medicinal and food uses. Response surface methodology (RSM) is a useful statistical tool, which has been applied in research for optimizing various processes including transesterification reaction of vegetable oils: *Moringa oleifera* (Rashid et al., 2011), *Jatropha* oil (Tiwari et al., 2007) and cottonseed oil (Zhang et al., 2011) to mention a few. The main advantage of RSM is the ability to reduced number of experimental runs needed to provide sufficient information for statistically acceptable results. In this present study, an effort was made to optimize the process conditions for the transesterification step of Sorrel oil. Emission characteristics of the SOME in Internal Combustion (I.C.) engine were also investigated to determine its suitability.

2. METHODOLOGY

2.1. Extraction of Sorrel seed oil

The method of Betiku and Adepoju (2012) was employed for this study. Sorrel seeds were collected from Adamawa State, Nigeria. Chaffs were winnowed from the oilseeds and the cleaned oilseeds were milled into powder by grinding with plate machine. A 5-liter Soxhlet apparatus and n-hexane as solvent were used for the oil extraction.

2.2. Experimental design of SOME production

In this study, the central composite rotatable design (CCRD) was employed to optimize the SOME production. Five-level-four-factors design was applied, which generated 30 experimental runs. This included 16 factorial points, 8 axial points, and 6 central points to provide information regarding the interior of the experimental region, making it possible to evaluate the curvature effect. Selected factors for

the transesterification process from the Sorrel seed oil were reaction temperature (X1), catalyst amount (X2), reaction time (X3) and methanol/oil molar ratio (X4). The coded levels of the independent factors are given in Table 1. The experiments were randomizes to minimize the effects of unexplained variability in the observed response due to extraneous factors.

Table 1: Factors and Their Levels for Composite Central Design

Variable	Symbol	Coded factor levels				
		-2	-1	0	1	2
Reaction temperature (°C)	X_1	50	55	60	65	70
Catalyst amount (wt %)	X_2	0.7	0.8	0.9	1.0	1.1
Reaction time (min)	X_3	40	45	50	55	60
Methanol/oil ratio	X_4	4	5	6	7	8

2.3. SOME production procedure

Base catalyst transesterification reaction was applied for the SOME production, due to the low FFA value of the seed oil. A known weight of NaOH pellet was dissolved in a known volume of anhydrous methanol and was quickly transferred into the seed oil in the reactor and the reaction was monitored according to the design variables. At the completion of the reaction, the product was transferred to a separating funnel for glycerol and SOME separation. Glycerol was tapped off and the SOME left was washed with distilled water to remove residual catalyst, glycerol, methanol and soap. The washed SOME was further dried over heated $CaCl_2$ powder. The SOME yield was determined gravimetrically as described in Eq.1

$$SOME\ yield = \frac{weight\ of\ SOME\ produced}{weight\ of\ Sorrel\ seed\ oil\ used} \quad (1)$$

2.4. Statistical data analysis

SOME production data were analyzed statistically using RSM, so as to fit the quadratic polynomial equation generated by the Design-Expert software version 8.0.3.1 (Stat-Ease Inc., Minneapolis, USA). To correlate the response variable to the independent factors, multiple regressions was used to fit the coefficient of the polynomial model of the response. The quality of the fit of the model was evaluated using test of significance and analysis of variance (ANOVA). The fitted quadratic response model is given by Eq. 2.

$$Y = b_0 + \sum_{i=1}^{k} b_i X_i + \sum_{i=1}^{k} b_{ii} X_i^2 + \sum_{i<j}^{k} b_{ij} X_i X_j + e \quad (2)$$

where, Y is response factor (SOME), b_o is the intercept value, b_i (i= 1, 2,..., k) is the first order model coefficient, b_{ij} is the interaction effect, and b_{ii} represents the quadratic coefficients of X_i, and e is the random error.

2.5. Quality and fuel properties of SOME

Fuel properties namely, moisture content, specific gravity, kinematic viscosity at 40 °C, iodine value, acid value, saponification value, higher heating value, flash point, cloud point and cetane number of both Sorrel seed oil and SOME were determined following standard methods and compared with American and European standards (ASTM and DIN EN 14214).

2.6. Emissions Assesment

In order to test the suitability of the SOME produced in I.C engine as well as compare the emissions with that of neat diesel (AGO), B10, B20, B30, ..., B90 blends of pure SOME with AGO at different loads (0-2.7 kW) were used, 100% AGO and 100% SOME were burnt in succession and emissions such as CO and NO were measured with the aids of MutiRAE and ToxiRAE gas analyzers, respectively.

3. RESULTS AND DISCUSSION

3.1. Optimization of the transesterification step

Table 2 depicts the coded factors considered in this study with experimental results, predicted values as well as the residual values obtained. The highest SOME yield obtained was 99.30 % (w/w) at reaction temperature of 60 °C, catalyst amount of 0.90% (w/w), reaction time of 50 min and methanol/oil molar ratio 6:1. While the lowest SOME yield of 89.29% (w/w) was observed at reaction temperature of 60 °C, catalyst amount of 0.70% (w/w), reaction time of 50 min and methanol/oil molar ratio 6:1. Design Expert 8.0.3.1 software was employed to evaluate and determine the coefficients of the full regression model equation and their statistical significance. Table 3a shows the results of test of significance for every regression coefficient. The results showed that the p-value of the model terms were significant, i.e. $p < 0.05$. In this case, the four linear terms (X_1, X_2, X_3, X_4), five cross-products (X_1X_2, X_1X_3, X_1X_4,X_2X_3, X_3X_4) and the four quadratic terms (X_1^2, X_2^2 ,X_3^2 and X_4^2) were all remarkably significant model terms at 95% confidence level except X_2X_4. However, all other model terms were more significant than both X_4 and X_1X_2. In order to minimize error, all the coefficients were considered in the design. Table 3b shows the analysis of variance (ANOVA) of the regression equation. The model F-value of 361.87 implied a high significant for the regression model (Yuan et al., 2008). The goodness of the fit of a model was checked by the coefficient of determination (R^2). R^2 should be at least 0.80 for the good fit of a model (Guan and Yao, 2008). The R^2 of 0.9941 in this case indicated that the sample variation of 99.41% for SOME yield was attributed to the independent factors and only 0.59% of the total variation are not explained by the model.

Table 2: Central Composite Design, Experimental, Predicted and Residual Values for Five – Level-Four Factor Response Surface Analysis

Std order	X_1	X_2	X_3	X_4	Experimental value (w/w %)	Predicted value (w/w %)	Residual values (w/w%)
1	-1	-1	-1	-1	89.30	89.35	-0.050
2	1	-1	-1	-1	90.00	89.79	0.210
3	-1	1	-1	-1	93.92	93.87	0.050
4	1	1	-1	-1	94.79	94.86	-0.066
5	-1	-1	1	-1	90.90	90.87	0.031
6	1	-1	1	-1	90.17	90.21	-0.039
7	-1	1	1	-1	93.67	93.57	0.096
8	1	1	1	-1	93.56	93.47	0.091
9	-1	-1	-1	1	86.99	86.88	0.110
10	1	-1	-1	1	90.70	90.78	-0.084
11	-1	1	-1	1	91.20	91.15	0.051
12	1	1	-1	1	95.78	95.61	0.170
13	-1	-1	1	1	90.73	90.65	0.077
14	1	-1	1	1	93.61	93.46	0.150
15	-1	1	1	1	93.10	93.11	-0.013
16	1	1	1	1	96.54	96.48	0.062
17	-2	0	0	0	90.15	90.22	-0.072
18	2	0	0	0	93.88	94.02	-0.140
19	0	-2	0	0	89.29	89.39	-0.097
20	0	2	0	0	96.80	96.92	-0.120
21	0	0	-2	0	90.64	90.73	-0.093
22	0	0	2	0	93.00	93.12	-0.120
23	0	0	0	-2	91.00	91.06	-0.058
24	0	0	0	2	91.44	91.60	-0.160
25	0	0	0	0	98.49	98.91	-0.420
26	0	0	0	0	99.30	98.91	0.390
27	0	0	0	0	99.10	98.91	0.190
28	0	0	0	0	98.65	98.91	-0.260
29	0	0	0	0	99.07	98.91	0.160
30	0	0	0	0	98.87	98.91	-0.043

The value of adjusted determination coefficient (Adj. R^2 = 0.9962) was also very high, supporting a high significant of the model (Khuri and Cornell, 1987) and all p-value coefficients were less than 0.0001, which implied that the model proved suitable for the adequate representation of the actual relationship among the selected variables. The lack-of-fit term of 0.9589 was not significant relative to the pure error. The final equation in terms of coded factors for the response surface quadratic model is expressed in Eq. (3).

Table 3a: Test of Significance for Every Regression Coefficient CCRD

Source	Sum of squares	df	Mean Square	F-value	p-value
X_1	21.66	1	21.66	453.37	< 0.0001
X_2	85.05	1	85.05	1780.23	< 0.0001
X_3	8.54	1	8.54	178.84	< 0.0001
X_4	0.43	1	0.43	9.04	0.0088
X_1X_2	0.31	1	0.31	6.45	0.0227
X_1X_3	1.20	1	1.20	25.10	0.0002
X_1X_4	12.04	1	12.04	252.03	< 0.0001
X_2X_3	3.28	1	3.28	68.57	< 0.0001
X_2X_4	0.060	1	0.060	1.26	0.2800
X_3X_4	5.09	1	5.09	106.44	< 0.0001
X_1^2	79.07	1	79.07	1655.12	< 0.0001
X_2^2	56.91	1	56.91	1191.17	< 0.0001
X_3^2	83.68	1	83.68	1751.53	< 0.0001
X_4^2	98.67	1	98.67	2065.28	< 0.0001

Table 3b: Analysis of Variance of Regression Equation

Source	Sum of squares	df	Mean Square	F-value	p-value
Model	361.87	14	25.85	541.03	< 0.0001
Residual	0.72	15	0.048		
Lack of Fit	0.26	10	0.026	0.28	0.9589
Pure Error	0.46	5	0.092		
Cor Total	362.59	29			

R^2 = 99.40%, R^2(adj) = 99.62%

$$Y(w/w\ \%) = 98.91 + 0.95X_1 + 1.88X_2 + 0.60X_3 + 0.13X_4 + 0.14X_1X_2 - 0.27X_1X_3 + 0.87X_1X_4 - 0.45X_2X_3 - 0.061X_2X_4 + 0.56X_3X_4 - 1.70X_1^2 - 1.44X_2^2 - 1.75X_3^2 - 1.90X_4^2 \quad (3)$$

All the X_1, X_2, X_3, X_4, X_1X_2, X_1X_4 and X_3X_4 had positive effect on the SOME yield while the rest had negative influence on the yield (Table 4).

Table 4: ANOVA for Response Surface Quadratic Model for Intercept.

Factors	Coefficient estimate	df	Standard error	95%CI low	95% CI high	VIF
Intercept	98.91	1	0.089	98.72	99.10	-
X_1	0.95	1	0.045	0.85	1.05	1.00
X_2	1.88	1	0.045	1.79	1.98	1.00
X_3	0.60	1	0.045	0.50	0.69	1.00
X_4	0.13	1	0.045	0.039	0.23	1.00
X_1X_2	0.14	1	0.055	0.022	0.26	1.00
X_1X_3	-0.27	1	0.055	-0.39	-0.16	1.00
X_1X_4	0.87	1	0.055	0.75	0.98	1.00
X_2X_3	-0.061	1	0.055	-0.57	-0.34	1.00
X_2X_4	0.56	1	0.055	-0.18	0.55	1.00
X_3X_4	-1.70	1	0.055	0.45	0.68	1.00
X_1^2	-1.44	1	0.042	-1.79	-1.61	1.05
X_2^2	1.75	1	0.042	-1.53	-1.35	1.05
X_3^2	-1.90	1	0.042	-1.84	-1.66	1.05
X_4^2	98.67	1	0.042	-1.99	-1.81	1.05

In general, the 3D response surface plot is a graphical representation of the regression equation for the optimization of the reaction variables. Figure 1(a-f) described the 3D surfaces linked to the effect of two variables on the yield of SOME (biodiesel).

The curvatures nature of 3D surfaces in Fig. 1b, c and f indicated mutual interaction of the reaction time with reaction temperature, methanol/oil molar ratio with reaction temperature and methanol/oil molar ratio with reaction time, respectively. Meanwhile, there was a moderate interaction between methanol/oil molar ratio with catalyst amount and catalyst amount with reaction temperature, (Fig.1a and e), but no interaction was observed between reaction time and catalyst amount as represented in Fig.1d. The optimal condition predicted by the model were methanol/oil molar ratio 6.21, catalyst amount 1.03 (%wt.), reaction temperature 51 °C, and reaction time 63 min, which gave 99.71% (w/w). Using these optimal condition values for three independent experimental replicates, an average SOME yield of 99.23% (w/w) was achieved, which was within the range predicted by the model.

3.2. Quality and fuel properties of SOME

Table 5 shows the properties of the SOME in comparison with ASTM biodiesel and DIN EN 14214 standards. All the tested characteristics and fuel properties of the SOME satisfied both the ASTM D 6751 and DIN EN 1424 standards. Gas chromatography analysis of fatty acids present in the SOME is shown in Table 6. The results indicated that SOME was highly unsaturated. The dominant fatty acids were: oleic (58.34%), arachidic (1.55%), palmitic (18.28%) and linoleic (21.19%). The total unsaturated fatty acid composition of the SOME was 79.53%.

3.3. Engine performance of various SOME blends

The performance characteristics of SOME and diesel blends are shown in Fig. 2(a and b). For CO monitoring, the lowest values of the pollutant was observed at engine speed range of 1600-2000 rpm while the highest levels of the pollutant was observed at 600-1000 rpm. Whereas for NO monitoring, the lowest values of the pollutant was observed at 2100-2500 rpm and the highest levels of the pollutant was observed at 1100-1500 rpm. The results revealed 70% reduction of CO at B80 and 80% reduction of NO concentration at B40.

4. CONCLUSIONS

In this study, RSM was used to determine the effects of four reaction factors namely methanol/oil molar ratio, reaction temperature, catalyst concentration and reaction time on SOME yield in the transesterification of the Sorrel seed oil. The maximum SOME conversion yield was validated as 99.23% (w/w) at the reaction temperature of 63 °C, a catalyst amount of 1.03 wt %, methanol/oil molar ratio of 6.21 and reaction time of 51 min. The fuel properties of the SOME were within the ASTM D6751 and DIN EN 14214 specifications. Emission assessment revealed 70% reduction of CO at B80 and 80% reduction of NO concentration at B40.

Table 5: Properties of SOME in Comparison with Biodiesel Standards

Parameters	SOME	ASTM D6751	DIN EN 14214
Specific gravity@15 °C	0.882	0.86-0.90	0.85
Viscosity at 40 °C (cP)	5.80	1.9-6.0	3.5-5.0
Iodine value (g I_2/100g)	64.47	-	120 max
Acid value	0.24	< 0.80	0.5 max
Density (kg/m^3) at 25 °C	0.92	0.84	0.86-0.90
Saponification value (mg KOH/g oil)	148.49	-	-
Higher heating value (MJ/kg)	42.48	-	-
Diesel index	81.94	50.40	-
API	32.65	36.95	-
Cetane number	69.0	47 min	51 min
Aniline point	250.96	331.00	-
Pour point (°C)	-15	-	-
Cloud point (°C)	+5	-	-
Flash point (°C)	186	93 min	120 min

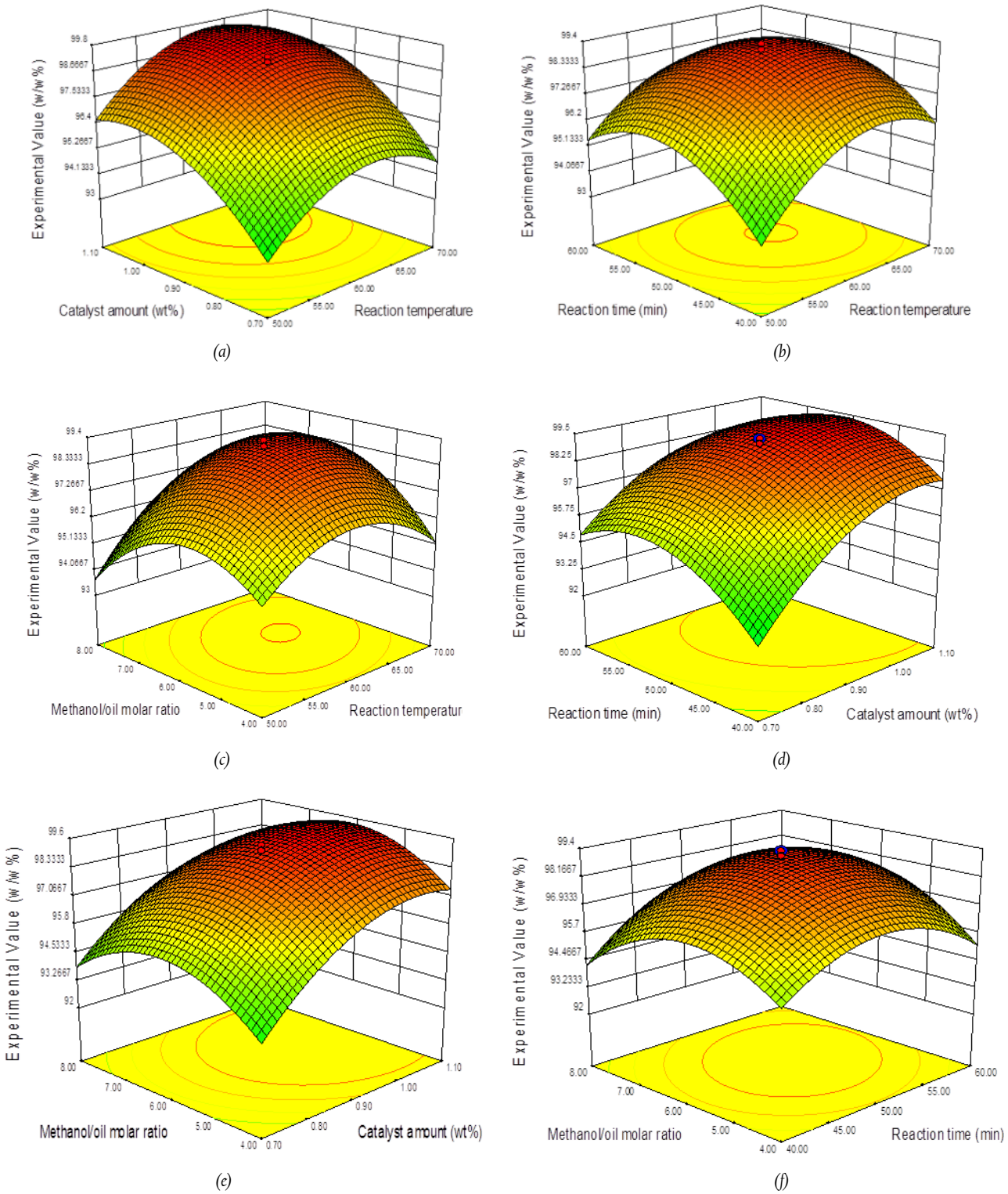

Figure 1: Response surface plots for SOME production

ACKNOWLEDGEMENTS

E. Betiku gratefully acknowledged equipment donation by the World University Service, Germany and provision of relevant literature by the DAAD. Technical supports offered by Mr. A.D. Oyinlola in SOME analysis and Dr. J.A. Sonibare in pollutants analysis are acknowledged.

REFERENCES

Al-Wandawi, H., Al-Shaikhaly, K. and Abdu-Rahman, M., Roselles Seeds: A Source of Protein. J. Agric. Food Chem. 32:510-512, 1984.

Bouanga-Kalou, G., Kimbongila, A., Nzikou, M., Ganongo-Po, F.B., Moutoula, F.B., Tchicaillat-Landou, M., Bitsangou, R.M., Silou, T.H. and Desobry, S., Chemical Composition of Seed Oil from Roselle (*Hibiscus sabdariffa* L.) and the kinetics of Degradation of the Oil during Heating. *JASET.* 3(2):117-122, 2011.

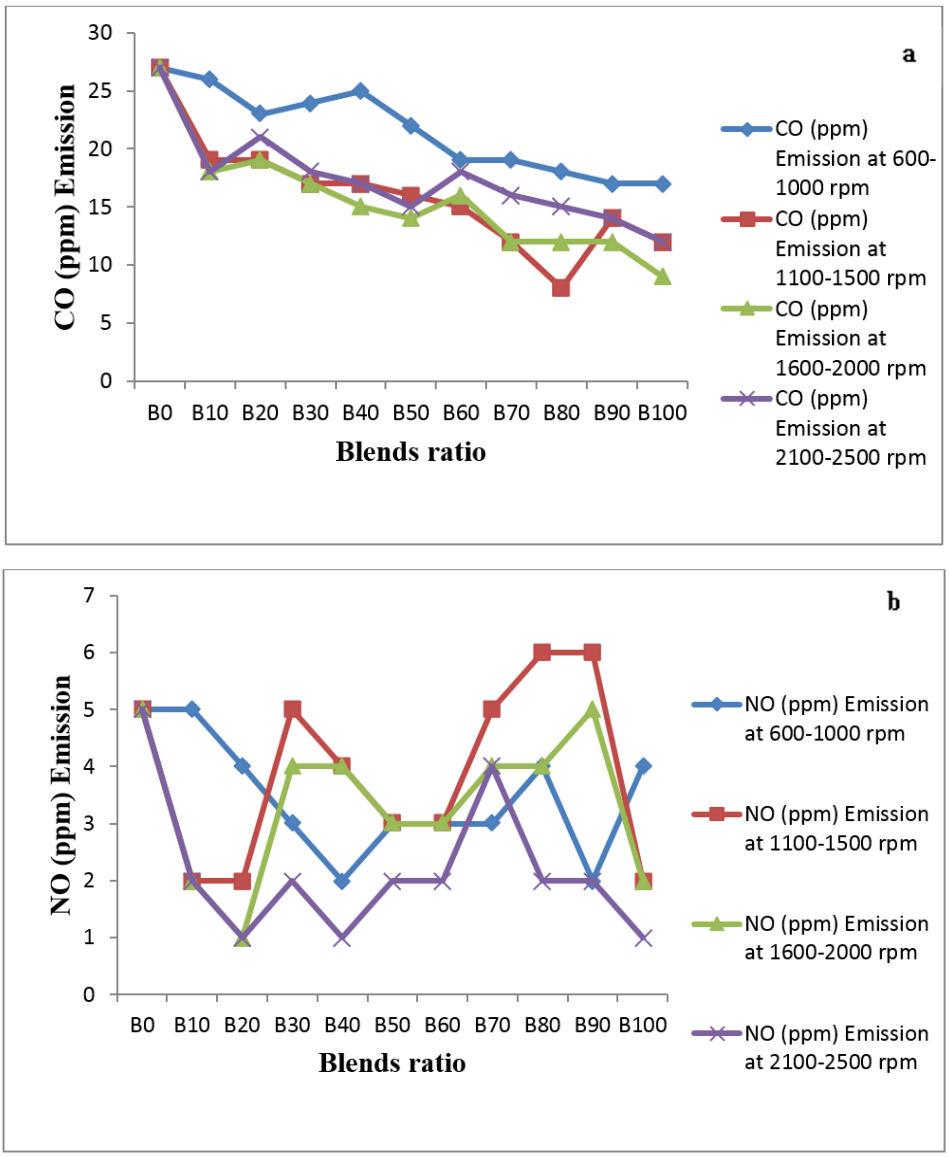

Figure 2: Plots of CO and NO Concentrations of SOME and diesel blends

Table 6: Fatty Acids Compositions of the SOME Produced

Fatty acid	Compositions %
Palmitic acid (C16:0)	18.280
Palmitoleic acids (C16:1)	0.055
Stearic acids (C18:0)	0.213
Oleic acids (C18:1)	58.337
Linoleic acids (C18:2)	21.194
Linolenic acid (C18:3)	0.165
Myristic acid (C14:0)	0.0943
Arachidonic acid (C20:4)	1.548
Other	0.114
Total	100

Emirbas, A., Comparison of Transesterification Methods for Production of Biodiesel from Vegetable Oils and Fats. *Energ. Convers. Manage.* 49:125–30, 2008.

Duke, J.A. and Atchley, A.A., Properties of Sorrel Seeds and its Compositions. ***J. Agric. Food Chem.*** 23:136-140, 1984.

Guan, X. and Yao, H., Optimization of Viscozyme L-assisted Extraction of Oat Bran Protein using Response Surface Methodology. *Food Chem.* 106:345-351, 2008.

Ismail, A., Ikram, E.H.K. and Nazri, H.S.M., Roselle *(Hibiscus sabdariffa* L.) Seeds–Nutritional Composition, Protein Quality and Health Benefits. *Foods* 2(1):1-16, 2008.

Khuri, A. I. and Cornell, J. A., *Response surfaces: design and analysis*. Marcel Dekker: New York, 1987.

Knothe, G., Krahl, J., and Gerpen, J.V., *The biodiesel handbook*. Champaign, IL: AOCS Press, 2007.

Nakpong, P. and Wootthikanokkhan, S., Roselle (*Hibiscus sabdariffa* L.) Oil as an Alternative Feedstock for Biodiesel Production in Thailand. *Fuel* 89: 1806–1811, 2010.

Omobuwajo, T.O., Sanni, L.A. and Balami, Y.A., Physical Properties of Sorrel (*Hibiscus sabdariffa*) seeds. *J. Food Eng.* 45:37-41, 2000.

Rashid, U., Anwar, F., Ashraf, M., Saleem, M., and Yusup, S., Application of Response Surface Methodology for Optimizing Transesterification of *Moringa oleifera* Oil: Biodiesel Production. *Energ. Convers. Manage.* 52:3034–3042, 2011.

Tiwari, A.K., Kumar, A., and Raheman, H., Biodiesel Production from Jatropha Oil (*Jatropha curcas*) with High Free Fatty Acids: An Optimized process. *Biomass Bioenergy* 31:569-575, 2007.

Yuan, X., Liu, J., Zeng, G., Shi, J. and Huang, G., Optimization of Conversion of Waste Rapeseed Oil with High FFA to Biodiesel using Response Surface Methodology. *Renew. Energ.* 33:1678-1684, 2008.

Zhang, X. W. and Huang, W., Optimization of the transesterification reaction from cottenseed oil using a statistical approach. *Energ. Sources* 33:1107-1116, 2011.

Full Paper

NUTRITIONAL EVALUATION OF COMPLEMENTARY FOODS PRODUCED FROM MALTED WHITE MAIZE AND SOY CONCENTRATE BLENDS

A.V. Ikujenlola
Department of Food Science and Technology
Obafemi Awolowo University, Ile- Ife
avjenlola@oauife.edu.ng

S.O. Oguntuase
Department of Food Science and Technology
Federal University of Technology, Akure

ABSTRACT

Complementary foods are foods given to infant in addition to breastmilk as from the 4-6th month of age. White maize grains were malted to produce malted maize flour.Soybean seeds were processed into soyconcentrate. The resulting flours were formulated at the ratio of 70:30 (maize product : soybean product) for complementary foods' production.The resulting complementary foods were assessed for proximate composition and protein quality assessment using animals feeding experiment . The results showed that protein content of the processed maize increased with soyconcentrate supplementation. The protein contents (18.10 - 25.30%) of the supplemented diets were significantly higher ($p<0.05$) than that of the commercial diet (control) (15.00%).There was no significant difference ($p >0.05$) between the proximate parameters of processed maize supplemented with similar additives. The malted maize based diet gave better growth and high Protein Efficiency Ratio (PER) and food efficiency ratio than the unmalted maize diets. The PER ranged between 1.46 and 2.38 for all the formulated diets. The biological value,true digestibility and net protein utilization were of higher values with respect to the supplemented diets and compared favourably with the commercial diet and casein. The malted maize and soyconcentrate blend is superior ($p<0.05$) to the commercial diet (control) diet.The blend of malted maize and soyconcentrate could be produced by mothers and caregivers; fed to infants in order to reduce the prevalence of protein energy malnutrition in the developing countries.

Keywords: *Complementary foods, maize, soyconcentrate, malted, biological assessment, protein efficiency ratio,*

1. INTRODUCTION

Exclusive breastfeeding for the first 6 months and continued breastfeeding with appropriate complementary feeding for up to 2 years and beyond is recommended by the World Health Organization (WHO,1998). Complementary feeding period is the time when malnutrition starts in many infants contributing significantly to the high prevalence of malnutrition in children under 5 years of age worldwide (Anigo *et al*., 2010). Many factors contribute to the vulnerability of children to malnutrition during the complementary feeding period. In most developing countries, the prevalence of malnutrition during the complementary feeding is attributable not only to inadequate amounts of food but also to the poor nutritional quality of the available food supply (Hotz *et al*., 2007; Brown, 1991).

Infants generally show symptoms of protein energy malnutrition (PEM) during their early stage of life when family foods are introduced to complement the breast milk. Most of the foods that are offered to the infants are not hygienically produced which may result to intoxication, while some have the problem of high dietary bulk which makes feeding difficult and cumbersome for some mothers and causing choking in babies (Desikachar,1980; Ikujenlola and Fashakin, 2005). The nutritional quality of the food in terms of the protein and other nutrients is of major concern because some of the home made diets are made from cereals as the sole protein source. Cereals are regarded as incomplete protein due to the fact that cereals generally lack lysine and tryptophan. These problems are responsible for high infantile mortality in many developing countries Nigeria inclusive where maize is a major staple (Obayanju and Ikujenlola, 2002; Adelekan, 2003).

Maize (*Zea mays*) is a cereal crop which is grown in every part of Nigeria and it has a very high yield. Because of its abundance, it is usually utilized in the production of various food items for both adults and infants. The common product used as complementary food among the low income earners is called "ogi" which is produced by soaking, wet milling, wet sieving and settling (Inyang and Idoko, 2006). This product has been reported to contain very poor protein quality and cannot support growth of rats as well as children (Ikujenlola, 2004; Ghasemzadeh and Ghavidel 2011; Ikujenlola, 2010). Soy beans (*Glycine max*) a leguminous crop is known to be of good quality protein, its protein quality compares well with that of animal origin. It has been utilized in the production of soy milk, soy flour, soy isolate, soy concentrate e.t.c.(Iwe, 2003). Because of the protein quality of soy bean it could be used to supplement the inadequate protein present in maize in order to produce diet of high nutritional quality; that could maintain a healthy living and support growth among the infants. The objectives of this study were to produce nutritious complementary food from malted white maize and soy bean, and to assess its nutritional quality using animal feeding experiment.

2. MATERIALS AND METHODS

The white maize grains and soy bean seeds used were purchased from the International Institute of Tropical Agriculture, Ibadan, Nigeria.

2.1. Methodology

2.1.1. Production of Malted Maize and Unmalted Maize Flours

The maize grains were cleaned by sorting and floatation processes to remove dirts and extraneous materials. The grains were washed thoroughly and soaked for 8 hours to moisten the grains to increase the moisture content to about 40% . The moistened grains were spread in the germinating chamber at about 1.5cm loading depth

and allowed to sprout for a period of 72 hours with watering every 12 hours. The germinated grains were washed and dried in a cabinet dryer at 60 ^{0}C for 20 hours. The dried sprouts were de-vegetated to remove the rootlets and plumules. The de- vegetated grains were milled, sieved (60 mesh), packaged and stored in a refrigerator until needed (Ikujenlola,2004; Marero *et al*.,1988). The unmalted maize flour was produced from cleaned grains by milling and sieving(60 mesh), packaging and stored in a refrigerator until needed (Ikujenlola, 2010). Figure 1 shows the unit operations involved in the production of malted maize and unmalted maize flours.

2.1.2. Production of Soybea full fat and Soy concentrate flours

Soy bean full fat flour was produced from soy bean seeds that were cleaned of all extraneous materials by winnowing and hand sorting. The seeds were soaked in warm water for 2 hours, thereafter the seeds were dehulled, cooked for 2 hours (to destroy the anti-nutrition factors), drained, washed in fresh water and dried (in cabinet dryer for 12 hours at 60 ^{0}C) milled and sieved.

The soy concentrate was produced from a portion from the soy full fat flour which had been defatted using solvent (hexane), and thereafter by dissolving the defatted soy flour in 60% alcohol solution to remove water soluble carbohydrates and other oligosaccharides responsible for flatulence. The meal from the extraction was dried and packaged for further utilization. Figure 2 shows the flow diagram for Soy full fat flour and soy concentrate production (Iwe, 2003).

2.1.3. Determination of Chemical composition of the blends

The chemical composition of the blends was determined by the standard methods of A.O.A.C. (1990). The parameters determined were protein (Kjeldahl method; N x 6.25), fat (Soxhlet extraction), ash, crude fibre, moisture content, carbohydrate (by difference) and energy {Atwater factor (9 x fat) + (4 x protein) + (4 x carbohydrate)} Kcal.

2.1.4. Biological evaluation of the complementary diets

For this study, forty albino (wistar var.) rats between three and four weeks of age were used. They were weighed, randomly distributed in metabolic cages and were adapted to the basal diet over a period of five days. After this period of acclimatisation the animals were re-weighed and re-grouped. The average weight per group was approximately the same (zero block design). The animals were fed with the experimental diets for a period of 28 days. Water was supplied *ad libitum*. During this period, dietary intake and growth were recorded. The urine and faecal discharge were collected appropriately. After the completion of the experiment the animals were anaesthetized and sacrificed. Tissue specimens were obtained and weighed. The data collected during feeding trial were used in computing the protein quality parameters (protein efficiency ratio, feed efficiency ratio, biological value, true digestibility, net protein utilization) (Dahiya and Kapoor, 1993; Ikujenlola and Fashakin,2005; Ikujenlola, 2010).

2.1.5. Formulation of various blends

The complementary diets were produced by blending the maize products (maize flour and malted maize flour) and soy products (soy full fat and soy concentrate) separately at a ratio of 100:0 and 70:30 respectively according to FAO/WHO(1985).

2.1.6. Basal diet formulation

The basal diet was patterned after the basal diet composition reported by Fashakin and Unokiwedi (1993).

2.1.7. Statistical analysis

Experimental results were subjected to analysis of variance. The level of significance was determined according to the method of Alika (1997).

Table 1: Basal diet formulation

Component	g/kg
Corn Starch	800
Vegetable Oil	100
Sugar	60
Mineral Salt	10
Vitamin mix	10
Salt	15
Cod Liver Oil	5
Energy (Kcal)	438.50

Source: Fashakin and Unokiwedi (1993)

3. RESULTS AND DISCUSSION

3.1. Proximate composition of the diet

Table 2 shows the proximate composition of the diets formulated from maize products (unmalted and malted) and soy bean products (full fat and concentrate). There was no significant difference ($p > 0.05$) in the proximate parameters of the processed maize to which similar additives have been added. The protein content ranged between 10.70 (Unmalted maize) and 25.30% (Malted maize + Soy concentrate). The addition of soy products increased the level and quality of protein of the fortified maize diets. Soy concentrate contains over 60% crude protein with improved amino acid profile (Iwe, 2003). The complementary effect of the protein (amino acids) in the soy bean and maize will no doubt be of valuable advantage to the end user of the formulated diets that is the infants. Since the sulphur bearing amino acids – methionine is abundant in maize but insufficient in legumes (soy bean) generally while the soy bean will make up for the inadequate quantity of lysine and tryptophan in maize (Ghasemzadeh and Ghavidel, 2011)

In infant nutrition, the quantity and quality of protein are of high importance, food that are high in protein are expected to be of reasonable quality in terms of essential amino acid. The protein content of the samples containing soy concentrate were significantly higher ($p < 0.05$) than that of the commercial diet.

Table 2: Proximate composition of formulated diets (%)

Sample	Moisture Content	Protein	Fat	Crude fibre	Ash	Carbohydrate	Energy (Kcal)
Maize flour	8.95^{b}	10.70^{d}	5.62^{c}	2.69^{cd}	2.25^{bc}	69.79^{a}	372.54^{b}
Malted Maize flour	8.78^{b}	11.50^{d}	6.02^{c}	3.13^{c}	2.64^{b}	67.93^{a}	371.90^{b}
Maize flour + Soyfull fat	9.55^{a}	18.12^{b}	8.53^{a}	3.30^{c}	2.98^{b}	57.52^{b}	379.33^{b}
Malted maize flour + Soy full fat	7.65^{c}	18.10^{b}	8.24^{a}	2.98^{c}	2.30^{b}	60.73^{bc}	389.48^{a}
Maize flour + soy Concentrate	9.35^{a}	24.26^{a}	5.93^{c}	7.80^{ab}	2.01^{b}	56.65^{d}	377.01^{b}
Malted maize flour + Soy Concentrate	9.61^{a}	25.30^{a}	6.15^{c}	2.20^{d}	1.90^{b}	54.84^{d}	375.91^{b}
Control	8.59^{b}	15.00^{b}	9.00^{a}	4.00^{b}	5.00^{a}	58.41^{b}	374.64^{b}

Means of the same column followed by different letters are significant ($p < 0.05$)

The addition of soy full fat flour to the maize flour increased the fat content however, the addition of soy concentrate did not increase the level of the fat owing to the fact that soy bean flour was defatted during soy concentrate production. The fat content was below 10% for all the samples while the commercial diet was 9.00% fat, high fat level is associated with ranscidity and it promotes off flavour during prolong storage. The recommendation of PAG (1971) was that fat content of diet meant for infant should not be more than 10%. This is to prevent the occurrence of off flavour and change in taste.

There was no significant difference (p › 0.05) between the ash contents of the diets except in the control. The ash content indicates the level of mineral content of the product. The control had the highest crude fibre (5.00 %) compared to the other samples. The carbohydrate ranged between 54.84 and 69.79 %. The estimated energy derivable from the diet ranged between 371.90 and 389.48kcal. The energy value of the control was 374.64 kcal.

The moisture content ranged from 7.65 to 9.61%. The moisture content was less than 10% in the all the samples. The lower the moisture content of the product the better; to prolong the shelf-life especially in rural areas where storage facilities may not be available. Higher moisture content encourage caking of floury product (Onuorah and Akinjide, 2004; Owolabi *et al*., 2012).

3.2. Animal Feeding Experiment

The feed intake ranged between 165.5g (basal diet) and 208.5g (Commercial - Control diet). The highest feed was consumed by the groups fed on the malted maize based diet and control groups. The least feed (165.5g) was consumed by the group fed with basal diet. The feeding trials of the diets showed that the dispositions of the experimental animals to the diets varied. The disposition of rats fed with the malted maize-soy concentrate blend and Commercial - control diet groups were better compared to the rats fed with other formulated diets; they were more agile and increased in weight. The group of rats fed with basal diet were reducing in weight and did not exhibit similar agility seen in the other groups during the period of feeding trials. Ikujenlola and Fashakin (2005) reported similar observation about the inability of basal and unsupplemented maize diets to support growth. According to Wardlaw (2000) lack of protein in responsible for weight reduction which is otherwise referred to as stunted growth and if this persist death can be the last result.

Figure 3 shows the changes in the growth weight of experimental rats during the period of feeding trial. The data showed that malted maize based diet had better growth and higher overall weight increase than unmalted maize based diet. Although the addition of soy full fat to maize enhanced the growth of the rats better than those diets which contained no soy supplement; the addition of soy concentrate to malted maize further boosted the rate at which the diet enhanced the rats' growth. Malting according to Marero *et al.*(1988) and Sajilata *et al.*(2002) enhanced the level of protein and this invariably improves the growth and tissue development of animal and man. The observation in this result showed the complementary effect of both soy bean and maize especially as it affects the protein quality of the supplemented diets. This result also confirm the inability of maize flour as sole protein source to support adequate growth.

There was no significant difference (p ›0.05) between the muscle tissue (Table 3) of the experimental rats fed with the various formulated diets except the basal and maize flour samples. The weights of the kidney and liver followed a similar trend as observed in the muscle tissue. The weight of the various organs of the experimental rats revealed the influence of the various formulated diets on the size of the organs. These organs are required for various metabolic processes of the body. Table 3 shows the weights of the various organs from the experimental rats. The weights of the organs from the formulated diets compared favourably with those of the control diet, however the weights of similar organs reported by Ikujenlola (2010) were bigger.

The Protein Efficiency Ratio (PER) and Food Efficiency Ratio (FER) of the diets are presented in Table 4. The PER ranged between (1.46 - 2.38) for the formulated diets. The PER is one of the methods of measuring the quality of protein in foods. The PER of diets supplemented with processed soybean had PER above 2.00 which showed no significant difference (p ›0.05) from that of commercial-control diet. It has been reported earlier that maize protein is regarded as incomplete because it lacks lysine and tryptophan this is confirmed with the low PER in the diets to which no soy bean was added. Low PER accounts for the inability of the diets to support growth, at best the weight could be maintained for sometimes however, the growth diminished after a while. Howbeit, the inclusion of processed soy bean enhanced the growth of the experimental rats as observed in the study (Fig.3). Soy bean according to Iwe (2003) contain protein of high quality in terms of amino acids. The results of PER in this study compared well with the reports of Malleshi *et al.* (1989) who prepared weaning food from malted ragi and green gram (7:3) with PER 2.2. Also the PER of 2.13 – 2.58 was reported by Gupta and Sehgal (1992) for bajra, barley, green gram and amaranth blends, while Ikujenlola (2010) reported 2.1- 2.43 for processed quality protein maize - soy bean blends. The PAG (1971) recommended PER of 2.1 for diet meant for complementary feeding for infants. The PER of malted maize supplemented with soy bean products and the control were higher than the recommended value.

The FER (Table 4) ranged between 0.15 and 0.24 for all the formulated samples. The least value for feed efficiency came from the group of rats fed with unmalted maize diet while the highest value was found in the group of rats fed with malted maize supplemented with soy concentrate diet. The well-being of infant depends majorly on both the quality and quantity of food stuff they consume (Ghasemzadeh and Ghavidel, 2011; Ikpeme-Emmanuel *et al*.,2009). When both conditions are not met malnutrition result. According to Ojofetimi *et al.* (2001) malnutrition is responsible high percentage of death in the developing countries.

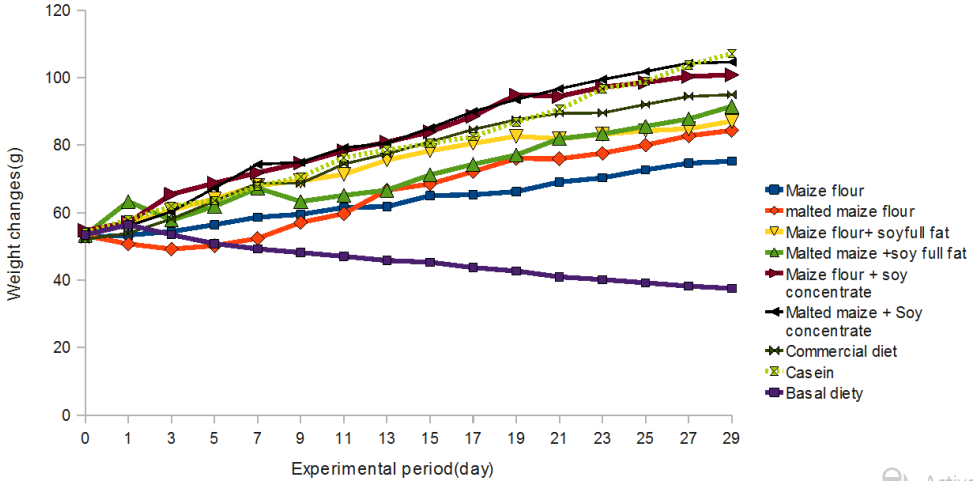

Fig. 3: Growth performance of the experimental animals

Table 3. The Mean Weight of Selected Organs of the Experimental Animal (g)

Sample	Muscle	Kidney	Liver
Unmalted Maize flour	0.16^{c}	0.14^{c}	0.14^{b}
Malted Maize flour	0.20^{b}	0.17^{ab}	0.20^{a}
Unmalted Maize flour+Soyfull fat	0.20^{b}	0.17^{ab}	0.20^{a}
Malted maize flour + Soy full fat	0.20^{b}	0.15^{b}	0.18^{a}
UnmaltedMaize flour + Soy Concentrate	0.28^{a}	0.20^{a}	0.20^{a}
Malted maize flour + Soy Concentrate	0.24^{a}	0.17^{b}	0.19^{a}
Commercial diet	0.19^{ab}	0.19^{a}	0.18^{a}
Casein	0.28^{a}	0.18^{a}	0.19^{a}
Basal diet	0.15^{c}	0.11^{c}	0.14^{b}

Means of the same column followed by different letters are significant ($p < 0.05$)

Table 4: The Corrected Protein Efficiency Ratio (CPER), Food Efficiency Ratio (FER) and Food intake of formulated diets

Sample	CPER	FER	Food Intake
Unmalted maize flour	1.46^{c}	0.15^{c}	175.8^{c}
Malted maize flour	1.59^{c}	0.16^{c}	178.4^{bc}
Unmalted maize flour +Soy full fat	2.00^{b}	0.20^{b}	180.2^{ab}
Malted maize flour + Soy full fat	2.15^{ab}	0.22^{ab}	176.8^{c}
Unmalted maize flour + Soy Concentrate	2.25^{ab}	0.23^{ab}	188. 6^{ab}
Malted maize flour + Soy Concentrate	2.38^{a}	0.24^{a}	205.4^{a}
Commercial diet	2.30^{a}	0.23^{a}	208.6^{a}
Casein	2.50^{a}	0.25a	206.6^{a}
Basal diet	-	-	165.5^{d}

Means of the same column followed by different letters are significant ($p < 0.05$).

The true digestibility (Fig. 4) of the diets varied between 74.70 (unmalted maize diet) and 90.30% (Casein). There was no significant difference ($p > 0.05$) between the commercial diet and the formulated diets containing soy concentrate. The casein has true digestibility higher than commercial and formulated diets. Formulation based on malted maize has higher true digestibility than the unmalted maize diet. The level of crude fibre affects the digestibility of the diets. Malting is usually carried out to increase digestibility and reduce the buklk density (Hofvander and Underwood,1987). Gupta and Sehgal (1992) reported a similar true digestibility for complementary foods based on germinated cereal grains. The biological value and the net protein utilization of the formulated complementary diets varied between (64.50 - 78.24%) and (48.18 - 66.70%) respectively. The casein has the highest biological value and net protein utilization (Fig. 4), the commercial diet was not significantly higher ($p > 0.05$) than the diets containing soy concentrate. The biological value expresses the percentage of the nitrogen which was retained by the body for repair or the construction of nitrogenous tissue.

4. CONCLUSIONS

There was improvement in the nutrient quality of the formulated complementary foods from malted maize supplemented with soy concentrate which supported better growth. This study also infered that malted maize- soy concentrate blend has better tendency of retaining high nitrogen in the body which will be needed for growth and development. These diets could be prepared at household level for infants in regions where maize is a staple and malnutrition is prevalent.

REFERENCES

A.O.A.C., Official Methods of Analysis 15th Edn. Association of Official Analytical Chemist. Washington D.C.,1990.

Adelekan, D.A., Childhood Nutrition and Malnutrition in Nigeria. *The International Journal of Applied and Basic Nutritional Science*,19, Issue 2:179-181, 2003.

Akingbala, J.O., Rooney, L.W. and Faubion, M.A., Laboratory Procedure for the Preparation of Ogi- a Nigerian Fermented. *Journal of Food Science*, 46:1523-1526,1981.

Alika, J.E., Statistics and Research methods. Ambik Press Benin City, First edition. 1-103,1997.

Anigo, K. M., Ameh, D. A., Ibrahim, S. and Danbauchi, S. S., Nutrient composition of complementary food gruels formulated from malted cereals, soy beans and groundnut for use in North-western Nigeria. *African Journal of Food Science*, 4 (3) 65-72, Available online http://www.acadjourn.org/ajfs, 2010.

Brown, K.H., Appropriate diets for the rehabilitation of malnourished children in the community setting. *Acta Paediatric Scand*., 374:151-159,1991.

Dahiya, S. and Kapoor, A.C., Biological evaluation of protein quality of home processed supplementary foods for pre- school children. *Food Chemistry*, 48 : 183 - 188,1993.

Desikachar, H.S.R.,Development of Weaning foods with high caloric density and low hot paste viscosity using traditional technology. *Food and Nutrition Bulletin*, 2 (4):21-23,1980.

FAO,Guidelines for Development of Supplementary Foods for Older Infants and Young Children. Report of the 14th session of the codex committee on Foods for special Dietary Uses: Appendix 12, 1985.

FAO/WHO/UNU, Energy and Protein requirements. Reports of a joint FAO/WHO.UNU Expert consultation World Health Organization Technical Report Series, 724:86-98,1991.

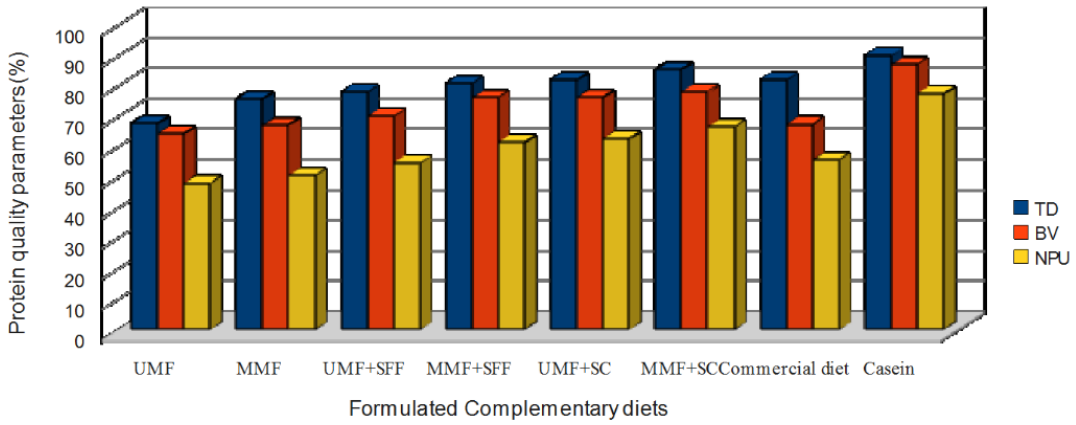

Fig. 4: The true digestibility, Biol;ogical value, and net protein utilization

Fashakin, J.B. and Unokiwedi, C.C.,Nutritional Evaluation of Warankasi and Wara egusi prepared from cow milk partially substituted with melon milk. *Nigerian Food Journal*, 2: 128 -134,1993.

Ghasemzadeh, R. and Ghavidel,R. A., Processing and assesment of quality charactristic of cereals - legumes composite weaning foods . 2011 International Conference on Bioscience, Biochemistry and Bioinformatics. IPCBEE IACSIT Press, Singapore,5 :1-3,2011.

Gupta, C. and Sehgal, S., Protein quality of developed home made weaning foods. *Plant Foods Human Nutrition*, 42: 239 –246,1992.

Hofvander, Y. and Underwood, B.A.,Processed supplementary foods for older infants and young children, with special reference to developing countries. *Food and Bulletin*, 9:(1) 1-1,1987.

Hotz ,C. and Gibson, R.S.,Traditional Food Processing and Preparation practices to enhance the Bioavailability of micro-nutrients in plants-diets. *The Journal of Nutrition*, 137:1097-1100, 2007.

Ihekoronye, A.I. and Ngoddy, P.O., Integrated Food Science and Technology for the Tropics. Macmillan Publishing Co. London, 253-257,1985.

Ikujenlola, A. V.,Quality Evaluation of weaning food Produced from Malted cowpea and rice blends. *Knowledge Review*, 8 (1):83-87, 2004.

Ikujenlola, A.V. and Fashakin, J.B.,Bioassay assessment of a complementary diet prepared from vegetable proteins. *Journal of Food Agriculture and Environment*, Finland, 3(3): 23-26, 2005.

Ikujenlola, A.V.,The effects of malting and fermentation on the nutritional qualities of complementary produced from maize varieties and soy bean grains. Ph.D Thesis Obafemi Awolowo University, Ile-Ife, Nigeria, 2010.

Ikpeme-Emmanuel, C. A., Okoi, J. and Osuchukwu, N. C., Functional, anti-nutritional and sensory acceptability of taro and soybean based weaning food. *African Journal of Food Science*, Available online http://www.acadjourn.org/ajfs. Accessed on March 12, 2012, 3(11) 372-377,2009.

Inyang, C.U. and Idoko, C.A.,Assessment of the quality of "Ogi" made from malted millet. African Journal of Biotechnology, 5: 2334 – 2337,2006.

Iwe, M.O., The Science and Technology of Soybean: Chemistry, Nutrition, Processing and Utilization. 1st edn. Rojoint Communication Services Ltd. Enugu, Nigeria. 115-116, 2003.

Malleshi, N.G.,Daodu,M.A. and Chandrasekar,A., Development of weaning Food formulations based on malting and roller drying of sorghum and cowpea. *Int. J. Food Sci. Tech.*, 24: 511-519, 1989.

Marero, L.M., Payumo, E.M., Lirando, E.C. Larez, W.N., Gopez, M.D. and Horma, S.,Technology of Weaning food formulation prepared from germinated cereals and legumes. *Journal of Food Science*, 53: 1391-1398, 1988.

Obayanju, V.S. and Ikujenlola, A.V.,Formulation and Nutritional Assessment of Weaning food from soy bean and Acha. *Journal of Agricultural Technology*, 10 (2): 22-27,2002.

Ojofeitimi, E.O., Abiose, S.H., Ijadunola, R.T., Pedro, T. and Jinadu, M.K.,Modification and Improvement of Nutritive quality of corn pap Ogi' with cowpea and groundnut milk, *Nutrition and Health*, 15:47-53,2001.

Onuorah, C.E. and Akinjide, F.A., Comparative Evaluation of four formulated weaning foods and a commercial product. *Nigerian Food Journal*, 22: 48-53, 2004.

Owolabi, A.O., Ndidi, U.S., James, B.D. and Amune, F.A., Proximate, Antinutrient and Mineral Composition of Five Varieties (Improved and Local) of Cowpea, (*Vigna unguiculata*), Commonly Consumed in Samaru Community, Zaria-Nigeria, *Asian Journal of Food Science and Technology*, 4(2): 70-72, 2012.

PAG, Protein Advisory Groups of the United Nations Guideline No 8, New York, 1-7,1971.

Sajilata, G., Rekha, S., Singhal, O. and Kulkarni, P.R., Weaning Foods A review of the Indian Experience, *Food and Nutrition Bulletin*, 23 (2): 208-226,2002 .

Wardlaw, G. M., Contemporary Nutrition Issues and Insights. 4th ed. McGraw. Hall Higher Education, USA,450-475, 2000.

W.H.O.,Complementary feeding of young children in developing countries. A review of current scientific knowledge. Available at: http://www.who.int/nutrition/ publications/ infantfeeding/ WHO. NUT. 98.1/en/index.html. Accessed 29 June 2009.1998.

Full Paper

EFFECT OF SOME PRESERVATION TECHNIQUES ON THE MICROBIOLOGICAL CHARACTERISTICS OF *FURA DE NUNU* DURING STORAGE

A.A. Adepoju
Department of Food Science and Technology, Obafemi Awolowo University, Ile-Ife.
adepojuadekunbi@yahoo.com
080-28466459

S.H. Abiose
Department of Food Science and Technology, Obafemi Awolowo University, Ile-Ife.

H.A. Adeniran
Department of Food Science and Technology, Obafemi Awolowo University, Ile-Ife.

ABSTRACT

The study focused on the effect of pasteurisation, with or without addition of sodium benzoate or sorbic acid on the microbiological characteristics of *fura de nunu* samples stored at ambient and refrigeration temperatures. This was carried out with the view of extending the shelf-life of this locally prepared dairy based drinkFreshly prepared *fura* was added to fresh *nunu* at ratio 1: 3, different batches were each subjected to pasteurisation, with or without sodium benzoate at two concentrations (300 mg/l and 200 mg/l) and sorbic acid at two concentrations (1000 mg/l and 750 mg/l). Samples were stored at refrigeration (4 ±1 °C) and ambient temperatures (28 ±2 °C) over a period of four weeks. The Total Viable Count (TVC), Lactic Acid Bacteria (LAB) and Yeast counts of the *fura de nunu* during storage were enumerated and identified. Results showed that the TVC and LAB counts of untreated sample ranged from 6.76 - 14.90, and 6.64 - 13.72 (log cfu ml^{-1}), respectively while pasteurised samples treated with 300mg L^{-1} sodium benzoate were found to have TVC and LAB of 0 - 4.88, and 0 - 3.84 ((log cfu ml^{-1}), respectively over the four weeks storage. The microorganisms were identified as *Lactobacillus delbrueckii*, *Lactobacillus brevis*, *Lactobacillus plantarum*, *Lactobacillus helveliticus*, *Leuconostoc mensenteroides*, *Streptococcus thermophilus*, *Saccharomyces cerevisiae*, *Saccharomyces lactic*, *Rhodotorula glutinis*, *Hansenula anomala*, *Torulopsis versatalis*, *and Candida mycoderma.* In conclusion, the combination of pasteurisation and 300mg L^{-1} sodium benzoate effectively lowered the microbial load during the period of storage. Sorbic acid was also effective, but it had minimal effect on the growth of lactic acid bacteria.

Key words: *fura de nunu*, *microbial load*, *preservation*, *microbiological characteristics*, *probiotics.*

1. INTRODUCTION

Fura de nunu (fermented milk and millet mix) is a highly nutritious beverage which is a two-in-one product, consisting of cereal, "*Fura*" made from millet grains and '*nunu*' a fermented milk product (with acid taste) similar to yoghurt. Depending on the consistency, the product is used as food, refreshing drink and a weaning food for infants (Umoh *et al*., 1988). The mixture of fermented milk and cooked spiced millet (*fura de nunu*) is almost a complete food with milk serving as a source of protein while cooked spiced millet provides energy. The sour taste is known to be particularly suited for quenching thirst (Owusu-kwanteng *et al*., 2010). It, however, does not appeal to majority of the people because of the apparent unhygienic conditions in which it is prepared, and its poor shelf life (Wallander and Samson, 1967; Yahuza, 2001).

Nunu is a delicious and refreshing beverage (Olalokun, 1976) that evolved empirically some centuries ago by allowing milk to sour at warm temperature (Adebesin *et al*., 2001). The fermentation occurs spontaneously without starter cultures at ambient temperature. The fermented milk is then churned using a wooden ladle. Fat accumulates as a result of the churning and is removed. Excess whey is drained off to obtain a product with a thick consistency which is the *nunu*, consumed alone or with *fura* (Owuzu-kwateng *et al*., 2010).

Fermented milk contains probiotics which are live microbial food supplements that benefits the health of consumers by maintaining or improving their intestinal microbial balance. Lactic acid bacteria in fermented milk break down lactose into glucose and galactose in the intestine by synthesizing the enzyme lactase. People with lactose intolerance can consume fermented milk product because of its lower lactose content and availability of live probiotics (Adolfsson *et al*., 2004).

Most foods deteriorate in quality following harvest, slaughter or manufacture, in a manner that is dependent on food types, its composition and storage conditions. The principal cause of deterioration of foods may be microbiological, enzymatic, chemical and physical. Methods by which the microbial decomposition of foods can be delayed or prevented include; restriction of access of microorganisms to foods by aseptic packaging, removal of microorganisms by filtration or centrifugation, slowing or preventing the growth and activity of microorganisms by reducing the temperature, water activity and pH, removal of oxygen, modified atmosphere packaging and addition of preservatives, and inactivation of microorganisms by heat (Gupta, 2007).

Pasteurisation conditions are designed to give maximum protection from milk-borne diseases with minimum reduction in nutritional properties, and at the same time to retain as fully as possible the appearance and flavour of raw fresh milk (Ihekoronye and Ngoddy, 1985). Organic acids such as sorbic acid and sodium benzoates also help in killing or inactivating target organisms in food. Preservatives may be microbicidal and kill the target organism or they may be microbiostatic in which case they simply prevent them from growing, thus improving the shelf-life of the product (Fawole and Osho, 2002). Preservatives may also inhibit microorganism by interfering with the cell membrane, enzyme activity or genetic mechanism of microorganisms (William and Westhoff, 1995). Since food spoilage is usually a result of chemical reactions mediated by

microbial and endogenous enzymes, the useful life of foods can be increased at low temperatures (Adam and Moss, 1999). Nebedum and Obiakor (2007) reported the use of pasteurisation and application of sorbic acid and sodium benzoate on fermented milk (*nunu*) for seven days at refrigeration and ambient temperatures. Abiose and Adeniran (2010) reported the use of pasteurization and application of sodium benzoate/ sodium metabisulphite in extending the shelf-life of *Hibiscus sabdariffa* extract for six weeks. This study investigated the effect of pasteurisation with or without sodium benzoate or sorbic acid on the microbial population and microbial types in *fura de nunu* during storage at refrigeration and ambient temperatures.

2. MATERIALS AND METHODS

Fresh cow milk was obtained from Fulani settlement at Alakowe, Ile-Ife, Nigeria. Millet grains were obtained from a local market in Ile-Ife, Nigeria. The media and chemicals were of reagent grade.

2.1. Preparation of *fura*

Millet grains (700 g) were sorted, cleaned, steeped for 18 *h* and then wet milled. The paste was hand- moulded into balls of about 10 cm in diameter and then cooked for about 30 minutes. The cooked millet balls were pounded with mortar and pestle. The balls were finally moulded into much smaller balls of about 4 cm diameter known as *fura* (Owuzu-Kwanteng *et al*., 2010).

2.2. Preparation of *nunu*

Cow milk was collected, sieved, and left to ferment for 48 *h* in a covered container at ambient temperature. The fermented milk was churned using a wooden ladle. Fat and excess whey were drained off to obtain a product with a thick consistency (*nunu*) (Akabanda *et al*., 2010).

2.3. Preparation of *fura de nunu*

Nunu was added to *fura* at ratio 3:1 by blending and the mixture was then packaged in sterile plastic bottles. Sodium benzoate and sorbic acid were added at different. The mixture was split into six portions A-F; A was unpasteurised, B-F were pasteurised at 70 ^{o}C for 15 *min* in sterile plastic bottles. Sample B was only pasteurised, sample C was treated with 300 mg L^{-1} sodium benzoate, sample D was treated with 1000 mg L^{-1} sorbic acid, sample E was treated with 200 mg L^{-1} sodium benzoates, and sample F was treated with 750 mg L^{-1} sorbic acid. Samples were kept at ambient (28 ±2^{o}C) and refrigeration temperatures (4 ±1) ^{o}C for a period of four weeks.

2.4. Microbiological evaluation of *fura de nunu*

2.4.1. Enumeration of microbes

Serial dilution was carried out by first mixing 1 ml of *fura de nunu* sample with 9 ml of peptone water to obtain 10^{-1}dilution. From this subsequent dilutions were made serially until the desired level of dilution was achieved. From each dilution, 1.0ml was plated on sterile petridish before 20ml each of molten Nutrient Agar (NA), de Man Rogosa and Sharpe (MRS) and Potato Dextrose Agar (PDA) for total viable count, Lactic acid bacteria count, and yeast count respectively, using pour plate technique (Harrigan and McCance, 1976; McLandsborough, 2005).

Plates were incubated in an inverted position in the incubators set at 37 ^{o}C for total viable microorganism and lactic acid bacteria for 24 and 72 *h*, respectively. Plates were incubated at 28 ^{o}C ± 2 ^{o}C for yeast for 3 to 5 days. The microbial load was determined by counting distinct colonies with the aid of a colony counter. Plates with 25 -250 colonies were reckoned with and the number of colonies on each plate was multiplied with the reciprocal of the dilution factor to obtain the count (Harrigan and McCance, 1976; Harrigan, 1998).

2.4.2. Characterization and identification of microbes

Pure cultures were obtained from distinct colonies by repeated streaking on fresh agar plates and subjected to microscopic examination and biochemical tests (such as catalase test, gram staining, oxidase test, sugar fermentation test and production of carbon dioxide). Relevant bacterial and yeast identification schemes of Harrigan and McCance (1976), and Holt (1996) were employed for identification.

3. RESULTS AND DISCUSSIONS

3.1. Total Viable Count

There was a general increase in the total viable count of *fura de nunu* with increase in the period of storage (Tables 1a and 1b). All the samples except the unpasteurised *fura de nunu* had no count at week zero. Unpasteurised *fura de nunu* had the highest count at refrigeration and ambient temperatures. A range of total viable count reported for fresh *fura de nunu* has been put at 10^{-4} to 10^{-7} (Adebesin *et al*., 2001; Owuzu-kwateng *et al*., 2010). At refrigeration temperature the total viable count of pasteurised *fura de nunu* treated with 300 mg/l sodium benzoate increased from zero count at week 0 to 3.66 at week 1 and 4.69 (cfu ml^{-1}) at the end of week 4 of storage. In the pasteurised samples treated with 200 mg/l sodium benzoate, there was no count at week zero, the count increased to 3.82 at the first week and 4.81 (cfu ml^{-1}) at week 4 of refrigeration storage. At ambient temperature, a similar trend was observed. There was no significant difference ($p > 0.05$) in the total viable count of pasteurised sample treated with sodium benzoate at refrigeration temperature and ambient temperature. There was significant increase ($p > 0.05$) in the total viable count of unpasteurised and pasteurised *fura de nunu* at refrigeration and ambient temperatures.

Total viable count of pasteurised samples treated with sorbic acid increased significantly from week one to week four but the counts were significantly lower than the count in pasteurised sample. The result showed that pasteurisation destroyed the microorganisms in *fura de nunu* at the initial stage but some microorganisms that were able to survive the process later grew, but the growth was lower at refrigeration temperature than at ambient temperature. The best result was obtained in pasteurised sample treated with 300 mg L^{-1} sodium benzoate at refrigeration temperature. Pasteurisation of raw milk was reported to be effective in eliminating all but the thermoduric microorganisms and occasionally some Gram-negative rods (Jay, 1996). The use of preservatives such as sodium benzoate and sorbic acid further reduced the total viable count of *fura de nunu.* Psychrotrophs can grow at refrigeration temperatures below 7 °C, produce enzymes, toxins and other metabolites (Jay, 1996) and contribute to high TVC in both raw and pasteurised milk. Microorganisms also hinder the effort of increasing the shelf life of pasteurised milk (Frank, 1997).

3.2. Lactic acid bacteria count

Lactic acid bacteria count increased as the period of storage increased (Tables 2a and 2b). There was no count in all the samples except in the unpasteurised sample at week zero. Unpasteurised sample had the highest lactic acid bacteria count at refrigeration and ambient temperatures at different stages of storage (6.64 -13.26 cfu ml^{-1}). There was significant difference ($p > 0.05$) in the lactic acid bacteria count of unpasteurised sample and pasteurised sample at refrigeration and ambient temperature.

The count in pasteurised *fura de nunu* treated with 300mg L^{-1} sodium benzoate increased from week zero to week one (0 – 3.38 cfu ml^{-1}) and also increased at the second week but reduced at the third week (4.72 – 3.40 cfu ml^{-1}) but slightly increased at the fourth week of storage (3.44 cfu ml^{-1}). There was no significant difference ($p > 0.05$) in the lactic acid bacteria count of pasteurised *fura de nunu* treated with sodium benzoate at refrigeration and ambient temperatures. Pasteurised *fura de nunu* treated with 300mg/l sodium benzoate had the

Table 1a: Total Viable Count of fura de nunu stored at Refrigeration Temperature (log cfu ml^{-1})

Weeks	Samples					
	A	B	C	D	E	F
0	6.76 ± 0.01^{b}	0.00± 0.00^{a}	0.00± 0.00^{a}	0.00± 0.00^{a}	0.00± 0.00^{a}	0.00± 0.00^{a}
1	9.86 ± 0.09^{d}	5.92 ± 0.44^{c}	3.66 ± 0.17^{a}	3.82 ± 0.14^{a}	4.77± 0.17^{b}	4.78 ± 0.24^{b}
2	11.59 ± 0.59^{d}	7.40 ± 0.38^{c}	3.66 ± 0.13^{a}	4.72 ± 0.17^{b}	4.81 ± 0.14^{b}	4.82 ± 0.18^{b}
3	12.78 ± 0.38^{d}	9.53 ± 0.14^{c}	4.72 ± 0.16^{a}	4.76 ± 0.16^{a}	5.69 ± 0.30^{b}	5.80 ± 0.14^{b}
4	14.41 ± 0.07^{d}	10.54 ± 0.13^{c}	4.69 ± 0.20^{a}	4.81 ± 0.18^{a}	6.58 ± 0.20^{b}	6.71 ± 0.17^{b}

n=3, ±Standard Deviation. Means in the same row with the same superscript are not significantly different at (p › 0.05).

Table 1b: Total Viable Count of fura de nunu stored at Ambient Temperature (log cfu ml^{-1})

Weeks	Samples					
	A	B	C	D	E	F
0	6.76 ± 0.01^{b}	0.00± 0.00^{a}	0.00± 0.00^{a}	0.00± 0.00^{a}	0.00± 0.00^{a}	0.00± 0.00^{a}
1	11.99 ± 0.18^{d}	6.62 ± 0.54^{c}	3.79 ± 0.24^{a}	3.86 ± 0.11^{a}	4.81± 0.16^{b}	4.84 ± 0.02^{b}
2	13.98 ± 0.25^{d}	9.73 ± 0.17^{c}	4.83 ± 0.17^{a}	4.78 ± 0.20^{a}	5.69 ± 0.28^{b}	5.72 ± 0.21^{b}
3	14.94 ± 0.33^{d}	11.86 ± 0.08^{c}	4.78 ± 0.08^{a}	4.91 ± 0.10^{a}	6.68 ± 0.11^{b}	6.78 ± 0.11^{b}
4	14.90 ± 0.18^{d}	12.98 ± 0.14^{c}	4.88 ± 0.21^{a}	4.96 ± 0.24^{a}	6.87 ± 0.14^{b}	6.88 ± 0.23^{b}

n=3, ±Standard Deviation. Means in the same row with the same superscript are not significantly different at (p › 0.05). A: Unpasteurised *fura de nunu*, B: Pasteurised *fura de nunu*, C: Pasteurised *fura de nunu* treated with 300 mg/l sodium benzoate, D: Pasteurised *fura de nunu* treated with 200 mg/l sodium benzoate, E: Pasteurised *fura de nunu* treated with 1000 mg/l sorbic acid. F: Pasteurised *fura de nunu* treated with 750 mg/l sorbic acid.

Table 2a: Lactic Acid Bacteria Count of fura de nunu stored at Refrigeration Temperature (log cfu ml^{-1})

Weeks	A	B	C	D	E	F
0	6.64 ± 0.14^{b}	0.00± 0.00^{a}	0.00± 0.00^{a}	0.00± 0.00^{a}	0.00± 0.00^{a}	0.00± 0.00^{a}
1	9.68 ± 0.17^{c}	5.49 ± 0.14^{b}	3.38 ± 0.30^{a}	3.58 ± 0.13^{a}	3.64 ± 0.14^{a}	3.80 ± 0.33^{a}
2	11.38 ± 0.17^{c}	7.89 ± 0.13^{b}	4.72 ± 0.16^{a}	4.75 ± 0.10^{a}	4.75 ± 0.28^{a}	4.89 ± 0.20^{a}
3	12.91± 0.14^{d}	9.46 ± 0.16^{c}	3.40 ± 0.27^{a}	3.77 ± 0.33^{a}	5.38 ± 0.13^{b}	5.85 ± 0.14^{b}
4	13.26 ± 0.25^{d}	9.68 ± 0.16^{c}	3.44 ± 0.21^{a}	3.58 ± 0.24^{a}	6.40 ± 0.23^{b}	6.83 ± 0.20^{b}

n=3, ±Standard Deviation. Means in the same row with the same superscript are not significantly different at (p › 0.05).

Table 2b: Lactic Acid Bacteria Count of fura de nunu stored at Ambient Temperature (log cfu ml^{-1})

Weeks	A	B	C	D	E	F
0	6.64 ± 0.14^{b}	0.00± 0.00^{a}	0.00± 0.00^{a}	0.00± 0.00^{a}	0.00± 0.00^{a}	0.00± 0.00^{a}
1	10.80 ± 0.28^{c}	6.66 ± 0.17^{b}	3.68 ± 0.20^{a}	3.79 ± 0.16^{a}	3.81± 0.24^{a}	3.88 ± 0.18^{a}
2	12.71 ± 0.35^{c}	8.83 ± 0.17^{b}	4.83 ± 0.20^{a}	4.83 ± 0.20^{a}	4.83 ± 0.20^{a}	4.89 ± 0.20^{a}
3	13.52 ± 0.30^{d}	10.61 ± 0.23^{c}	4.55 ± 0.16^{a}	4.56 ± 0.16^{a}	5.76 ± 0.20^{b}	5.85 ± 0.14^{b}
4	13.72 ± 0.30^{d}	9.97 ± 0.23^{c}	3.76 ± 0.28^{a}	3.84 ± 0.20^{a}	6.62 ± 0.32^{b}	6.83 ± 0.20^{b}

n=3, ±Standard Deviation. Means in the same row with the same superscript are not significantly different at (p › 0.05). A: Unpasteurised *fura de nunu*, B: Pasteurised *fura de nunu*, C: Pasteurised *fura de nunu* treated with 300 mg/l sodium benzoate, D: Pasteurised *fura de nunu* treated with 200 mg/l sodium benzoate, E: Pasteurised *fura de nunu* treated with 1000 mg/l sorbic acid. F: Pasteurised *fura de nunu* treated with 750 mg/l sorbic acid.

lowest count at both refrigeration and ambient temperature. Lactic acid bacteria count in pasteurised *fura de nunu* treated with sorbic acid was higher than that of pasteurised *fura de nunu* treated with sodium benzoate but lower than the lactic acid bacteria count in pasteurised sample. According to Adam and Moss (1999) sorbic acid is active against yeast, moulds and catalase-positive bacteria but, less active against catalase-negative bacteria. The result showed that it was not effective against all the lactic acid bacteria in *fura de nunu.* Thus, it can be used in the preservation of probiotic food to keep the beneficial lactic acid bacteria viable during the period of storage.

3.3. Yeast count

Yeast counts in unpasteurised *fura de nunu* were higher than in pasteurised *fura de nunu* at refrigeration and ambient temperatures. There was significant increase (p › 0.05) in yeast count of pasteurised and unpasteurised *fura de nunu* at refrigeration and ambient temperatures.

There was a general increase in yeast count of *fura de nunu* at refrigeration and ambient temperatures except in pasteurised sample treated with sorbic acid. At refrigeration temperature, pasteurised *fura de nunu* treated with 1000 mg L $^{-1}$ sorbic acid increased from initial count 0 to 3.60 cfu ml^{-1} at the first week and then reduced to 2.46 cfu ml^{-1}at the fourth week.

There was no significant difference (p › 0.05) in yeast count of pasteurised *fura de nunu* treated with sorbic acid at refrigeration and ambient temperatures.

Pasteurised *fura de nunu* treated with sorbic acid had a lower yeast count than pasteurised *fura de nunu* treated with sodium benzoate. Yeast count of pasteurised sample treated with sodium benzoate was significantly lower than in pasteurised sample. Sorbic acid is more effective at lower pH levels because more will exist in the undissociation form, allowing entry into the cell (Foegeding and Busta, 1999). The highest count was recorded in the unpasteurised *fura de nunu* because the growth process was not controlled.

3.4. Identity of Microbial Isolates

3.4.1. Lactic acid bacteria

Lactic acid bacteria identified in fura de nunu were Lactobacillus plantarum, Leuconostoc mensenteroides, Streptococcus thermophilus, Lactobacillus delbrueckii, Lactobacillus brevis, and Lactobacillus helveliticus (Table 4). This high number of lactic acid bacteria, coupled with the low values of pH and high acidity may be responsible for the sour taste, flavour and unique aroma of fura de nunu. The production of lactic acid gives the fermented product a desired sour taste. In addition to this, various flavour compounds are

Table 3a: Yeast Count of fura de nunu stored at Refrigeration Temperature (log cfu ml^{-1})

Weeks	A	B	C	D	E	F
0	5.53 ± 0.30^{b}	0.00± 0.00^{a}	0.00± 0.00^{a}	0.00± 0.00^{a}	0.00± 0.00^{a}	0.00± 0.00^{a}
1	8.94 ± 0.17^{c}	4.64 ± 0.14^{b}	3.49 ± 0.24^{a}	3.65 ± 0.28^{a}	3.60 ± 0.28^{a}	3.68 ± 0.18^{a}
2	10.51 ± 0.31	6.90 ± 0.14^{c}	2.84 ± 0.13^{a}	3.41 ± 0.16^{b}	3.56 ± 0.14^{b}	3.61 ± 0.17^{b}
3	11.98 ± 0.17^{d}	8.83 ± 0.16^{c}	3.26 ± 0.25^{b}	3.51 ± 0.08^{b}	2.51 ± 0.27^{a}	2.56 ± 0.16^{a}
4	13.75 ± 0.20	10.74 ± 0.35	4.00 ± 0.30^{b}	4.20 ± 0.14^{b}	2.46 ± 0.13^{a}	2.76 ± 0.24^{a}

n=3, ±Standard Deviation. Means in the same row with the same superscript are not significantly different at (p › 0.05).

Table 3b: Yeast Count of fura de nunu stored at Ambient Temperature (log cfu ml^{-1})

Weeks	A	B	C	D	E	F
0	5.53± 0.30^{b}	0.00± 0.00^{a}	0.00± 0.00^{a}	0.00± 0.00^{a}	0.00± 0.00^{a}	0.00± 0.00^{a}
1	9.81± 0.27^{c}	5.95± 0.18^{b}	3.52 ± 0.28^{a}	3.69 ± 0.18^{a}	3.84 ± 0.18^{a}	3.85 ± 0.24^{a}
2	11.49 ± 0.13^{c}	7.99 ± 0.27^{b}	3.56 ± 0.14^{a}	3.58 ± 0.24^{a}	3.69 ± 0.33^{a}	3.78 ± 0.21^{a}
3	12.76 ± 0.14^{d}	10.72 ± 0.21^{c}	3.72 ± 0.20^{b}	3.81 ± 0.21^{b}	2.72 ± 0.16^{a}	2.76 ± 0.18^{a}
4	13.90 ± 0.30^{d}	12.52 ± 0.45^{c}	4.50 ± 0.16^{b}	4.72 ± 0.23^{b}	2.67 ± 0.20^{a}	2.75 ± 0.27^{a}

n=3, ±Standard Deviation. Means in the same row with the same superscript are not significantly different at (p › 0.05). A: Unpasteurised *fura de nunu*, B: Pasteurised *fura de nunu*, C: Pasteurised *fura de nunu* treated with 300 mg/l sodium benzoate, D: Pasteurised *fura de nunu* treated with 200 mg/l sodium benzoate, E: Pasteurised *fura de nunu* treated with 1000 mg/l sorbic acid. F: Pasteurised *fura de nunu* treated with 750 mg/l sorbic acid.

Table 4: Identification of Lactic Acid Bacteria in fura de nunu

Tests	Isolates					
	B1	B2	B3	B4	B5	B6
Morphology	Rods	Cocci	Cocci	Rods	Rods	Rods
Colour of colony	Cream	Cream	Cream	Cream	Cream	Cream
Gram reaction	+	+	+	+	+	+
Catalase test	-	-	-	-	-	-
Growth at:						
15°C	-	+	-	+	-	+
45°C	+	+	+	-	+	-
Growth in:						
4 % NaCl	-	-	-	-	-	-
6.5 % NaCl	-	-	-	-	-	-
Production of CO_2	-	+	-	-	-	+
Sugars fermentation:						
Glucose	+	+	+	+	+	+
Galactose	+	+	+	-	+	+
Lactose	+	+	+	+	+	+
Arabinose	-	+	-	+	+	+
Trehalose	+	+	-	-	+	-
Salicin	+	+	-	+	-	+
Sucrose	+	+	-	+	-	+
Maltose	+	+	-	-	+	+
Raffinose	-	+	+	+	-	+
Dextran production	-	+	-	-	-	-
Probable identity of Organism	*Lactobacillus Delbrueckii*	*Leuconostoc mesenteroides*	*Streptococcus thermophilus*	*Lactobacillus plantarum*	*Lactobacillus helveliticus*	*Lactobacillus Brevis*

formed and these are responsible for the specific taste of different products. Such flavour compounds can be formed from citrate, when the important flavour compounds diacetyl, acetic acid and carbon dioxide are formed (Akabanda et al., 2010). Many microorganisms in fermented dairy products stabilize the bowl micro flora, and some appear to have antimicrobial properties. Several lactobacilli have antitumor compounds in their cell walls. Such findings suggest that diets including lactic acid bacteria may contribute to the control of colon cancer (Prescott et al., 2002). Leuconostoc mesenteroides was isolated from unpasteurised fura de nunu at week zero (Table 2). Leuconostoc mesenteroides and Leuconostoc lactis are the dominant Leuconostoc in milk and fermented milk product (Marshal, 1987). Leuconostoc mesenteroides was only present in the fresh unpasteurised fura de nunu. Leuconostoc sp have also been shown to exhibit a weak competitive ability during the fermentation of milk (Wood and Hozapfel, 1995).

3.4.2. Yeasts

Yeast isolates identified in *fura de nunu* were *Saccharomyces cerevesiae*, *Hansenula anomala*, *Torulopsis versatalis*, *Rhodotorula glutinis*, and *Candida mycoderma* (Table 5). Yeasts have been reported to make a useful contribution to the improvement of flavour and acceptability of fermented cereal gruels (Owuzu-kwanteng et al., 2010). Yeasts appear to be commonly associated with traditional fermented dairy products and have been reported in several studies (Mathara *et al*., 2004; Isono *et al*., 1994; Gadaga *et al*., 1999; Beukes *et al*., 2001; Adebesin *et al*., 2001; Akabanda *et al*., 2010). Yeasts are common in several fermented foods and beverages including *ogi* , *fufu*, *kunu*, and *nunu* produced in the tropical part of the world (Odunfa, 1985, Adegoke and Babalola, 1988, Halm *et al*., 1993; Akabanda *et al*., 2010).

3.5. Occurrence Pattern of Lactic Acid Bacteria in during Storage

Leuconostoc mesenteroides was isolated from unpasteurised *fura de nunu* at week zero (Table 6). *Leuconostoc mesenteroides* and *Leuconostoc lactis* are the dominant *Leuconostoc* in milk and fermented milk product (Marshal, 1987). *Leuconostoc mesenteroides* was only present in the fresh unpasteurised *fura de nunu*. *Leuconostoc* have practical importance in the

role they play in changing the organoleptic quality and texture of fermented food products such as milk, butter, cheese and meat.

Lactobacillus delbrueckii was isolated from fresh unpasteurised *fura de nunu* and from pasteurised *fura de nunu* at the first week of storage (Table 6). *Streptococcus thermophilus* was isolated from all *fura de nunu* samples except from pasteurised *fura de nunu* treated with sodium benzoate (Table 6). This showed that *Streptococcus thermophilus* can grow at high temperature. Wood and Holzaphel, (1995) reported that *Streptococcus thermophilus* can be found in heated or pasteurised milk. *Lactobacillus plantarum* was isolated from all the samples from the first week to the fourth week of storage, except in unpasteurised *fura de nunu* which contain *Lactobacillus plantarum* at week zero. *L. plantarum* has been identified as the dominant organism at the end of several natural lactic acid fermentations (Nout, 1980; Mbugua, 1984; Braunman *et al*., 1996; Olasupo *et al*., 1997; Kunene *et al*., 2000; Mugula *et al*., 2003), probably due to its acid tolerance (Fleming and McFeters, 1981) and superior ability to utilize the substrate including dextrins (Akinrele, 1970). *Lactobacillus helveliticus* was isolated from freshly prepared unpasteurised milk, from pasteurised *fura de nunu*, pasteurised *fura de nunu* treated with sodium benzoate and sorbic acid at the second week of storage. *Lactobacillus brevis* was isolated from freshly prepared unpasteurised *fura de nunu*. *L. brevis* has also been often found to occur in fermenting plant material (Corsetti *et al*., 2001) and have been isolated from fermented maize dough (Halm *et al*., 1993, Hounhouigan *et al*., 1993).

3.6. Occurrence Pattern of Yeasts in during Storage

Yeast isolates identified in *fura de nunu* were *Saccharomyces cerevesiae*, *Hansenula anomala*, *Torulopsis versatalis*, *Rhodotorula glutinis*, and *Candida mycoderma* (Table 5). *Torulopsis versatilis* was isolated from unpasteurised *fura de nunu* at the third week of storage while *Candida mycoderma* was isolated from unpasteurised *fura de nunu* at week zero,

Table 5: Identification of Yeast in Fura de nunu

Test	Isolates					
	Y1	Y2	Y3	Y4	Y5	Y6
Morphology:						
Pellicle	-	+	-	-	-	+
Colour	White	Cream	Pink	Cream	Cream	Cream
Shape	Ovoid	Cylindrical	Ovoid	Ovoid	Ovoid	Ovoid
Reproduction	Budding	Budding	Budding	Budding	Budding	Budding
Sugar fermentation:						
Glucose	+	+	-	+	+	-
Sucrose	+	+	-	+	+	-
Maltose	+	+	-	-	+	-
Galactose	+	+	-	+	+	-
Raffinose	+	+	-	+	+	-
Lactose	-	-	-	+	-	-
Sugar assimilation:						
Glucose	+	+	+	+	+	+
Sucrose	+	+	+	+	+	-
Maltose	+	+	+	+	+	-
Galactose	+	+	+	+	+	-
Raffinose	-	-	-	+	-	-
Lactose	-	-	-	+	+	-
Nitrate assimilation	-	+	-	-	+	-
Probably identity of organism	*Saccharomyces cerevisiae*	*Hansenula anomala*	*Rhodotorula glutinis*	*Saccharomyces lactis*	*Torulopsis versatalis*	*Candida mycoderma*

Table 6: Occurrence Pattern of Lactic Acid Bacteria in during Storage

Sample code	Lactic acid bacteria	Week 0	Week 1	Week 2	Week 3	Week 4
A	*Lactobacillus plantarum*	+	+	+	+	-
	Lactobacillus debrueckii	+	+	-	-	-
	Lactobacillus brevis	+	-	-	-	-
	Leuconostoc mesenteriodes	+	+	-	-	-
	Streptococcus thermophilus	+	+	-	-	-
	Lactobacillus helveliticus	+	+	+	-	-
B	*Lactobacillus plantarum*	-	+	+	+	+
	Streptococcus thermophilus	-	+	+	-	-
	Lactobacillus helveliticus	-	-	-	-	-
C	*Lactobacillus plantarum*	-	-	+	+	+
D	*Lactobacillus plantarum*	-	-	+	+	+
E	*Lactobacillus plantarum*	-	-	+	+	+
	Streptococcus thermophilus	-	-	+	+	+
	Lactobacillus brevis	-	-	+	+	+
F	*Lactobacillus plantarum*	-	-	+	+	+
	Streptococcus thermophilus	-	-	+	+	+
	Lactobacillus brevis	+	-	+	+	+

A: Unpasteurised *fura de nunu*, B: Pasteurised *fura de nunu*, C: Pasteurised *fura de nunu* treated with 300 mg/l sodium benzoate, D: Pasteurised *fura de nunu* treated with 200 mg/l sodium benzoate, E: Pasteurised *fura de nunu* treated with 1000 mg/l sorbic acid, F: Pasteurised *fura de nunu* treated with 750 mg/l sorbic acid.

+: Present, -: Absent

week one and week two (Table 7). Akinrele, (1970) reported the contribution of *Candida mycoderma* to the flavour acceptability of *ogi. Saccharomyces cerevesiae* was isolated from all *fura de nunu* samples. *Saccharomyces cerevisiae* is the most encountered yeast in fermented beverages and food based vegetables (Adam and Moss, 1999). *Saccharomyces lactis* was isolated from freshly prepared unpasteurised fura *de nunu* and pasteurised *fura de nunu* at the first week of storage.

It was also present in *fura de nunu* treated with sodium benzoate at the second and third week of storage (Table 7). *Hansenula anomala was* isolated from unpasteurised *fura de nunu* at the initial stage, from pasteurised *fura de nunu* at the second week of storage and from pasteurised *fura de nunu* treated with sodium benzoate at the fourth week of storage (Table 7). *Rhodotorula glutinis* was isolated from unpasteurised *fura de nunu* at the second week of storage. Yeasts appear to be commonly associated with traditionally fermented dairy products and have been reported in several studies (Beukes *et al*., 2001; Adebesin *et al*, 2001; Akabanda *et al*., 2001). Yeasts have been reported to make a useful contribution to the improvement of flavour and acceptability of fermented cereal gruels (Baningo *et al*., 1974; Odunfa and Adeyele, 1985).

3.7. pH of fura de nunu

The pH of *fura de nunu* samples decreased as the storage period increased. At refrigeration temperature (Figure 1), the pH of pasteurised *fura de nunu* treated with 300 mg/l sodium benzoate was stable with the value of 5.00, 4.97, 4.95 and 4.93 from week 0 to the third week and the decrease was significant at the fourth week of refrigeration storage. At ambient temperature the pH was stable from week 0 to the first week and reduced significantly ($p > 0.05$) at the third week. There was significant difference ($p > 0.05$) in the pH of pasteurised *fura de nunu* treated with sodium benzoate at refrigeration and ambient temperatures (Figure 4). pH of the pasteurised sample treated with sorbic acid was stable at week zero and week one but there was significant decrease from week two to week four at both refrigeration and ambient temperatures. There was no significant difference ($p > 0.05$) in pH of pasteurised *fura de nunu* treated with sorbic acid at refrigeration and ambient the pH of pasteurised *fura de nunu* treated with 300 mg/l sodium benzoate was stable with the value of 5.00, 4.97, 4.95 and 4.93 from week 0 to the third week and the decrease was significant at the fourth week of refrigeration storage. At ambient temperature the pH was stable from week 0 to the first week and reduced significantly ($p > 0.05$) at the third week. There was significant difference ($p > 0.05$) in the pH of pasteurised *fura de nunu* treated with sodium benzoate at refrigeration and ambient temperatures. pH of the pasteurised sample treated with sorbic acid was stable at week zero and week one but there was significant decrease from week two to week four at both refrigeration and ambient temperatures. There was no significant difference ($p > 0.05$) in pH of pasteurised *fura de nunu* treated with sorbic acid at refrigeration and ambient temperature during the four weeks of storage. Decrease in pH of *fura de nunu* was significant ($p > 0.05$) at week 0 and week four in unpasteurised *fura de nunu* and pasteurised sample, and there was a significant difference in their pH at refrigeration and ambient temperatures. There was progressive decrease in pH of the unpasteurised *fura de nunu* and the decrease was similar to that of pasteurised sample from the first week to fourth week of storage. It was observed that while the pH decreases, the titratable acidity increases with weeks of storage. It appears however, that the higher the storage temperature, the more pronounced the decrease in pH. This is expected, since the higher the storage temperature, the higher the rate of metabolism of sugar, hence, the higher the rate of acid production by the relevant microorganisms. Oyeyiola (1990) reported that production of acid during fermentation led to decrease in pH. These observations are in agreement with those reported by Fraizer, (1978) and Adebayo *et al*., (2010) who reported the production of acid from sugar by various metabolic microorganisms such as lactic acid bacteria, acetic and butyric acid bacteria.

3.8. Microbiological stability of fura de nunu

The shelf life of *fura de nunu* was extended by the combination of pasteurisation and chemical preservatives. The unpasteurised *fura de nunu* sample had the highest total viable count with less than one week shelf life when compared with fresh *fura de nunu* sample. Sodium benzoate was considered to be the best preservative in terms of lower microbial count. It was effective against lactic acid bacteria and other bacteria but, it was less effective against yeast. Pasteurised *fura de nunu* treated with sorbic acid had a good keeping quality throughout the storage period of 4 weeks especially at refrigeration temperature. The inhibitory effect of sorbic acid against yeast was observed as their number decreased over the period of storage at both ambient and refrigeration temperature. The lower the pH of *fura de nunu* the higher the inhibitory effect of sorbic acid against yeast but lactic acid bacteria count increased progressively with the storage period. In terms of viability of lactic acid bacteria, sorbic acid was considered as the best because it had little effect on the activities and growth of lactic acid bacteria. The microbial counts of *fura de nunu* samples were lower at refrigeration temperature than ambient storage temperature. There was no evidence of coliform in all the *fura de nunu* samples at ambient and refrigeration temperatures during the four weeks period of storage.

Table 7: Occurrence Pattern of Yeast in fura de nunu during Storage

Sample code	Yeast and mould	Week 0	Week 1	Week 2	Week 3	Week 4
A	*Saccharomyces cerevisiae*	-	-	-	-	-
	Hansenula anomala	-	-	-	-	-
	Rhodotorula glutinis	-	-	+	-	-
	Saccharomyces lactis	-	-	-	-	-
	Torulopsis versatalis	-	-	-	+	+
B	*Hansenula anomala*	-	-	+	+	+
	Saccharomyces lactis	-	+	+	+	-
	Saccharomyces cerevisiae	-	+	+	+	+
C	*Saccharomyces cerevisiae*	-	+	+	+	+
	Hansenula anomala	-	-	-	-	+
D	*Saccharomyces cerevisiae*	-	+	+	+	+
	Hansenula anomala	-	-	-	-	+
E	*Saccharomyces cerevisiae*	-	+	+	+	+
F	*Saccharomyces cerevisiae*	-	+	+	+	+

A: Unpasteurised *fura de nunu*, B: Pasteurised *fura de nunu*, C: Pasteurised *fura de nunu* treated with 300 mg/l sodium benzoate, D: Pasteurised *fura de nunu* treated with 200 mg/l sodium benzoate, E: Pasteurised *fura de nunu* treated with 1000 mg/l sorbic acid, F: Pasteurised *fura de nunu* treated with 750 mg/l sorbic acid.

+: Present, -: Absent

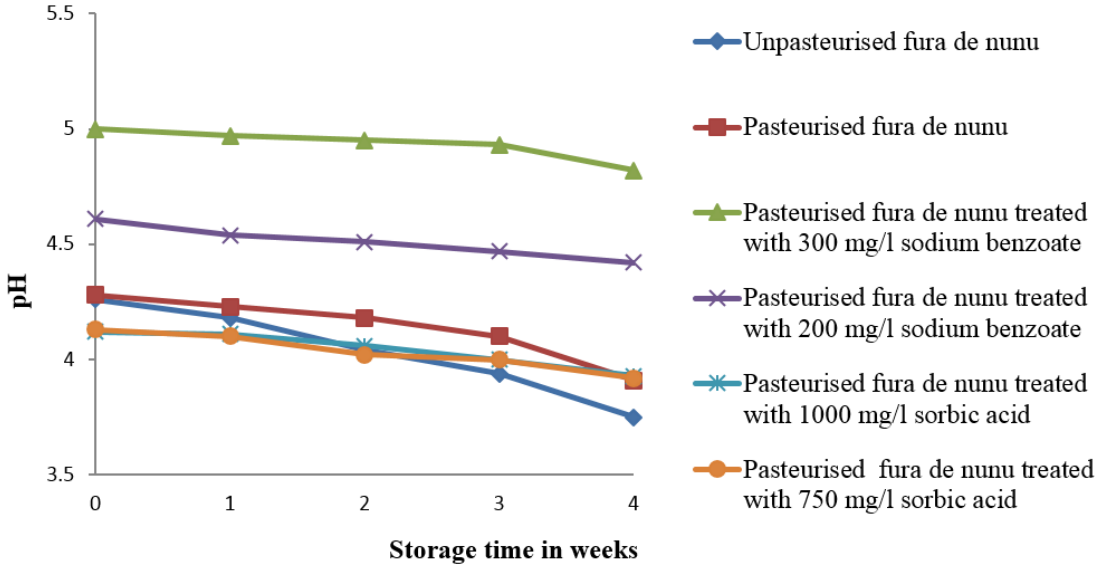

Figure 1. pH of Fura de nunu at Refrigeration Temperature

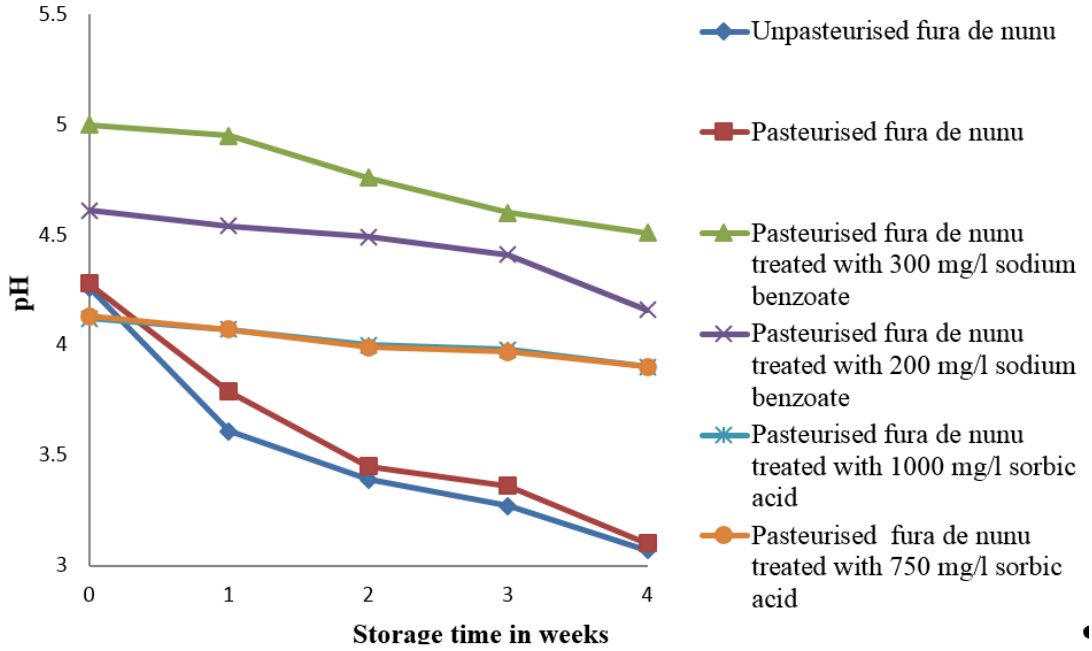

Figure 2. pH of Fura de nunu at Ambient Temperature

Akabanda *et al*., 2010 reported that *nunu*, however, was found to be microbiologically safe as no Enterobacteria survived by 48 h of fermentation when pH decreased below 4.0. The results showed that good quality *fura de nunu* with better shelf life can be produced by pasteurisation and addition of sodium benzoate and sorbic acid. Pasteurised *fura de nunu* sample treated with sodium benzoate had the lowest lactic acid bacteria population. The number of lactic acid bacteria in pasteurised *fura de nunu* treated with sorbic acid had higher population of lactic acid bacteria which are potentially probiotic organisms that help in maintaining intestinal balance.

4. CONCLUSION

The study has established that 200 and 300 mg L^{-1} of sodium benzoate when applied in combination with pasteurization at 70 °C for 15 minutes could effectively suppress Total Viable count, Lactic acid bacteria count and yeast count in *fura de nunu* for 4 weeks at ambient and refrigeration temperatures. It has also been found from this study that sorbic acid applied at 750 and 1000 mg L^{-1} together with pasteurization was also effective in extending the shelf-life of fura de nunu at both storage temperatures, though to a lesser extent. Also established in this study are the microbes associated with microbial deterioration of *fura de nunu* which are mainly LAB and yeasts.

REFERENCES

Abiose and Adeniran, H.A., Studies on Extension of Shelf-life of Roselle (*Hibiscus sabdariffa*) Extract Ife *Journal of Technology*, 19 (1): 34-39, 2010.

Adam, M. R. and Moss, M. O., Food Microbiology. Published by the Royal Society of Chemistry, Thomas Graham House, Science Park, Cambridge, 1999.

Adebayo, G. B., Otunola, G. A. and Ajao, T. A. Physicochemical, Microbiological and Sensory Characteristics of Kunu Prepared from Millet, Maize and Guinea Corn and Stored at Selected Temperatures. *Advance Journal of Food Science and Technology*, 2(1): 41-46, 2010.

Adebesin, A. A., Amusa, N. A. and Fagade, S. O., Microbiological qualities of locally fermented milk (nono) and fermented cereal mixture (fura

de nono) drink in Bauchi. *The Journal of Food Technology in Africa*, 6: 87-89, 2001.

Adegoke, G. O. and Babalola, A. K., Characteristics of microorganisms of importance in the fermentation of fufu and ogi - two Nigerian foods. *Journal of Applied Bacteriology*, 65: 449- 453, 1988.

Adolfsson, O., Meydani, S. N. and Russel, R. M., Yoghurt and gut function. *The America Journal of Clinical Nutrition*, 80: 245-256, 2012.

Akinrele, I. A., Fermentation studies on maize during the preparation of a traditional African starch cake. *Journal of the Science of Food and Agriculture*. 21: 619-625, 1970.

Akabanda, F., Glover, R. L. K., Owusu-Kwanteng, J. and Tano-Debrah, K., Microbiological characteristics of fermented milk product, "nunu". *Nature and Science*, 8(9): 178-187, 2010.

Baningo, E. O. I., De Man., J. M. and Duitschaever, C. L., Utilization of high-lysine corn for the manufacture of ogi using a new improved processing system. *Cereal Chemistry*, 52: 559-572, 1974.

Beukes, E. M., Bester B. H., Mostert, J. F., The microbiology of South African traditional fermented milk. *International Journal of Food Microbiology*, 63: 189-197, 2001

Corsetti, A., Lavermicocca, P., Morea, M., Baruzzi, F., Tosti, N. and Gobbetti, M., Phenotypic and molecular identification and clustering of lactic acid bacteria and yeast from wheat (species *Triticum durum* and *Triticum aestivum*) sourdoughs of southern Italy. *International Journal of Food Microbiology*, 64: 95- 104, 2001.

Fawole, M. O. and Osho, B. A., Laboratory Manual of Microbiology. Spectrum Books, Ibadan, 2002.

Foegeding, P. M. and Busta F. F., Chemical food preservatives. In: Block, S. S. (ed.) Disinfection, Sterilization and Preservation, 4th edition. Lea and Febiger, Philadelphia, 1991.

Fraizer, W. C. and Westhoff, D. C., Food Microbiology. 3rd Edn., Tata Mc Graw-Hill Publishing Company, New York, 1978.

Frank, J. F., Milk and dairy products. In: Food Microbiology, Fundamentals and Frontiers (Eds.: Doyle, M. P., Beuchat, L. R., Montwille, and T. J.). *American Society for Microbiology*,Washington, DC., pp. 101–116, 581–594, 1997.

Gadaga, T. H., Mutukumira, A. N., Narvhus, J. A. and Feresu, S. B. (1999). A review of traditional fermented foods and beverages of Zimbabwe. *International Journal of Food Microbiology*, 53: 1-11, 1999.

Gibbs, B. M and Shapton, D. A., Identification Methods for Microbiologist. Academic Press Inc, London, 1968.

Gupta, R. K., Food and Industrial Microbiology. Food Preservation. Duala Khan, New Delhi, 2007.

Halm, M., Lillie, A., Spreusen A. K. and Jakobsen, M., Microbiological and aromatic characteristics of fermented maize doughs for kenkey production in Ghana. *International Journal of Food Microbiology*, 19: 135-143, 1993.

Harrigan, J. R. and McCance, M., Laboratory Methods in Food and Dairy Microbiology, Academic Press, London, 1976.

Harrigan, W.F., Laboratory Methods in Food Microbiology. San Diego: Academic Press, 1998.

Isono, Y., Shingu, I. and Shimizu, S., Identification and Characteristics of lactic acid bacteria isolated from Masaï fermented milk in Northern Tanzania. *Bioscience Biotechnology Biochemistry*, 58: 660-664, 1994.

Mathara, J. M., Schillingera, U., Kutima, P. M., Mbugua, S. K., Holzapfel, W. H., Isolation, identification and characterisation of the dominant microorganisms of kule naoto: the Maasai traditional fermented milk in Kenya. *International Journal of Food Microbiology*, 94: 269– 278, 2004.

Mclandsborough, L., Food Microbiology Laboratory. CRC Press, Boca Raton, 2005.

Nebedum, J. O. and Obiakor, T., The effects of different preservation methods on the quality of nunu, a locally fermented Nigerian dairy product. *African Journals of Biotechnology*, 6 (4): 454-458, 2007.

Jay, J. M., Modern Food Microbiology (5th ed.). Chapman and Hall, New York, 1996.

Odunfa, S. A., African fermented foods. In: Wood, B. J. B. (Ed.). Microbiology of Fermented Foods. Elsevier Applied Science Publishers, London, 1985.

Olalokun, E. A., Milk production in West Africa: objectives and research approaches. Journal *of Association of Advancement Agriculture in Africa*, 3: 5-13, 1976.

Oyeyiola, G. P., Microbiological and biochemical changes during the fermentation of maize (*Zea mays*) grain for masa production. World Journal of Microbiology and Biochemistry, 6: 171-177, 1990.

Prescott, L. M., Harly. J. P. and Kleen, D. A., Food Microbiolgy. 5th Edn., McGraw Hill Book, New York, 2002.

Umoh, V. J., Adesiyuh, A. C. and Gomwalk, N. E., Enterotoxin production by Staphylococcus isolates from fermented milk product. *Journal of Food Protection*, 5: 534- 537, 1998.

Wallander J. F, Samson, A. M., Effect of certain heat treatments on the milk lipase system. *Journal of Dairy Science*, 50: 949-955, 1967.

William. C. F and Westhoff, D. C., Food Microbiology fourth Edition. Mcgraw-Hill Publishing Company limited, New Delhi, 1995.

Wood, B. J. B. and Holzapfel, W. H., The Genera of Lactic Acid Bacteria Vol. 2. Blakie Academic and Professional, an Imprint of Chapman and Hall, Wester Cleddens Road, Bishopbriggs, Glasgow, 1995.

Yahuza, M. L., Small - holder dairy production and marketing constrains in Nigeria. In: Rangnekegr, D. and Thorpe, W. (Eds). Proceedings of a South – South workshop held at National Dairy Development Board (NDDB). Anand, India, and ILRI (International Livestock Research Institute), Nairobi, Kenya, 2001.

Full Paper

EFFECTS OF NON-POTABLE WATER ON THE STRENGTHS OF CONCRETE

A.M. Olajumoke
Department of Civil Engineering, Obafemi Awolowo University, Ile-Ife.
aolajumo@yahoo.co.uk,

I.A. Oke
Department of Civil Engineering, Obafemi Awolowo University, Ile-Ife.

K.A. Olonade
Department of Civil Engineering, Obafemi Awolowo University, Ile-Ife.

A.A. Laoye
Department of Civil Engineering, Obafemi Awolowo University, Ile-Ife.

ABSTRACT

Concrete is a composite material made from a mixture of cement, aggregates and water. This study presents the effects of non-potable water on the strengths of concrete. Tap, stream and partially polluted stream water samples were used in moulding the concrete. Optimum water-cement ratios (w/c) were determined for each of the water samples. Concrete specimens were prepared using nominal mix proportion of 1:2:4 and optimum water-cement ratio (w/c) of the known water quality. The concrete specimens were cured by total immersion in water. Compressive and flexural strengths of the concrete were determined using standard methods. The results showed that the optimum w/c were 0.65, 0.55 and 0.65 for concrete made with tap water (A), non-polluted stream water (B) and polluted stream water (C) respectively. At 28-day curing, their compressive strengths were 18.3, 17.13 and 18.00 N/mm^2 while at 56-day curing the compressive strengths were 25.60, 20.87 and 22.56 N/mm^2 respectively. The pHs of the water samples (A, B, C) were 6.7, 9.5 and 6.7 respectively. The concrete made with water (A) gave the highest compressive and flexural strengths while the concrete made with water (B) gave the least strengths. It was concluded that the two stream waters (B and C) are acceptable for concrete production but concrete made with water (C) gave better results. The stream water polluted by partially treated effluent from biological treatment plant does not have serious adverse effect on the strengths of concrete.

Keywords: *Concrete, strength, stream water, suspended solid, treated wastewater.*

1. INTRODUCTION

Concrete is a versatile construction material. It can be easily produced and within short time hardens and develops considerable strength to sustain large loads. Water is an essential ingredient of concrete production as it activates the exothermic chemical reaction with cement. The reaction usually results in the formation of strength giving cement gel in which the quantity and quality of water used are important in this regard. Gross shortage of potable water for domestic use has necessitated the search for alternative sources of water for concreting. This is a common practice almost everywhere, especially in developing countries, like Nigeria, where the cost of water treatment is prohibitive and potable water is almost not available. In addition to the scarcity of potable water for mixing concrete, indiscriminate disposal of domestic and industrial wastes into rivers and streams is making availability of adequate water for concreting more critical. In fact, the substitution of potable water with water from another source for concrete production has many associated problems and risks that must be removed in order to ensure adequate quality and performance of concrete. The study of effects of impurities in water on concrete properties is attracting interest of many researchers because of indispensable nature of concrete to infrastructural development

Impurities (liquid and solid types) can adversely affect performance of concrete. In the work of Oktar *et al*. (1996), impurities in mixing water has been implicated to have been responsible for efflorescence, staining, corrosion of reinforcement, volume instability and reduced durability of concrete. Akinkurolere *et al*. (2007) investigated the effect of salt water on compressive strength of concrete for a constant water-cement ratio (w/c) over different periods of curing with four different possibilities of casting and curing. These are casting and curing with fresh water, casting and curing with salt water, casting with fresh water and curing with salt water and casting with salt water and curing with fresh water. They found that, concrete cast and cured with salt water had drastic increase in 28-day compressive strength. However, use of adequate water-cement ratio (w/c) is important for strength development especially in hot climate, as adequate moisture needed to be available during the first few hours of placing the concrete to aid the hydration process (Ait-Aider *et al*. 2007).

It should be noted that BS EN 1008 (2002) permits the use of natural water and industrial waste water for making concrete but recommends that appropriate tests be carried out to determine their suitability. However, in order not to compromise strengths and durability, limits are usually set for the amount of chloride, sulphate, alkalis and suspended solids in water for concrete production. Also, BS EN 1008 (2002) recommends that the compressive strength of concrete made with water from source other than potable water should not be less than 90% of that made with potable water. Consequently, many authors (Cebeci and Saatci, 1989; Lee et al., 2001; Tahaet al. 2010) have reported on the use of alternative water sources to make concrete. Cebeci and Saatci (1989) reported that untreated domestic sewage is not recommended for mortar and concrete production as it increases the initial setting time and entrained air as well as reduces strength. The effects of all these are detrimental to durability of concrete. The authors added that the characteristics of treated sewage need to be determined for conformity to standards before use for mortar and concrete production. The use of wash water, underground water, ground water and production water for concrete production have been studied by some authors (Su et al. 2007; Al-

Harthyet al., 2005). They found concrete made with wash water or underground water to give compressive strength that was as good as that made with tap water. Al-Harthy et al. (2005) reported that concrete made with groundwater and production water gave lower compressive strength than that made with tap water but the strength was within the acceptable range for flowable fill mixes at 28-day. Flowable fill is a low strength, self-compacting material usually for backfill purposes. Similarly, the use of production and brackish water did not have serious adverse effects on setting time and strength of mortar and concrete (Tahaet al., 2010). On the other hand, Ayininuola (2009) investigated the effects of Ogunpa (Ibadan) stream water on the compressive strength of concrete and found it to be unsuitable for concrete production due to its high level of pollution. Also, El-Nawawy and Ahmad (1991) reported that use of treated effluent alone is unsuitable for concrete production but found the use of up to 20% of treated effluent with potable water gives concrete of acceptable strength.

These show that not all non-potable waters are suitable for concrete production. Therefore, there is need to document results of research on the effects of non-potable water (stream water, partially polluted water or treated sewage effluents) around us on the strengths of concrete before use. By this, correct strength would have been used in the design of concrete structures and this will prevent collapse of such structures that may be due to inadequate strength. Also, this will allow us to identify suitable alternative sources of water for concrete production in order to reduce the need for potable water in sandcrete and concrete production in Nigeria. This is important because currently potable water supply per capita in the country is below the World Health Organisation (WHO) limit of 100 litres per capital per day (lcd) (Oke, 2010).

The focus of this study is to investigate the effects of water from selected sources (of know quality) on the concrete strengths. The study is initiated based on the field observations that many contractors are using these alternative sources of water under study for concrete production without having adequate information on their quality characteristics. It is also noted that treated effluent from biological plant is commonly used for irrigation purposes, but information on its usage for making and curing concrete is limited in Nigeria. Therefore, the results of this study would be a useful guide to potential contractors and house owners in choosing better alternative source(s) of water for mixing concrete. It will also reduce their dependence on the scarce potable water supply for concrete production which has potential for sustainable infrastructural development in concrete structures.

2. MATERIALS AND METHOD

The cement used was Ordinary Portland Cement (OPC) of brand name Elephant and produced by Lafarge/WAPCO Cement Company of Nigeria. It was purchased from a main distributor in Ile-Ife, Osun State. The chemical composition of the cement was determined by X-ray fluorescence (XRF) analysis. The fine aggregate used was obtained from a location beside the new site of the Natural History Museum at Obafemi Awolowo University (OAU), Ile-Ife, Osun State. The particle size distribution curve of the aggregate was determined in accordance with BS 812-103-1 (1985) procedure. Coarse aggregate of maximum size 19 mm was used in this study and was obtained from a construction site at the OAU campus, Ile-Ife. Three sources of water for this study were from Ile-Ife area, Osun State. The tap water, A, as control was obtained from OAU campus; 'unpolluted' stream water, B, was taken under a bridge (at the maintenance junction along Road 1, OAU main gate, Ile-Ife) at one kilometer downstream the dam and stream water, C, was taken under a bridge (one kilometer away from OAU campus main gate along Ife-Ede Road) and at 1.5 km downstream from point of effluent discharge into the stream from an educational institutional oxidation pond. The stream waters were collected during the dry season when pollution and suspended solids of surface water are usually high.

Water samples collected from the three sources were analysed using standard methods (APHA, 1998) to determine the pH value, chloride, sulphate and suspended solids. The concrete cubes were made in accordance with procedure in BS 1881; Part 108 (1983). Batching by weight was used in the concrete production of nominal mix of 1:2:4 at optimum water-cement ratios (w/c) of 0.65, 0.55 and 0.65 for waters (A), (B) and (C) respectively. Optimum w/c for each of the water was used to ensure that the concrete mixes were properly hydrated. The use of adequate w/c is a means of ensuring good curing practice as enough moisture needed to be available during the first few hours of placing the concrete especially in hot climate (Ait-Aidut et al., 2007). Due to small quantity of concrete per batch, manual mixing of the constituents on hard non-absorbent surface was adopted and the concrete cubes produced using steel moulds were of size 150 mm × 150 mm×150 mm. The filling of the mould in each case was in three layers and were manually compacted using 25 mm diameter steel rod at minimum strokes of 35 per layer. The cubes were demoulded after 24 hours and cured in the three water samples (A, B and C) for a period of 3, 7, 14, 21, 28, and 56 days under laboratory conditions. Concrete cube specimens were tested to determine the compressive strength at each curing age. The average crushing loads for three cubes was recorded in each case. Also, concrete beams were cast using steel mould of size 150 mm ×150 mm×500 mm. The mould was removed after 24 hours when the concrete had set. Thereafter, the beams were cured separately in the water samples for 28 and 56 days. The standard test method described by ASTM C 78 was followed using symmetrical two-point loading method. According to Shetty (2007) the two-point loading method gives lower yield value of modulus of rupture (MOR) than the central loading method, this gives conservative but safe design results. The load that caused failure of each beam was recorded. The flexural strength in terms of MOR was determined for the unreinforced beam specimens and the load carrying capacity determined for the reinforced concrete beam specimens. Average of three readings was recorded in each case.

3. RESULTS AND DISCUSSIONS

3.1. Properties of Cement and Fine Aggregate

Table 1 shows the chemical properties of the cement used in this study as determined from the X-ray fluorescence techniques. The chemical composition of the cement is within the acceptable range as specified by BS EN 196-2 (1995). The particle size distribution curve of the sieve analysis carried out on the fine aggregate is shown in Figure 1. The value of the uniformity coefficient (U_c) was 4.73 and that of coefficient of curvature (C_c) was 1.15 (not much different from 1.0). These indicate that the fine aggregate is well graded. Also, as too much fines (silt and clay) content in aggregate has adverse effects on strength of concrete, the percentage of fines was found to be 5.12% and 2.68% for silt and clay respectively. These were less than 10%, which makes the aggregate acceptable for concrete.

Table 1: Chemical composition of the cement

Major oxides	Chemical composition (%)								LOI
	SiO_2	Al_2O_3	Fe_2O_3	CaO	MgO	*Na_2O	K_2O	SO_3	
Cement used	20.8	3.1	2.5	64.5	1.7	0.23	0.85	2.5	3.4
BS EN 196-2 (1995) reference	18-24	2.6-8.0	1.5-7.0	61-69	0.5-4.0	-	0.2-1.0	0.2- 4.0	

*The Code considers the XRF method to determine the Na_2O content as inappropriate because of inadequate precision obtainable at present.

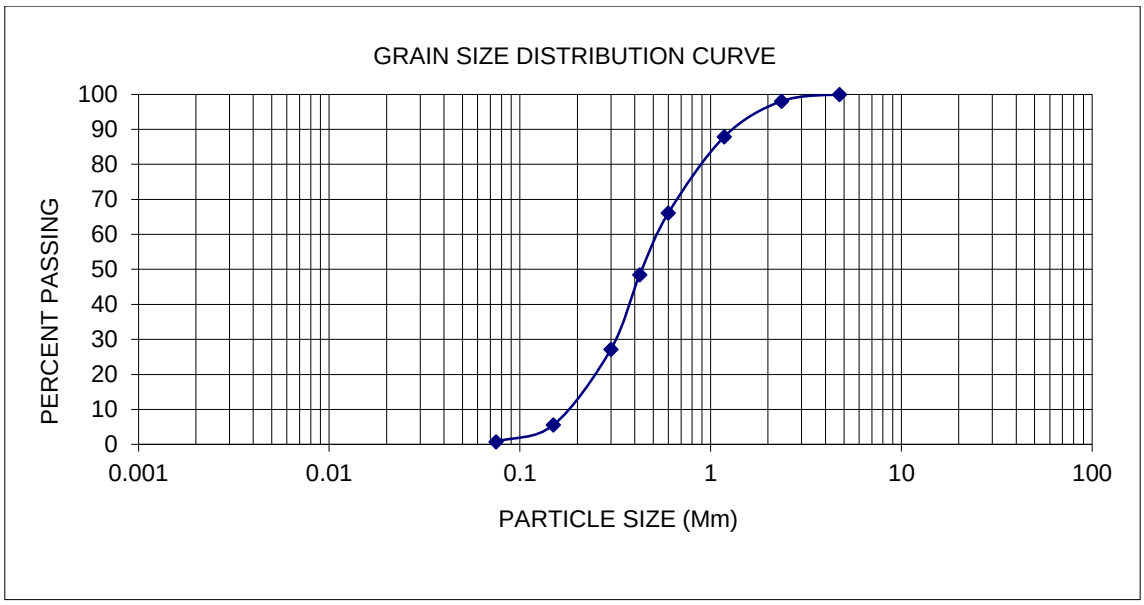

Figure 1: Particle size distribution curve of the fine aggregate.

Table 2: Comparison between qualities of water samples with the standard

Sample	Alkalinity (mg/L)	Chloride (mg/L)	Sulphate (mg/L)	Total solids (mg/L)	Total suspended solid (mg/L)	pH
A	63	16	82.50	300	60	6.7
B	12	17	111.15	760	170	9.5
C	48	18	40.65	240	160	6.7
SON	150	250	100	500	-	6.5 - 8.5

3.2. Water Quality Analysis

Physical observation of the two stream waters (B) and (C) showed that they had no offensive odour, no floating organic matter; but stream water (B) was a little bit turbid while stream water (C) was brackish in colour. The results of the analysis of water samples (A, B and C) which were compared with the standards specified by Standard Organization of Nigeria (SON, 2007) for drinking water in Nigeria are shown in Table 2. It is seen that the alkalinity and chloride contents of all the three water samples were below the maximum specified by the Standards (150 mg/L and 250 mg/L respectively). Similar trend is observed in sulphate content except that water (B) contained sulphate which is about 12% higher than specified (100 mg/L). It is suspected that the high content of sulphate in water (B) may be due to the discharge of the alum residues into the downstream of Opa River from which the water was taken. The pH value of stream waters (A and C) was 6.7 each which is in the range of 6.5 – 8.5 specified by SON whereas the pH value of stream water (B) was highest with a value of 9.5.

It is equally observed that stream water (B) had the highest total solids (760 mg/L) which is higher than the acceptable standard as well as total suspended solids (170 mg/L). This could also be due to the sludge from the waterworks being disposed into the river.

3.3. Effects of the Non-Potable Waters on Workability, Compressive and Flexural Strengths of Concrete

The slump values of the fresh concrete made with waters (A, B and C) at optimum water-cement ratio (w/c) were 50, 40 and 55 mm respectively. These show that concrete made with water (C) has the highest slump and was the most workable at optimum w/c. The slump value of the concrete made with stream water (B) was lower than that of stream water (C); this might be due to the quantity of total solids as shown in Table 2. Also, the effect of the three water samples on the compressive strength of the concrete made from and cured in them for 3, 7, 14, 21, 28 and 56 days was studied. The relationship between the curing ages and compressive strength for each water source is shown in Figure 2. The different effect of the waters on the compressive strength can be observed when they were used to mix and cure concrete. Compressive strength of concrete made with each of the water samples had positive logarithmic correlation (R^2 = 0.970, R^2 = 0.997 and R^2 = 0.989 for waters A, B and C respectively) with the increase in age.

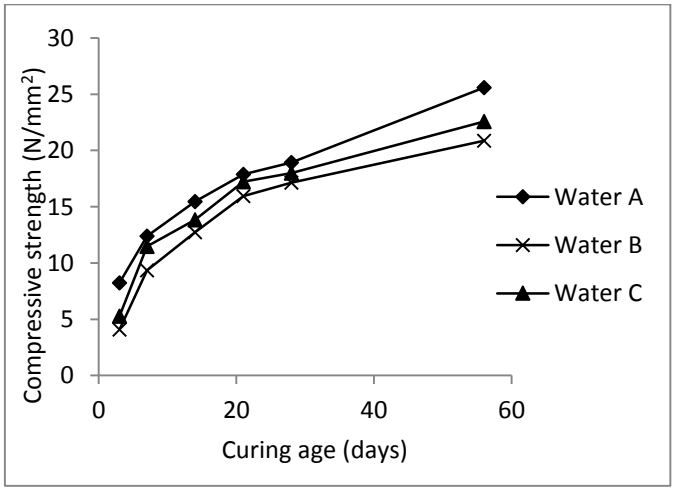

Figure 2: Compressive strength of concrete at different ages

It can also be observed from Table 3 that at 28-day curing, the highest compressive strength (18.93 N/mm^2) was obtained when tap water (A) was used while the concrete made with water (B) had the least compressive strength (17.13 N/mm^2). At 56-day curing the compressive strength was 25.60, 20.87 and 22.56 N/mm^{2}for waters A, B and C respectively. Also, at 28-day the compressive strength of

concrete made with water (B) was 90% of that made with water (A) while that of water (C) was 95% of that of water (A). However, at 56-day these were 81% and 88% respectively. These show that the concrete made with tap water (A) developed strength at higher rate than that made with waters B and C respectively.

Table 3: Compressive and flexural strengths of the concrete at 28-day and 56-day curing

Water sample	Water-cement ratio (w/c)	Compressive strength (N/mm^2)		Flexural strength (N/mm^2)	
		28-day	56-day	28-day	56-day
A	0.65	18.93	25.60	2.14	2.89
B	0.55	17.13	20.87	1.40	1.70
C	0.65	18.00	22.56	1.70	2.14

Noting from Table 3 that the compressive strength of concrete made with waters (B and C) at 28-day curing were 90 and 95% respectively of that made with potable water, the BS EN 1008 (2002) recommendations of 90% minimum for the acceptance of such water in concrete production was satisfied. However, the same mix proportion was used in this study; the strength results in Table 3 for concrete made with stream waters (B and C) could be improved if richer concrete mix was used. Therefore, it is recommended that the non-potable waters (B and C) considered in this study can be used for concrete making provided that they do not pose threat to the health of the handler(s).The advantage of the results of this study is that the need for potable water for concrete will be reduced and potable water would be available for domestic uses thereby reducing the prevalence of communicable diseases in our society.

Furthermore, from Table 3 the flexural strength as percentage of the compressive strength of concrete made with waters (A, B and C) at 28-day curing were 11.30, 8.17 and 9.44%, while at 56-day curing it is 11.29, 8.15 and 9.49% respectively. It had been established (Ghosh et al., 1972) that subject to maximum aggregate size, the flexural strength of concrete is about 10% of its compressive strength. In this case only the concrete made with potable water (A) met this criterion and marginally that of stream water C. However, in reinforced concrete structures design, the flexural (tensile) strength of concrete is not usually considered as the steel is assumed to be carrying all the tensile stress, but it is useful in the design of rigid pavement.

3.4. Effect of Non-potable Water on the Load Capacity of Reinforced Concrete Beams

The load carrying capacity at different steel ratio of the cured concrete beams made from the water samples was presented in Table 4. It was observed that for all the mixes, the failure load increased as the percentage of reinforcement increases. Also, similar trend in the compressive strength is observed here in which concrete made with water A gave best result and that made with water C had better result than that made with water B. For instance at 28-day, the percentage increase in the failure load of concrete made with water (C) over that made with water B at steel ratios 1.0, 1.5, 2.0, 2.5% and 3.0 were 18.7, 9.3, 5.2, 12.5 and 23.3% respectively, while at 56-day they were 21.6, 11.9, 8.6, 16.0 and 26.4%, respectively.

Table 4: Load carrying capacity of the beams at different steel ratios

Steel reinforcement percentage (%)		1.0	1.5	2.0	2.5	3.0
Water sample	Curing age (day)	Maximum failure load (kN)				
A	28	22.00	27.20	34.20	43.60	52.50
	56	29.70	36.72	46.18	58.86	70.88
B	28	15.00	20.50	26.80	30.40	35.20
	56	18.30	25.02	32.70	37.08	42.94
C	28	17.80	22.40	28.20	34.20	43.40
	56	22.26	28.00	35.50	43.00	54.26

4. CONCLUSION

This study examined the suitability of non-potable water for making concrete and concludes that:

Concrete made with the two stream waters (B and C) had lower strengths (compressive and flexural) and lower load carrying capacity when reinforced, compared to that made with tap water (A). However, based on the strength criterion, they were found suitable for use to make concrete as their compressive strength was within the permissible 90% of that made with potable water (A); but concrete made with water (C) performed better.

All the waters contained varied quantities of dissolved chemicals and suspended solids. However, water (C) polluted by the partially treated effluent from a biological treatment plant had all quality parameters considered to be within specified standards and did not have serious adverse effect on the strengths of concrete. This showed that water for concrete production does not necessarily have to be safe for drinking; a way of reducing the need for scarce potable water for concrete production.

There is need to determine necessary quality characteristics of alternative source of water other than potable water before use for concrete production in order not to compromise strengths and durability. Also, further studies are needed to ascertain the long term effects of these stream waters (B and C) on the deterioration of concrete due to carbonation and corrosion respectively.

REFERENCES

Ait-Aider, Hannachi, N.E. and Mouret, M.,'Importance of W/C ratio on compressive strength of concrete in hot climate'.Building and Environment. 42(6): 2461- 2465, 2007.

Akinkurolere, O.O., Cangru J. and Shobola, O.M.,'The influence of salt water on the compressive strength of concrete'. Journal of Engineering and Applied Sciences. 2(2): 412-415, 2007.

Al-Harthy, A.S., Taha, R. Abu-Ashour, J. Al-Jabir, K. and Al-Oraimi, S.,'Effect of water quality on the compressive strength of flowable fill mixtures'. Cement & Concrete Composite.Vol. 27: 33 – 39, 2005.

APHA, 'Standard Methods for the Examination of Water and Wastewater'. American Public Health Association. 20th edition, Washington, D.C., 1998.

ASTM Standard C 78, 'Flexural strength of concrete (using simple beam with third-point loading)'. ASTM International, West Conshohocken, DOI: 10.1520/C0078-09, 2009.

Ayininuola, G.M.,'Water quality effect on concrete compressive strength: Ogunpa stream water case study'. Civil Engineering Horizon. http://horizon.webinfolist.com/material/2009, 2009.Accessed on 16th June, 2012.

BS 1881: Part 108, 'Method for making test cubes from fresh concrete'. British Standard Institution, London, 1983.

BS 1881: Part 116, 'Method for determination of compressive strength of concrete'. British Standard Institution, London, 1983.

BS 812-103-1, 'Methods for determination of particle size distribution – Sieve tests'. British Standard Institution, London, 1985.

BS EN 1008,'Mixing water for concrete –Specification for sampling, testing and assessing the suitability of water, including water recovered from processes in the concrete industry, as mixing water for concrete'. British Standard Institution, London, 2002.

BS EN 196, Part 2, 'Method of testing cement – Chemical analysis of cement'. British Standard Institution, London, 1995.

Cebeci, O.Z and Saatci, A.M.,'Domestic sewage as mixing water in concrete'. Journal of American Concrete Institute, ACI.503 – 506, 1989.

El-Nawawy, O.A and Ahmad, A.S.,'Use of treated effluent in concrete mixing in arid climate'.Cement and Concrete Composite. Vol. 13: 137 – 141, 1991.

Ghosh, R.K., Chatterjee, M. R. and Lai, L.,'Flexural strength of concrete – Its variations, relationship with compressive strength and use in concrete mix design'. Central Road Institute, India. India Road Research Bulletin No. 126, 1972.

Lee, O.S. Saliu, M.R. Ismail, M and Ali, M.I.,'Reusing treated effluent in concrete technology'. *Jurnal Teknologi*. 34(F): 1- 10, 2001.

Oke, I.A., 'Engineering analysis and failure prevention of a water treatment plant in Nigeria'.Journal of Failure Analysis and Prevention. 10:105-119, 2010.

Oktar, O.N., Moral,H. and Tasdemir, M.A.,'Factors determining correlations between the concrete properties'. Cement and Concrete Research. 26(11): 1629-1637, 1996.

Shetty, M.S.,'Concrete technology: theory and practice'. 6th edition. S.Chand and company Ltd. Multicolour illustrative edition, 2007.

Standards Organisation of Nigeria (SON), 'Nigerian Standard for Drinking Water Quality'. Nigerian Industrial Standard Publication, ICS 13.060.20, 2007.

Su, N. Miao, B. and Liu, F-S., 'Effects of wash water and underground water on properties of concrete'.Cement and Concrete Research. Vol. 32: 777 – 782, 2007.

Taha, R.A. Al-Harthy, A.S. and Al-Jabri, K.S.,'Use of production and brackish water in concrete mixtures'.International Journal of Sustainable Water and Environmental System, IASKS. 1(2): 39 – 43, 2010.

Full Paper

ECO-FRIENDLY INHIBITORS FOR EROSION-CORROSION MITIGATION OF API-X65 STEEL IN CO2 ENVIRONMENT

O.O. Ige
Department of Materials Science and Engineering, Obafemi Awolowo University, Nigeria.
ige4usa@yahoo.com

M.D. Shittu
Department of Materials Science and Engineering, Obafemi Awolowo University, Nigeria.

K.M. Oluwasegun
Department of Materials Science and Engineering, Obafemi Awolowo University, Nigeria.

O.E. Olorunniwo
Department of Materials Science and Engineering, Obafemi Awolowo University, Nigeria.

L.E. Umoru
Department of Materials Science and Engineering, Obafemi Awolowo University, Nigeria.

ABSTRACT

The study of chemical mitigation of erosion-corrosion of API-X65 Steel in a multiphase system containing brine, CO_2 gas, and sand at different shear stresses with two eco-friendly inhibitors are reported. The inhibitors investigated are a commercial grade synthetic product and a natural inhibitor (*Aloe vera*). The mass loss, linear polarization, and scanning electron microscopy techniques were investigated. The results obtained show that both inhibitors maybe useful in oil and gas industry, the synthetic inhibitor have quantifiable advantage over the natural inhibitor. From the results obtained these inhibitors are expected to have credible technical performance and as such reduce considerably the adverse effects on health, safety, and environmental factors associated with inhibition in oil and gas industries.

Keywords: *Erosion-corrosion, Inhibitors, Multiphase system, Steel, Rotating cylinder electrode, and scanning electron microscopy.*

1. INTRODUCTION

The importance of corrosion inhibitors in the oil and gas industry is well established and cannot be underestimated. Corrosion inhibitors are known to prevent discharge of oil and gas through leakages to the environment (Obesekesere *et al.*, 2002). They also play a significant role in internal corrosion control associated with oil and gas production and transportation (Taj *et al.*, 2006). Due to rapid depletion and huge exploitation, future oil and gas productions are expected to occur more in remote areas. This will lead to increasing challenges relating to asset management, which includes; sand presence in production fluids and the shift towards deeper wells. All these may result in difficulties in maintaining the integrity of pipes and process equipment (Wang *et al.*, 2005).

In particular, there have been extensive studies of chemical inhibition of erosion-corrosion. Some of these studies have concluded that corrosion inhibitors are effective in controlling erosion corrosion mechanisms. The attention has been focussed on mechanisms of inhibition, inhibition efficiency, and material degradation phenomena, among others (McLaury *et al.*, 1995; Schmitt, 2001; Ramachandra *et al.*, 2005 and Wang *et al.*, 2005). Research efforts have also been deployed to study the effectiveness of inhibitors in the presence of erosive flows and at different shear stresses (Neville and Wang, 2009).

However, in the majority of these studies related to chemical mitigation of CO_2 corrosion, the focus has been more on superior performance with little or no emphasis on the health, safety, and environmental factors (Chen and Chen, 2002).

However national government of various countries have invoked tighter and stringent conditions due to more severe environmental constraints. Hence several attempts have been made to develop the chemistry that is considered green in nature (Obeyesekere *et al.*, 2000; Killars and Finley, 2001; Chen and Chen, 2002).

There is little previous work that investigated the performance of eco-friendly inhibitors in the erosion-corrosion control. Therefore, the aim of this work is to examine the behaviour of mild steel in the presence of a synthetic "green" chemistry based system and a natural product as corrosion inhibitors in a multiphase system containing brine, CO_2 gas, and sand at different shear stresses. The data obtained are compared for their performance in order to determine the effectiveness of the inhibitors as candidates for inhibition in oil and gas industry.

2. MATERIALS AND METHODS

2.1. Materials

The steel used in this study is as-received API 5L X65 carbon steel with Vickers hardness of 240 HV. The samples were cylindrical shaped with dimensions of 12 mm by 8 mm. The microstructure and chemical composition are as shown in Figure 1 and Table 1, respectively.

2.2. Media and Inhibitors

Table 2 shows the chemistry of the process solutions was prepared according to the work of Hu *et al.* (2011). Two different corrosion inhibitors were studied. They are referred to as Aloe vera and inhibitor NA. The Aloe vera represents a natural inhibitor with green chemistry while the inhibitor NA is a commercially available, high shear eco-friendly CO_2 – based inhibitor.

The Aloe vera leaves were sliced open at the edges and the gel was squeezed out, sieved in order to obtain a clear concentrated semi-liquid. No water was added. The liquid is viscous, colourless, transparent, consists of water (98.5%), and polysaccharides (0.3%) (WHO, 1999). The polysaccharide composition was analysed by gas

-

Table 1: Chemical or elemental compositions of API 5L X65 carbon steel

Element	C	Si	Mn	P	S	Cr	Mo	Ni	Ti	Fe
Wt (%)	0.10	0.18	1.21	0.009	0.003	0.10	0.16	0.07	<0.01	Balance

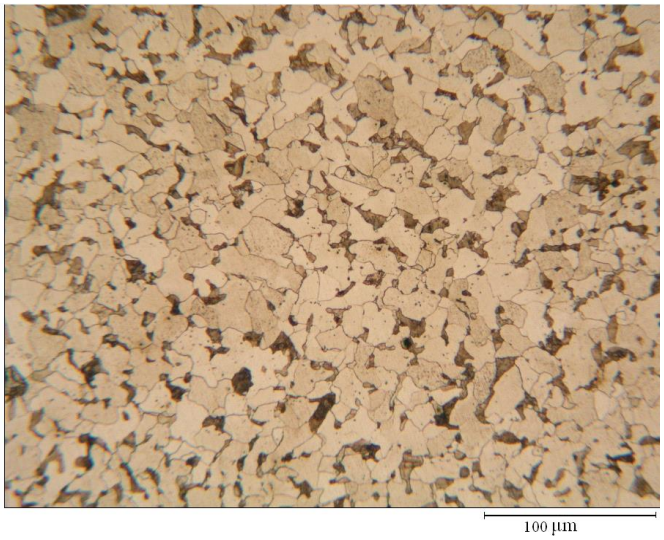

Figure 1: Optical microscope image of API 5L X65 carbon steel after being polished and etched in 2% nital solution for 10 seconds (dark background = pearlite and lighter background = ferrite)

Table 2: Composition of brine used in flow-induced corrosion and erosion-corrosion tests

Preparation	(mg/L)
NaCl (sodium chloride)	24090
KCl (potassium chloride)	706
$CaCl_2 \cdot 2H_2O$ (calcium chloride di-hydrate)	1387
$MgCl_2$ (magnesium chloride)	4360
$BaCl_2 \cdot 2H_2O$ (barium chloride di-hydrate)	16
$SrCl_2 \cdot 6H_2O$ (strontium chloride hexa-hydrate)	33
Na_2SO_4 (sodium sulphate)	3522
$NaHCO_3$ (sodium bicarbonate)	304

liquid chromatography and it reveals pectins, hemicellulose, glucomannan, acemannan, and mannose derivatives. It also contains amino acids, lipids, sterols, tannins and enzymes (WHO, 1999). The chemical preparation for inhibitor NA was based on a combination of ethandiol, ethoxylated imidazolines, carboxylic acid salts, and thioalcohol. The inhibitors were tested at concentrations of 0, 25, 50, 75, and 100 ppm (Table 3).

Table 3: Experimental matrix for rotating cylinder electrode (RCE)

Parameters	Conditions
Material	API 5L X65 in as-received condition
Temperature (°C)	50
CO_2 partial pressure (Bar)	1
Rotating cylinder speed (rpm)	1000, 3000, and 5000
Inhibitor	Aloe vera and G
Inhibitor concentrations (ppm)	0, 25, 50, 75, and 100
Stirrer speed (rpm)	750
Sand concentrations (mg/L)	0 and 500
Exposure duration (hours)	4

The inhibition efficiency was calculated using the following formula:

$$\text{Inhibition Efficiency} = \frac{(CRNI - CRWI)}{CRNI} X\ 100 \quad (1)$$

where CR_{WI} and CR_{NI} are the experimental corrosion rates with and without inhibition, respectively.

2.3. In-situ Corrosion Measurements

The erosion-corrosion tests were carried out using a rotating cylinder electrode (RCE) arrangement as shown in Figure 2. The RCE experiments were conducted in line with the work of Wang *et al.* (2005). The experimental matrix for the tests is as presented in Table 3. The hydrodynamic parameters of the RCE in terms of the Reynolds number R_e (Dalayan *et al.*, 1995) and wall shear stress (τ_ω) (Gabe and Walsh, 1983) used in this study are presented in Table 4. The tests were conducted with 500 mg/L of sand and the average diameter of the round silica sand used in these studies was 250 µm. The shape and size distribution are as illustrated in Figures 3a and 3b. The in-situ corrosion rate for the RCE was determined by using linear polarization resistance (LPR) technique according to the work of Hu *et al.* (2011). Also the specimens were weighed prior to exposure and after the tests to determine the total weight loss of each specimen using an analytical balance with the accuracy of 0.0001 g.

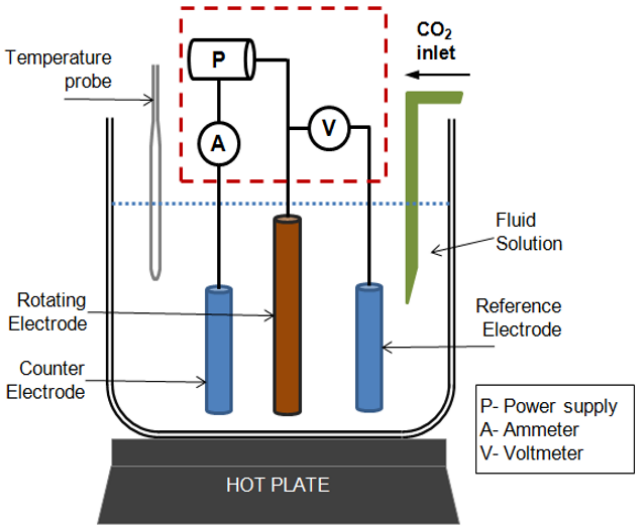

Figure 2: The set-up of the rotating cylinder electrode (RCE)

2.4. Scanning Electron Microscopy (SEM)

The possible mechanisms of degradation was investigated by SEM and the analysis revealed the extent and nature of the mechanical and electrochemical damage in the absence and presence of inhibitors (Figures 10a, b, and c).

3. RESULTS

3.1. Erosion-corrosion Mass Loss

A typical illustration of the total mass loss obtained for the steel samples subjected to different flow velocities is shown in Figure 4. There is a sharp reduction in the material degradation rates when *Aloe vera* inhibitor is added to the system at a lower velocity regime (1000 rpm) leading to almost 50% reduction in the thickness loss. Further decrease was observed when the synthetic inhibitor is added to the solution. However, a remarkable decrease in the material loss was observed when the inhibitors were added at a higher velocity (5000 rpm). Although the percentage reduction decreases as the velocity increases, the commercial inhibitor used still exhibits better

performance than the *Aloe vera* with about 50% reduction in corrosion rate compared to about 33% in the case of *Aloe vera*. It was observed that the corrosion rate increases as the flow velocity increases for uninhibited and inhibited solutions.

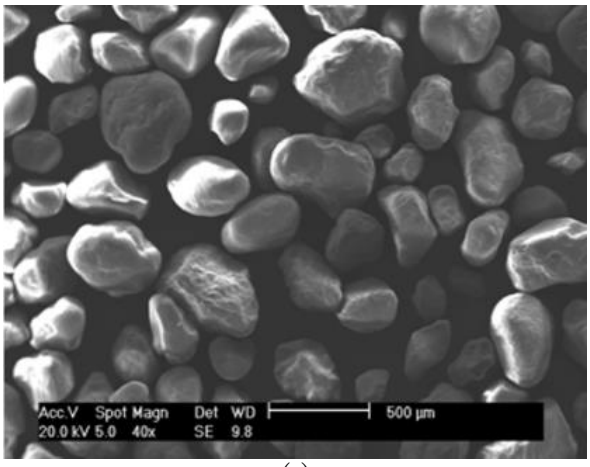

(a)

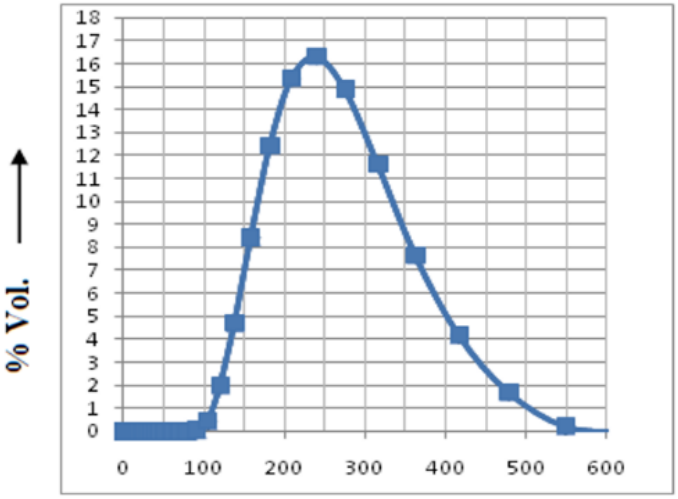

(b)

Figure 3: (a) Sand particles' shape and sizes from SEM and (b) Sand particles' size distribution from sieve analysis.

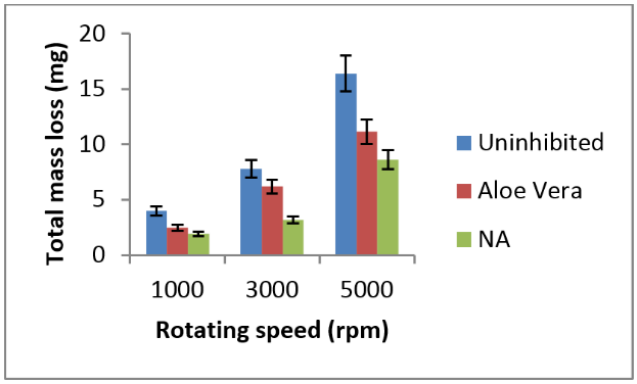

Figure 4: Comparison of total mass loss (mg) as a function of the rotating speed (rpm) and 50oC for uninhibited and 100 ppm of the inhibitors

3.2. In-situ Erosion-corrosion Analysis

The electrochemical measurements of the in-situ corrosion samples subjected to erosion-corrosion were carried out. The linear polarization resistance plot of the solutions when uninhibited and inhibited with *Aloe vera* and inhibitor NA is presented in Figure 5. The result shows that there is little change in the polarization resistance (R_p) for uninhibited solutions at different velocities. The data show that the R_p increases as the flow velocity increases with the highest rate obtained for the synthetic commercial inhibitor. Meanwhile at all velocity regimes the R_p decreases with the introduction of Aloe vera and further reduction occurs in solution inhibited with NA. The reduction becomes significant as the flow velocity increases.

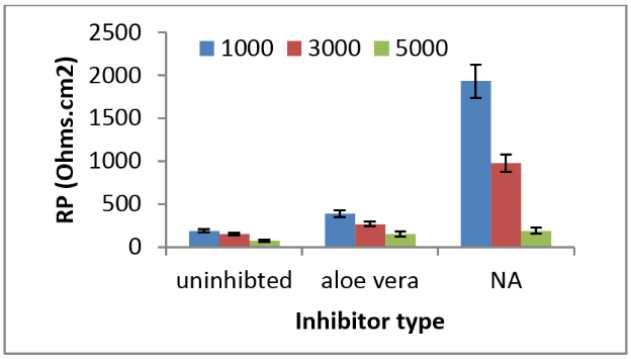

Figure 5: The Rp values from linear polarization at different rotating speeds and 50oC for the various inhibitors

Figure 6 shows the behaviour of the samples with and without inhibitors with respect to the open circuit potential (OCP). The results as presented are representative of a triplicate set of tests. In the uninhibited solution at different velocities, the OCP shifts to the positive direction as the velocity increases (Figure 6a). There is also a large shift towards the positive region as Aloe vera is introduced and a deeper shift is noticed as inhibitor NA is added (Figure 6b). This behaviour is representative of the characteristics of the inhibitors at different velocities.

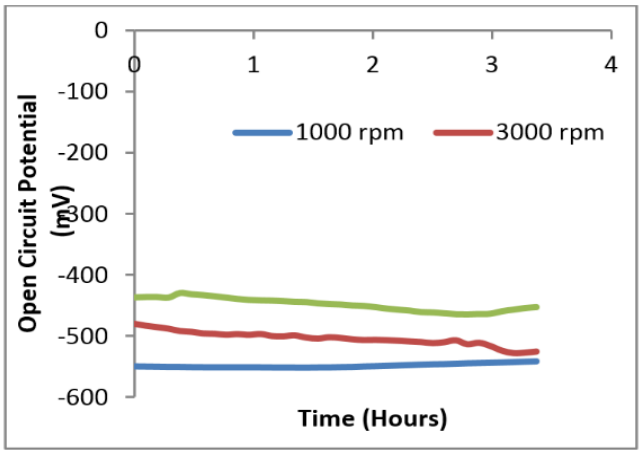

(a)

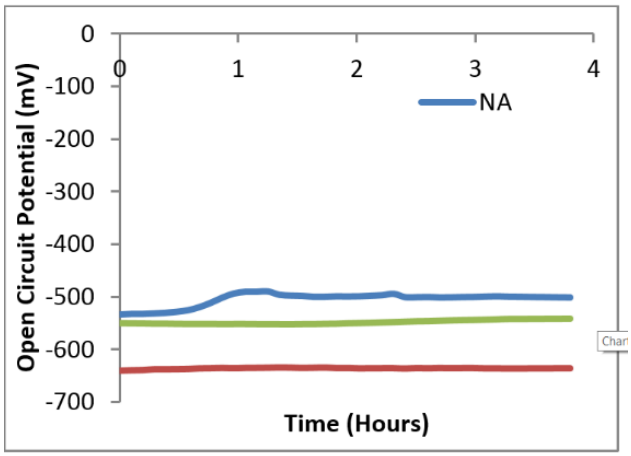

(b)

Figure 6: The effect of open circuit potentials (OCP) as a funtion of time at velocity of 1000 rpm (a) Uninhibited (b) 100 ppm

There were significant reductions in the erosion-corrosion rates as *Aloe vera* was added into the system at different velocities (Figure 7). The figure could be interpreted that there is an increase in the rates of degradation as the flow velocity increases for the uninhibited and inhibited solutions. However at each velocity regime there is considerable decrease in the erosion-corrosion rate with the addition of the inhibitors. At a flow velocity of 3000 rpm the erosion-corrosion rate is about 3 mm/yr, and about 0.5 mm/yr for samples inhibited with Aloe vera while it further reduced to about 0.15 mm/yr for inhibitor NA.

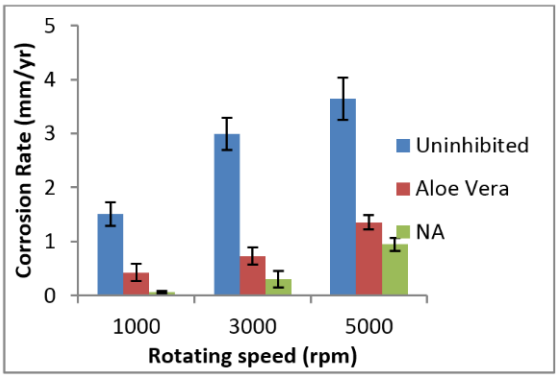

Figure 7: The in-situ corrosion rate of the samples at various rotating speed

3.3. Inhibition Efficiencies (IE%)

The inhibition efficiency is used to assess the performance of inhibitors and it is presented in Figure 8. Typically, the inhibition efficiency for total mass loss for *Aloe vera* decreases as the flow velocity increases. Interestingly the trend is reversed for inhibitor NA (Figure 8a). At lower flow regime the *Aloe vera* may offer better protection than the commercial inhibitor with a margin of about 15%.

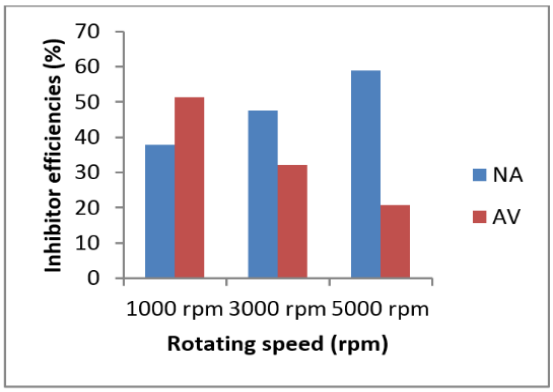

(a)

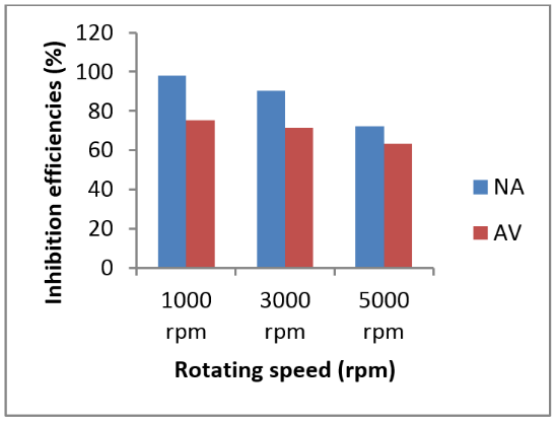

(b)

Figure 8: The inhibition efficiency at various rotating speed as a function of the techniques (a) TML (b) Electrochemistry

However, with increase in the velocity, the reverse occurs with inhibitor NA offering better coverage. Generally, the highest inhibition efficiency for the system is observed at 5000 rpm for inhibitor NA with about 60% while the least efficiency occurs at the same velocity with about 21% efficiency for *Aloe vera*. Figure 8b shows the inhibition efficiency of the inhibitors during in-situ corrosion measurement. Broadly, inhibitor NA exhibited better performance at all velocities and the efficiency decreases as the velocity increases as against the observation that was obtained for the total mass loss. The *Aloe vera* behaves similarly with a relatively lower protection efficiency at 1000 rpm. The maximum coverage occurs at 1000 rpm for inhibitor NA which is around 98% and the lowest is for *Aloe vera* at 5000 rpm with about 60% efficiency.

3.4. Shear Stress Evaluation

The erosion-corrosion rates of the samples as a function of wall shear stress is shown in Figure 9. The shear stress values for RCE were determined according to Silverman and Walsh (1987):

$$\tau_w = 0.0791 Re^{-0.3} \rho r^2 \omega^2 \quad (2)$$

where, Re is the Reynolds Number, ρ is the solution density (g cm^{-3}), ω is the rotation rate (rad/sec), and r is the radius of the outer diameter (cm).

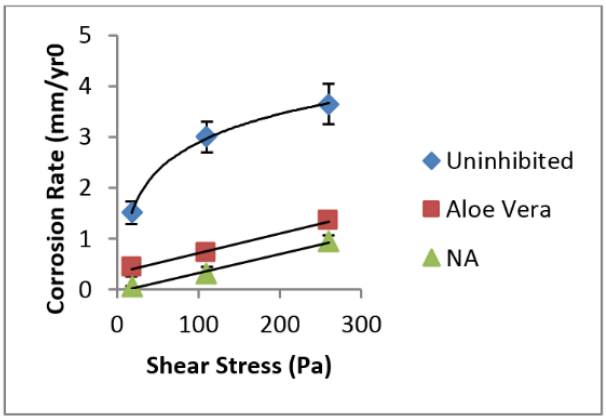

Figure 9: Shear stress vs Corrosion rate

It is observed that the corrosion rates increases as the shear stress increases for both uninhibited and inhibited solutions. The trend of the uninhibited solution displays a logarithmic series while the inhibited solutions show linear relationship.

3.5. Surface Analysis

The morphologies of the specimens subjected to 5000 rpm rotating speed were observed by SEM, as shown in Figure 10. This figure illustrates the behaviour of the samples at different velocities and inhibitor concentrations. Figure 10a is for the uninhibited sample which is characterized by material dissolution and scanty localized attacks. Uniform corrosion is dominant and the surface is roughened-like due to minimal plastic deformation coupled with impact trails. Compared with *Aloe vera* inhibited samples (Figure 10b), relatively higher material dissolution is prevalent, while the ferrite is dissolved leaving cementite protrusions. Carbonate films are suspected and confirmed by elemental composition analysis by energy-dispersive x-ray spectroscopy (EDX). The inhibitor NA adsorbs easily on the samples surface and this confirmed the earlier results reported above (Figure 10c). The adsorptions may have led to a uniform microstructure which consists of an unalloyed iron matrix with a homogeneous distribution of fine cementite (carbide).

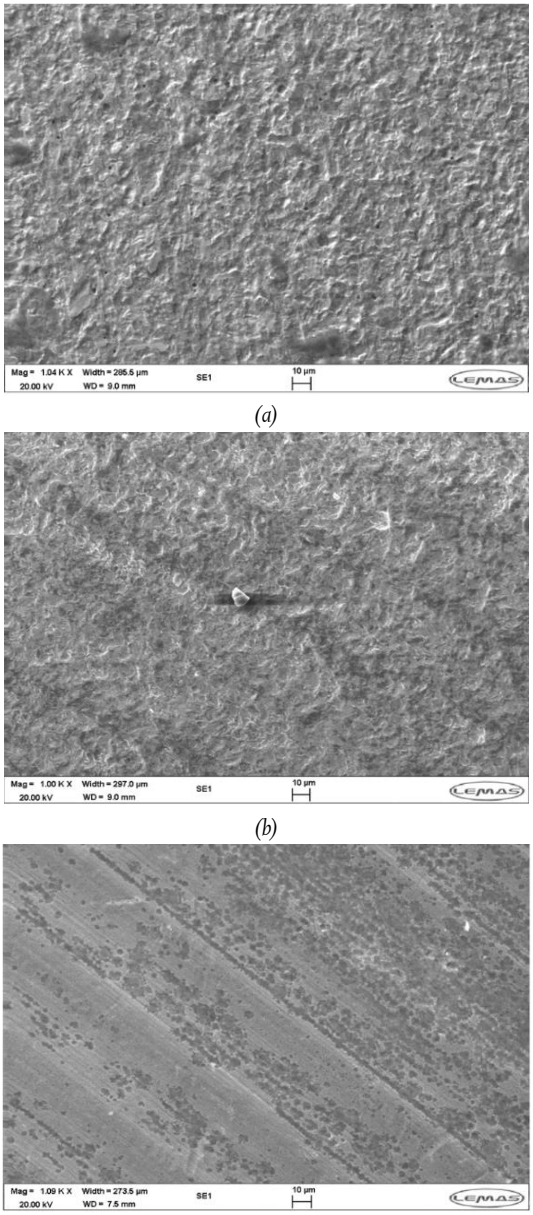

Figure 10: SEM micrograph of uninhibited and inhibited samples at 50 oC (a) uninhibited sample (b) 75 ppm Aloe vera (c) 75 ppm inhibitor NA

4. DISCUSSION OF RESULTS

4.1. Erosion-corrosion Mass Loss Assessment

From Figure 4 it could be inferred that the material loss increases with increase in the rotating speed (flow velocity). This is in agreement with earlier studies (Jiang *et al*., 2005 ; Musa *et al*., 2009). The presence of the inhibitors reduces the degradation tendency at all velocities. Inhibitor NA has the best coverage at all velocities and this can be attributed to the fact that it is a high shear formulated chemical package for CO_2 corrosion.

4.2. Electrochemical Analysis

The polarization resistance (R_p) are relatively stable over time at all velocities and this implies that the corrosion process is charge transfer controlled. The R_p decreases as the flow velocity increases which implies that there is an increase in the corrosion rate due to the increasing rate at which corrosion products are removed from corroded surfaces leading to greater attack on fresh metal surfaces (Figure 5). It has been reported that flow velocity increased the mass transport of electrolytes which may be beneficial in the presence of an inhibitor. However, this may lead to high shear stresses which will result in surface layer removal. This is harmful in the presence of an inhibitor (Jiang *et al*, 2005). The addition of sand may make surface layer removal to be the dominant mechanism because the sand will increase the kinetic energy of the impact on the metal surface. This will lead to an increase material dissolution.

It is observed that the open circuit potential (OCP) moves in the noble direction as the flow velocity increases as shown in Figure 6a. The Pourbaix diagram shows that iron dissolution will be prevalent and the anodic reaction will be the governing mechanism. The presence of inhibitors makes the OCP to move in the positive direction while the inhibitor NA shifts to the noble region, compared to that of *Aloe vera.* This implies that the inhibitors will suppress the anodic dissolution of the unalloyed iron from taking place. The anodic electrochemical reactions for low carbon steel corrosion in CO_2 – containing solution are as follows (Linter *et al*., 2009):

$$Fe = Fe^{2+} + 2e^- \quad (3)$$

$$Fe + H_2CO_3 = FeCO_3 + 2H^+ + 2e^- \quad (4)$$

$$Fe + HCO_3^- = FeCO_3 + H^+ + 2e^- \quad (5)$$

$$Fe + CO_3^{2-} = FeCO_3 + 2e^- \quad (6)$$

The surface morphology reveals that equation (1) is predominant and may be the one that is suppressed by the inhibitors. The inhibitors being organic are regarded as adsorption or film forming inhibitors on metal surface even at high shear stress multiphase system and in the presence of sand particles (Nesic *et al*., 1995; Neville and Wang, 2009).

Generally it is understood in CO_2 corrosion mechanism that mass transfer is important primarily at pH less than 5, when it will affect the limiting currents for H^+ reduction (Nesic *et al*., 1995). The inhibitors are mainly anodic and are expected to block the anodic areas more effectively. Consequently, as coverage increases the ratio between anodic and cathodic areas increases, and so the corrosion rate on the uncovered zones rises. This may leads to unfavourable galvanic effects due to area ratios.

The corrosion rate increasing with shear stress as a power function for uninhibited solution which is according to the work of Effird (1993) while the inhibited solutions have linear relationship and is not in agreement with the earlier study.

4.3. Correlation of Mass Loss and Corrosion Resistance

As shown in Figure 8 the inhibition efficiency of the *Aloe vera* is observed to decrease as the flow velocities increases for both erosion-corrosion mass loss and in-situ corrosion measurements. This confirms earlier studies (Wang *et al*., 2005; 2009). A significant result is that the inhibitor NA inhibition efficiency increases with flow velocity for erosion-corrosion mass loss which is contrary to what is obtained for in-situ corrosion measurement. It must be realised that this inhibitor is specially formulated for high shear CO_2 environment. It is believed that the inhibitors will be adsorbed and as such it can be deduced that inhibitor NA has good protection for the erosion parts (Wang *et al*., 2005; 2009). Although it can be inferred that Aloe vera behaves positively in suppressing the corrosion aspect, it did not perform well in reducing the erosion of the samples.

4.4. Surface Analysis

The surface morphology revealed by SEM characterization showed that material dissolution and defects reduced with addition of the inhibitors. A less damaged surface was found in the case of

inhibitor NA, which is in good agreement with the erosion-corrosion mass loss and in-situ corrosion results.

5. CONCLUSIONS

The results of this study have shown that increase in flow velocity for the erosion-corrosion samples caused a shift in corrosion potential towards positive directions. The inhibitors are anodic/mixed-type. The results show that inhibitor NA has better coverage for multiphase flow system in oil and gas industry. This study has shown that the chemistry of the inhibitors confer adequate inhibiting properties on the X65 steel in CO_2 environment by reducing damage in erosion-corrosion conditions.

ACKNOWLEDGEMENTS

The supervision and permission to use the facilities of iESTL, School of Mechanical Engineering, University of Leeds, UK by Prof A. Neville and Dr X. Hu are duely recognized. OOI will also like to thank the following organizations for their financial assistance: ETF, NIGERIA; NASENI, NIGERIA; Carnegie Corporation through OAU Linkages, NIGERIA and School of Mechanical Engineering, University of Leeds, UK.

REFERENCES

Chen, H.J., and Chen, Y. 'Environmentally friendly inhibitors for CO_2 corrosion', *CORROSION 2002*, NACE 02300, Houston, Texas, 2002.

Dalayan, E., Johar, T., Shadley, J.R. and Shirazi, S.A. 'Hydrodynamic correlations between pipe flow and rotating cylinder electrode (RCE) for oilfield corrosion – some insights', Houston, NACE International, CORROSION/95, paper no. 117, 1995.

Efird, K.D. Wright, E.J. Boros, J.A. and Hailey, T.G. 'Correlation of steel corrosion in pipe flow with jet impingement and rotating cylinder tests', *Corrosion*, 49 (12): 992-1003, 1993.

Gabe, D.R., and Walsh, F.C. 'The rotating cylinder electrode: A review of development', *Journal of applied electrochemistry*, 13 (1): 3-21, 1983.

Hu, X. Barker, R. Neville A. and Gnanavelu, A. 'Case study on erosion-corrosion degradation of pipework located on an offshore oil and gas facility', *Wear*, 271: 1295-1301, 2011.

Obeyekesere, N.N., Naraghi, A.R. and Zhou, S. 'Further advances of environmentally friendly corrosion inhibitors for CO_2 corrosion in North Sea oil fields' *CORROSION 2002*, Houston, Texas, NACE 02415, 2002.

Janine Killars, and Pat Finley. 'Move to environmentally acceptable products: How the OSPARCOM legislation affects the introduction of new products', *Symposium on oilfield chemistry*, SPE 65044, Houston, Texas, 2001.

Jiang, X. Zheng, Y.G. and Ke, W. 'Effect of flow velocity and entrained sand on inhibitor performances of two inhibitors for CO_2 corrosion of N80 steel in 3% NaCl solution', *Corrosion science*, 47: 2636-2658, 2005.

Linter, B.R. and Burstein, G.T. 'Reactions of pipeline steels in CO_2 solutions', *Corrosion science*, 41: 117-139, 1999.

McLaury, B.S., Shiraz, S.A., Shadley, J.R., and Rybick, E.F. 'Parameters affecting flow accelerated erosion and erosion-corrosion', NACE International, NACE 95120, 1995.

Musa, A.Y. Kadhum, A.H. Mohamad, A.B. Daud, A.R. Takriff, M.S. Kamarudin, S.K. and Muhamad, N. 'Stability of layer forming for corrosion inhibitor on mild steel surface under hydrodynamic conditions', *Int. J. Electrochem. Sci.* 4: 707-716, 2009.

Neville, A. and Wang, C. 'Erosion-corrosion mitigation by corrosion inhibitors – An assessment of mechanisms', *Wear*, 267: 195-203, 2009.

Neville, A. and Wang, C. 'Study of the effect of inhibitor on erosion-corrosion in CO_2-saturated condition with sand', *SPE projects, facilities and construction*, SPE 114081, 1-10, 2009

Nesic, S. Solvi, G.T. and Enerhaug, J. 'Comparison of the rotating cylinder and pipe flow test for flow-sensitive CO_2 corrosion', *Corrosion*, 51(10) : 773-787, 1995.

Obeyesekere, N., Narghi, A., Dharma Abayarathna, Prasad, R., Montgomeric, H. 'Environmentally friendly corrosion for CO_2 corrosion in north sea', Houston, Texas, NACE, *CORROSION 2000*, Paper 00020, 2000.

Ramachandran, S., Ahn, Y.S., Batrip, K.A., Jovancicevic, V., and Basset, J. 'Further advances in the development of erosion corrosion inhibitors', in: *CORROSION/2005*, NACE International, Houston, Texas, NACE 05292, 2005.

Schmitt, G. 'Drag reduction by corrosion inhibitors – A neglected option for mitigation of flow induced localized corrosion', *Materials and Corrosion*, 52 (5): 329-343, 2001.

Silverman, D.C. ' Rotating Cylinder Electrode – Geometry relationships for prediction of velocity – sensitive corrosion', *Corrosion*, Vol 44 (1: 42, 1987.

Taj, S. Papavinasam, S. and Revie, R.W. 'Development of green inhibitors for oil nd gas applications' *CORROSION 2006*, Houston, Texas, NACE 06656, 2006.

Wang, C., Neville, A., Ramachandran, S. and Jovancicevic, V. 'Alleviation of erosion-corrosion damage by liquid-sand impact through use of chemicals', *Wear*, 258, 649-658, 2005.

World Health Organizations. 'Aloe vera gel: in WHO monographs on selected medicinal plants' Volume 1, World Health Organization, Geneva, pp 43-49, 1999.

Full Paper

IMPLEMENTATION OF ADVANCED CONTROL LAWS ON A LABORATORY-SCALE THREE-TANK SYSTEM

A. Bamimore
Department of Chemical Engineering, Obafemi Awolowo University, Ile-Ife, Nigeria.

K.S. Ogunba
Department of Electronic and Electrical Engineering, Obafemi Awolowo University, Ile-Ife, Nigeria.

M.A. Ogunleye
Department of Electronic and Electrical Engineering, Obafemi Awolowo University, Ile-Ife, Nigeria.

O. Taiwo
Department of Chemical Engineering, Obafemi Awolowo University, Ile-Ife, Nigeria.

A.S. Osunleke
Department of Chemical Engineering, Obafemi Awolowo University, Ile-Ife, Nigeria.

R. King
Head of Measurement and Control Group, Institute of Process and Plant Technology, Technical University of Berlin, Hardenberger, Berlin, Germany

ABSTRACT

A laboratory-scale three-tank system for Control Engineering Education has been installed at the Process System Engineering Laboratory of Obafemi Awolowo University, Ile-Ife, Nigeria. This study gives a description of the physical features of the three-tank system and the mathematical description of the dynamics of the system. Subsequently, the design and implementation of controllers using five popular advanced control laws are demonstrated. The performance of the designed control laws is displayed in set-point simulations using MATLAB and SIMULINK. The designs are then implemented on the physical system using the Real-Time Interface. The similarities observed between the experimental and simulation results show the effectiveness of the control systems and the usefulness of the set-up in demonstrating the practical relevance of advanced control laws.

Keywords: *Multivariable IMC, Method of Inequalities, Model Predictive Control, Three-Tank system, simplified decoupler*

1. INTRODUCTION

Together with well-known experimental control systems like the Quadruple-tank processes (Johanson, 2000; Vadigepalli *et al*., 2001; Shneiderman and Palmor, 2010; Garido *et al*., 2012), the Ball and Plate mechanism, the Inverted Pendulum, the electric servo-motor, the gyroscope, distillation column, the spring mass damper system, and the virtual boiler (Goodwin *et al*., 2000; Gatzke *et al*., 2000), a process of three interconnected tanks, the three-tank system (3TS), has emerged as a benchmark for laboratory demonstrations of control concepts, including illustrations of linear and nonlinear control and, more recently, the issues of fault detection, isolation and diagnosis and remote experimentation (Wu *et al*., 2003; Kovacs *et al*., 2007; Lincon *et al*., 2007; Klinkhieo and Patton, 2009; Suresh *et al*., 2009). The levels of water in two of the three tanks are controlled by the manipulation of the volumetric flow-rates delivered by two pumps. The third tank is observed but not controlled.

In this study, the nonlinear state equations relating the manipulated and controlled variables are stated. A linear model is obtained via a tangential linearization procedure around nominal operating point. The linear model is subsequently used to design controllers using a number of popular controller design techniques. These techniques are (i) Method-of-Inequalities-Synthesized Decentralized PI Control (ii) Full Multivariable Internal Model Control (iii) Simplified Decoupling Control (iv) Linear Model Predictive Control (v) H_∞-based Decentralized Control. The set-point tracking capabilities of the designed controllers are compared in simulation and experimental graphical plots.

1.1. Mathematical Preliminaries

The principal structure of the three tank plant is as shown in Figure 1. It is a two-input, two-output process in which the controlled variables are the levels h_1 and h_2 inside tanks 1 and 2 and the manipulated variables are the volumetric flow-rates of two pumps q_1 and q_2 respectively. The tank level h_3 of tank 3 is observed but not controlled.

The transient balance equations for all the tanks are,

$$A\frac{dh_1}{dt} = q_1 - q_{13} - d_1 \quad (1)$$

$$A\frac{dh_3}{dt} = q_{13} - q_{32} - d_3 \quad (2)$$

$$A\frac{dh_2}{dt} = q_2 + q_{32} - q_{20} - d_2 \quad (3)$$

where d_1, d_2, and d_3 represent leaks from tanks 1,2, and 3 respectively, A represents the cross-sectional area of the tanks, and q_{13}, q_{32}, and q_{20} are flow rates across pipes connecting, respectively, tanks 1 and 3, tanks 3 and 2, and tanks 2 and the water reservoir and are given by the Torricelli rule:

$$q_{13} = \mu_1 . S_p . sgn(h_1 - h_3) . \sqrt{2g|h_1 - h_3|} \quad (4)$$

$$q_{32} = \mu_3 . S_p . sgn(h_3 - h_2) . \sqrt{2g|h_3 - h_2|} \quad (5)$$

$$q_{20} = \mu_2 . S_p . \sqrt{2gh_2} \quad (6)$$

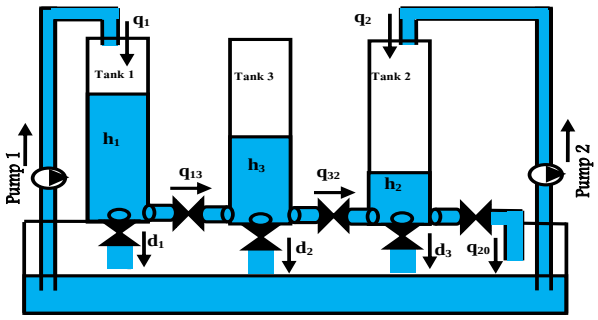

Figure 1: A Schematic of the Three-Tank System with Labels

with μ_i being the outflow coefficients out of tank $\boldsymbol{i}$, and $\boldsymbol{S_p}$ the cross-sectional area of the connecting pipes.

Making appropriate substitutions of equations (4) – (6) into equations (1) – (3) yields

$$\frac{dh_1}{dt} = -\left(1/_A\right).\mu_1.S_p.\sqrt{2g}.sgn(h_1-h_3).\sqrt{|h_1-h_3|} + \left(q_1/_A\right) - \left(d_1/_A\right) \quad (7)$$

$$\frac{dh_2}{dt} = \left(1/_A\right).\mu_3.S_p.\sqrt{2g}.sgn(h_3-h_2).\sqrt{|h_3-h_2|} - \left(1/_A\right).\mu_2.S_p.\sqrt{2g}.sgn(h_2).\sqrt{|h_2|} + \left(q_2/_A\right) - \left(d_2/_A\right) \quad (8)$$

$$\frac{dh_3}{dt} = \left(1/_A\right).\mu_1.S_p.\sqrt{2g}.sgn(h_1-h_3).\sqrt{|h_1-h_3|} - \left(1/_A\right).\mu_3.S_p.\sqrt{2g}.sgn(h_3-h_2).\sqrt{|h_3-h_2|} - \left(d_3/_A\right) \quad (9)$$

Linearizing the model equations (7)-(9) around the operating conditions given in equation (10).

$$\left.\begin{array}{c} h_{10} = 37.749, h_{20} = 15.145, h_{30} = 26.97 \\ \mu_{10} = 0.44, \mu_{20} = 0.87, \mu_{30} = 0.42 \\ q_{10} = 32\frac{cm^3}{s}, q_{20} = \frac{43cm^3}{s} \end{array}\right\} \quad (10)$$

yields linear model equation in s-domain.

$$\begin{bmatrix}\delta h_1 \\ \delta h_2\end{bmatrix} = \begin{bmatrix}g_{11} & g_{12} \\ g_{21} & g_{22}\end{bmatrix}\begin{bmatrix}\delta q_1 \\ \delta q_2\end{bmatrix} + \begin{bmatrix}g_{d11} & g_{d12} & g_{d13} \\ g_{d21} & g_{d22} & g_{d23}\end{bmatrix}\begin{bmatrix}\delta d_1 \\ \delta d_2 \\ \delta d_3\end{bmatrix} \quad (11)$$

$G(s)$ and $G_d(s)$ are used to denote the first and second terms of equation (11) and are defined as process and disturbance transfer functions respectively, given by:

$$\left.\begin{array}{l} g_{11} = \frac{0.006711s^2+0.0003003s+0.000002731}{s^3+0.05471s^2+0.0007534s+0.000001504} \\ g_{12} = \frac{6.072}{s^3+0.05471s^2+0.0007534s+0.000001504} \\ g_{21} = \frac{6.072}{s^3+0.05471s^2+0.0007534s+0.000001504} \\ g_{22} = \frac{0.000006072+0.0001946s+0.006711s^2}{s^3+0.05471s^2+0.0007534s+0.000001504} \end{array}\right\} \quad (12)$$

$$\left.\begin{array}{l} g_{d11} = \frac{-0.006711s^2-0.0003001s+0.000002726}{s^3+0.05471s^2+0.0007534s+0.000001504} \\ g_{d12} = \frac{-0.0000006068}{s^3+0.05471s^2+0.0007534s+0.000001504} \\ g_{d13} = \frac{-0.000006678s-0.000001714}{s^3+0.05471s^2+0.0007534s+0.000001504} \\ g_{d21} = \frac{-0.0000006068}{s^3+0.05471s^2+0.0007534s+0.000001504} \\ g_{d22} = \frac{-0.006711s^2-0.0001945s-0.0000006068}{s^3+0.05471s^2+0.0007534s+0.000001504} \\ g_{d23} = \frac{-0.00006099s-0.0000006068}{s^3+0.05471s^2+0.0007534s+0.000001504} \end{array}\right\} \quad (13)$$

2. Physical Layout of the Three-Tank System

The process being controlled in this experimental set-up is the three-tank plant shown in Figure 2, a combination of three transparent calibrated cylindrical Plexiglas tanks of equal dimensions. These tanks are connected together by cylindrical pipes with cross-sectional areas of $0.5\ cm^2$. The cross-sectional area of each tank is approximately $154\ cm^2$, while the maximum height of each tank is $62\ cm$ $(+/-1\ cm)$. The leftmost tank is labeled "tank 1," the middle tank "tank 3," and the rightmost tank "tank 2". The objective is to control the water levels of tanks 1 and 2 by the specification of reference command signals that ultimately results in the corresponding reaction of two diaphragm pumps.

Special differential pressure sensors are positioned behind each of the tanks to sense the levels of water in each of the three tanks. These differential pressure sensors sense the pressure differences between particular levels of water and a reference pressure level, and convert these pressure differentials into analog voltage values. An actuator device accepts signals from the sensors for Analog-to-Digital conversion before the digitized signals can be appropriately processed by the controlling equipment.

The controlling platform is a computer with a digital processing board, the dSPACE DS1104 R&D Controller Board. The board receives compiled codes from the computer and sends out a digital output signal to the AMIRA Actuator Device that corresponds to the control methodology's expected output unto a real system. This digital signal is then converted to an analog signal for transmission to the pumps.

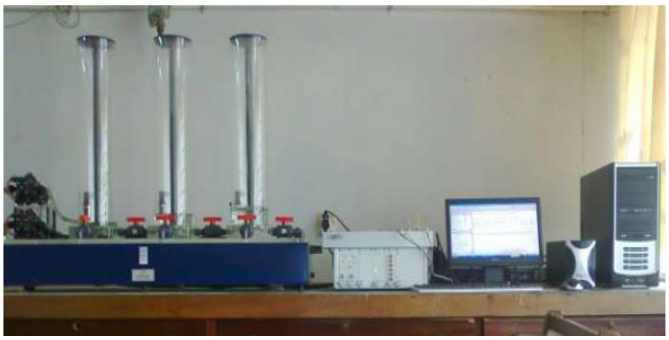

Figure 2: The Laboratory-Scale Three-Tank System for Real-Time Tank Height Control

Figure 3 gives the feedback representation of the components of the three-tank system set-up.

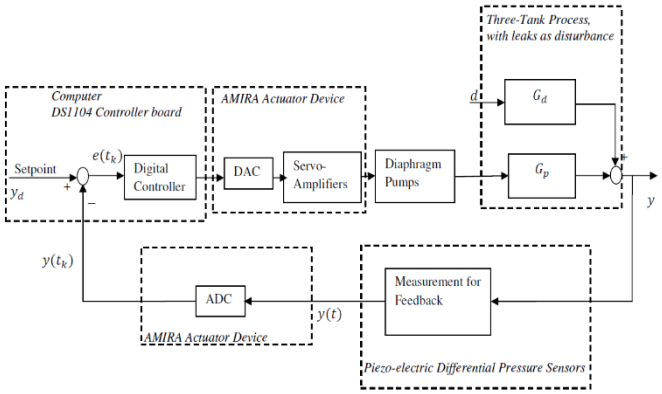

Figure 3: The Feedback Representation of the Components of the Three-Tank System Set-up

3. Input-Output Controllability Analysis

Here, simple analytical tools available are utilized to assess the controllability of the plant in order to evaluate any inherent performance limitations.

Scaling: While RGA, poles and zeros are independent of scaling, some other measures like singular values depend on it. All outputs,

set-points, inputs and disturbances are scaled by their "maximum acceptable deviation" from the desired operation conditions, such that the scaled variables stay within $\pm 1 \; \forall \; w$. The values used for scaling are given in (14) below:

$$\left.\begin{aligned} y_{maxdev} &= [h_1 \quad h_2] = [5 \quad 5] \\ u_{maxdev} &= [q_1 \quad q_2] = [53 \quad 43] \\ d_{maxdev} &= [d_1 \quad d_2 \quad d_3] = [20 \quad 20 \quad 20] \end{aligned}\right\} \tag{14}$$

Multivariable Interactions: Both the steady state relative gain array (RGA) and frequency dependent RGA were computed for the system to assess the level of interactions within the variables not only at steady state but at all frequencies. The steady state RGA is calculated as:

$$RGA = \begin{matrix} 1.29 & -0.29 \\ -0.29 & 1.29 \end{matrix} \tag{15}$$

It is clear that the interactions among the controlled variables are not so strong, meaning that the system is relatively decoupled. This indicates that decentralized control could be used with pairings $[h_1 \;\; q_1]$ and $[h_2 \;\; q_2]$.

The RGA elements as function of frequency are shown in Figure 4 reveal that the RGA elements decrease as frequency increases with almost negligible interactions at frequency greater than 0.1 rad/sec.

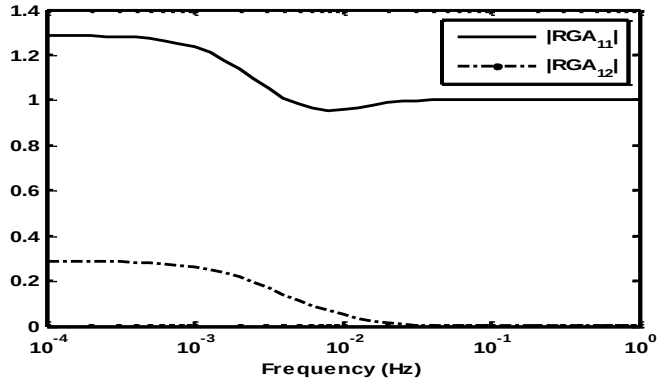

Figure 4: Input-Output controllability analysis: Frequency dependent RGA plot

Minimum-Phase (MP) Characteristics: The individual elements in the transfer function matrix have no right half plane (RHP) zeros. The multivariable transmission zeros of the process were equally calculated to be: $z_1 = -0.0024$, $z_2 = -0.018$ and $z_3 = -0.0336$, which shows that the process has no multivariable right half plane (RHP) zeros.

Sensitivity to Uncertainty: The condition number $\gamma(G)$ of the plant is plotted in Figure 5. It is of low order of magnitude indicating that the plant is not ill-conditioned. It is also higher at low frequency showing that the plant is more sensitive to unstructured uncertainty at steady state than at higher frequencies.

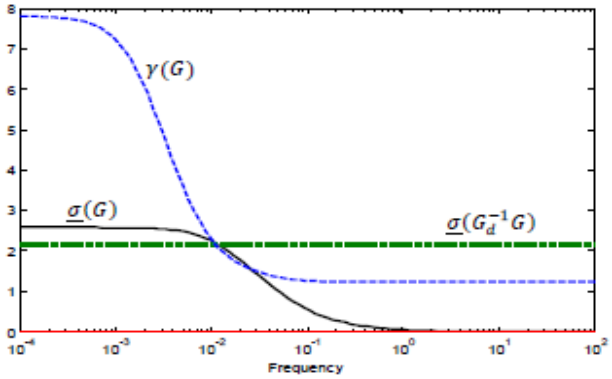

Figure 5: Input-output controllability analysis: Plots of $\underline{\sigma}(G), \gamma(G)$ and $\underline{\sigma}(G_d^{-1}G)$.

Functional Controllability: The system is functionally controllable as det[G(s)]≠ 0, ∀s .

Controllability (l): Consider a system m by m with transfer function G(s) whose McMillan standard form is

$$M(s) = diag\left(\epsilon_i(s) \Big/ \psi_i(s) \right), i = 1,2, \dots, m$$

where $\epsilon_i(s)$ and $\psi_i(s)$ are polynomials in s, G(s) is controllable if it is functionally controllable and none of the $\epsilon_i(s)$, has a zero in the closed loop. This plant satisfies this condition.

Modal Controllability (m): The condition here is that, matrix $[(sI - A), B]$ should be relatively left prime. This plant also satisfies this condition.

Input Saturation: Input saturation imposes a fundamental limitation on the control performance. The perfect control condition for reference tracking is given by:

$$\underline{\sigma}(R^{-1}G) \geq 1 \; \forall \; \omega \leq \omega_r \tag{16}$$

ω_r is the frequency up to which reference tracking is required. R is reference scaling matrix chosen as $R = I$. The condition for perfect disturbance rejection is given by (17) where $\boldsymbol{G_d}$ is the disturbance transfer function matrix.

$$\underline{\sigma}(G_d^{-1}G) \geq 1 \; \forall \; \omega \tag{17}$$

As shown in Figure 5, the minimum singular value of the plant, for reference tracking, is greater than 1 up to a frequency of $\omega = 0.046$. This is an upper bound on the controller bandwidth, ω_c due to input saturation considerations at high frequency. For disturbance rejection, the minimum singular value is greater than 1 at all frequencies, this shows that input saturation is not a serious problem for this plant.

4. Controller Design

In this work, the following control algorithms were considered for the control of the three-tank-system:

4.1. Multi-Objective Parameter Search for Multiloop PI Controller Design by Method of Inequalities (MoI)

The determination of controller parameters for multiloop Proportional-Integral (PI) controllers for the three-tank system was done using a multi-objective parameter-search optimization procedure called the Method of Inequalities (MoI) (Zakian and Al-Naib, 1973). The performance objectives were formulated as a set of algebraic inequalities

$$\phi_i(p) \leq \varepsilon_i, i = 1,2 \tag{18}$$

where $\phi_i(p)$ are objective functions for the two loops specified as functional of performance indices such as rise time, settling time, overshoot, stability margin, p is a vector $(p_1, p_2, \dots, p_q)$, and ε_i are real numbers chosen to limit the values of the objective functions.

Using the moving boundaries method with IMC parameterizations (Zakian and Al-Naib, 1973; Taiwo, 1978; Taiwo, 1980; Ogunleye, 2012), the PI controllers obtained are given by

$$g_{c1} = \left(23.79 + \frac{0.0608}{s}\right), g_{c2} = \left(39.81 + \frac{0.2202}{s}\right) \tag{19}$$

The comparisons of the set-point tracking manipulated and controlled variable plots of the experimental and simulation results for the implementation of the controllers of (19) are shown in Figure 6. The similarities between both plots are noteworthy.

4.2. Fixed-Structure $\mathbf{H}_\infty$ controller design

Here a H_∞ controller synthesis problem posed in equation 20 is solved as implemented in the MATLAB subroutine "hinfstruct".

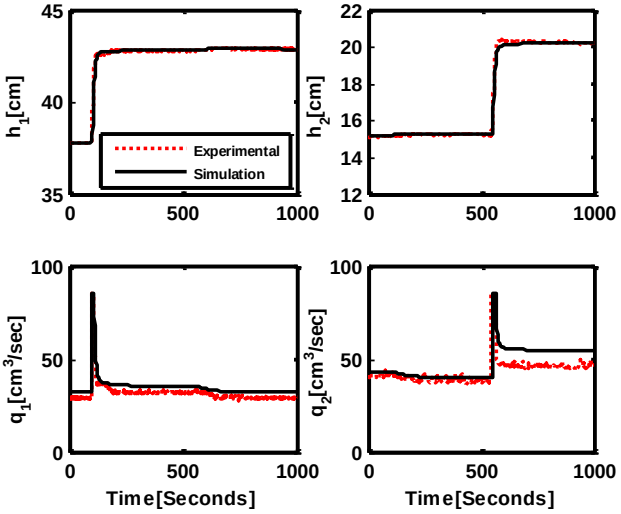

Figure 6: Setpoint Tracking Manipulated and Controlled Variable Plots of the Experimental and Simulation Results for the Implementation of the MoI-synthesized PI Controllers of (19)

$$\|\mathrm{H}(s)\|_\infty := \max_\omega \bar{\sigma}(\mathrm{H}(\mathrm{j}\omega)) < 1 \tag{20}$$

where

$$\mathrm{H}(s) = \mathrm{Diag}(\mathrm{w_S S}, \mathrm{w_T T}) \tag{21}$$

The details are well defined in the publication of Gahinet and Akparian (2011).

On solving the H_∞ optimization problem, the following controllers were obtained:

$$g_{c1} = \left(\frac{26.6s+0.104}{s}\right), g_{c2} = \left(\frac{33.4s+0.186}{s}\right) \tag{22}$$

Again, the setpoint tracking manipulated and controlled variable plots of the experimental and simulation results for the implementation of the controllers of (22) are shown in Figure 7. As was the case in Figure 6, the plots are strikingly similar.

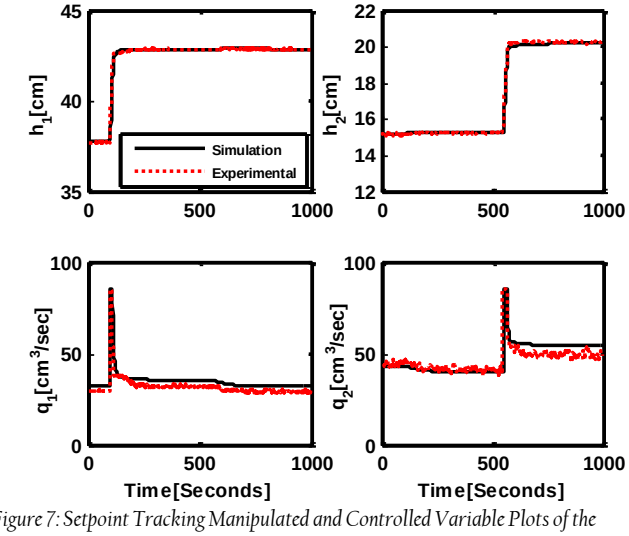

Figure 7: Setpoint Tracking Manipulated and Controlled Variable Plots of the Experimental and Simulation Results for the Implementation of the Fixed-Structure H_∞ Controllers of (22)

4.3. Multivariable Internal Model Controller (MIMC) design

A MIMC controller is designed by the inversion of the transfer function matrix of (13) and the subsequent augmentation of the inverse with a matrix of first-order filters i.e.

$$G_{IMC} = G^{-1}G_f \tag{23}$$

where

$$G_f = \begin{bmatrix} \frac{1}{\lambda_1 s+1} & 0 \\ 0 & \frac{1}{\lambda_2 s+1} \end{bmatrix} \tag{24}$$

By converting the G_{IMC} to a conventional feedback controller, G_c we obtained

$$G_c = \frac{G_{IMC}}{I-G_{IMC}G} = \begin{bmatrix} k_{11} & k_{12} \\ k_{21} & k_{22} \end{bmatrix} \tag{25}$$

where each controller k_{ij} $(i = 1,2; j = 1,2)$ is an 8th-order controller. The details are contained in Ogunba (2012).

Again, the plots of the manipulated and controlled variables of the implementation of the controllers of (25) are compared in Figure 8. The similarities are again noteworthy.

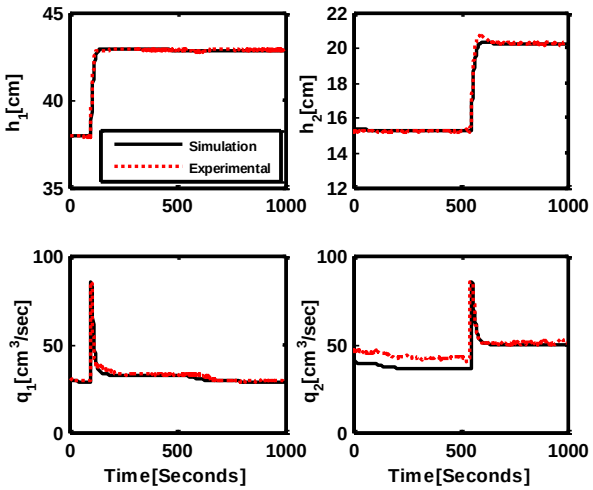

Figure 8: Setpoint Tracking Manipulated and Controlled Variable Plots of the Experimental and Simulation Results for the Implementation of Multivariable Internal Model Controllers of (25)

4.4. Simplified Decoupling Technique

Using the Decoupler Matrix $D(s)$ of (26) in the Simplified Decoupling framework (Waller, 1974; Waller *et al.*, 2003) yields an apparent process $Q(s)$ of (27) i.e.

$$D(s) = \begin{bmatrix} 1 & -\frac{g_{12}(s)}{g_{11}(s)} \\ -\frac{g_{21}(s)}{g_{22}(s)} & 1 \end{bmatrix} \tag{26}$$

$$Q(s) = \begin{bmatrix} g_{11}(s) - \frac{g_{12}(s)g_{21}(s)}{g_{22}(s)} & 0 \\ 0 & g_{22}(s) - \frac{g_{12}(s)g_{21}(s)}{g_{11}(s)} \end{bmatrix} \tag{27}$$

Using Single-Input, Single-Output Internal Model Control to generate SISO controllers and then converting the controllers to conventional unity feedback controllers yield the controllers of (28)

$$C(s) = \begin{bmatrix} c_{11}(s) & 0 \\ 0 & c_{22}(s) \end{bmatrix} \tag{28}$$

where each controller c_{ii} $(i = 1,2)$ is a 10th-order controller.

The multivariable controller is then given by (29)

$$G_c = D(s)C(s) \tag{29}$$

The plots of the manipulated and controlled variables of the implementation of the decoupler of (26) and the controllers of (28) are again compared in Figure 9. The similarities are again noteworthy.

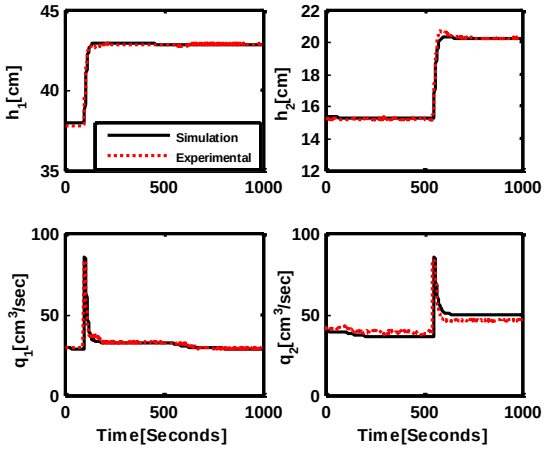

Figure 9: Set-point Tracking Manipulated and Controlled Variable Plots of the Experimental and Simulation Results for the Implementation of Simplified Decoupling Controllers of (26) and (28)

4.5. Model Predictive Controller Design

A MPC control problem consists of minimizing the cost function (Maciejowski, 2002 and Bamimore *et al*., 2011):

$$J(k) = \sum_{i=0}^{H_p-1} \|\hat{y}(k+i|k) - r(k+i|k)\|_Q^2 \quad + \sum_{i=0}^{H_u-1} \|\Delta\hat{u}(k+i|k)\|_R^2 \tag{30}$$

where $\hat{y}(k+i|k)$ are the predicted controlled outputs at time k, $\Delta u(k+i|k)$ are the predicted control increments, $r(k+i|k)$ are the set-point trajectories. The matrices $Q \geq 0$ and $R > 0$ are the weighing matrices, which are assumed to be constant over the prediction horizon. H_p is the length of the prediction horizon while H_u is the length of the control horizon.

On solving the optimization problem posed in equation (30), with the tuning parameters and process constraints specified as:

$H_p = 10$, $H_u = 2$, Q=diag([5,5]), R=0.005diag([1,1]), $\Delta q_{max} = \begin{bmatrix}10\\10\end{bmatrix}$, $\Delta q_{min} = \begin{bmatrix}-10\\-10\end{bmatrix}$, $q_{max} = \begin{bmatrix}85\\85\end{bmatrix}$, $q_{min} = \begin{bmatrix}0\\0\end{bmatrix}$, $h_{max} = \begin{bmatrix}62\\62\end{bmatrix}$, $h_{min} = \begin{bmatrix}0\\0\end{bmatrix}$,

a 9th-order controller is obtained. The details are contained in the appendix.

Again, the plots of the manipulated and controlled variables of the implementation of the controllers of are compared in Figure 10.

5. Conclusions

The experimental set-up of a laboratory-scale three-tank system of the Process System Engineering (PSE) Laboratory of Obafemi Awolowo University, Ile-Ife, Nigeria has been described. The usefulness of the set-up for the demonstration of advanced control laws has also been demonstrated with the design and implementation of popular control algorithms in literature. The striking similarities between controller implementations using SIMULINK and implementations on the real experimental set-up are noteworthy, with the major differences being in the noise introduced by the nonlinearities in the respective pumps. This set-up provides a massive opportunity for a practical demonstration of known control principles to engineering students.

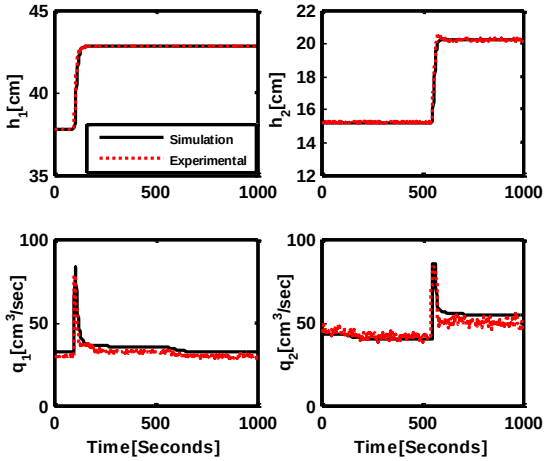

Figure 10: Set-point Tracking Manipulated and Controlled Variable Plots of the Experimental and Simulation Results for the Implementation of Linear Model Predictive Controllers of (31)

Acknowledgement

Prof. O. Taiwo acknowledges the donation of the Experimental System by Alexandria von Humbolt Foundation, Germany.

References

Bamimore, A., Taiwo, O. and King, R., "A Comparison of Two Nonlinear Model Predictive Control Methods and Implementation on a Laboratory Three Tank System." Proceedings of the 50th IEEE CDC-ECC Conference, 5242-5247, 2011.

Gahinet, P. and Apkarian, P., "Decentralized and Fixed-Structure H_∞Control in MATLAB." Proceedings of the 50th IEEE CDC-ECC Conference, 8205-8210, 2011.

Garrido, J., Vazquez, F., and Morilla, F., "Centralized Multivariable Control by Simplified Decoupling." Journal of Process Control, 22(6): 1044-1062, 2012.

Gatzke, E.P., Meadows, E.S., Wang, C., and Doyle III, F.J., "Model-Based Control of a Four-Tank System." Computers and Chemical Engineering, 24:1503-1509, 2000.

Goodwin, G. C., Graebe, S. F., and Salgado, M. E., "Control System Design", Prentice-Hall, Englewood Cliffs, New-Jersey, USA, 2000.

Johansson, K. H., "The Quadruple-Tank Process : A Multivariable Laboratory Process with an Adjustable Zero." IEEE Trans. Cont. Sys. Tech., 8 (3):456-465, 2000.

Klinkhieo, S. and Patton, R.J., "PLS based FDI of a Three-Tank Laboratory System." Proceedings of Joint 48th IEEE conference on Decision and Control and 28th Chinese Control Conference, Shanghai, China, 1896-1901, 2009.

Kovacs, L., Borbely, E., Benyo, Z., "Optimal control of the Three Tank System in H2/H-Inf Space." Fifth Slovakian-Hungarian Joint Symposium on Applied Machine Intelligence and Informatics, Poprad, Slovakia, 137-144, 2007.

Lincon, S.A., Sivakumar, D., Prakash, J., "State and Fault Parameter Estimation Applied To Three-Tank Bench Mark Relying On Augmented State Kalman Filter." ICGST-ACSE Journal, 7 (1):33-41, 2007.

Maciejowski, J. M., "Predictive Control with Constraints", Prentice-Hall, Harlow, England, 2002.

Ogunba, K. S., "Development of Generalized Internal Model Control (IMC) Techniques for Multivariable Control System Design." Unpublished M.Sc. Thesis, Obafemi Awolowo University, Ile-Ife, Nigeria, 2012.

Ogunleye, M. A., "Design of Controllers for Multivariable Systems using the Method of Inequalities." Unpublished M.Sc. Thesis, Obafemi Awolowo University, Ile-Ife, Nigeria, 2012.

Shneiderman, D. and Palmor, Z. J., "Properties and Control of the Quadruple-Tank Process with Multivariable Dead-Times." Journal of Process Control, 20:18-28, 2010.

Suresh, M., Srinivasan, G. J., Hemamalini, R. R., "Integrated Fuzzy Logic Based Intelligent Control of Three Tank System." Serbian Journal of Electrical Engineering, 6 (1):1-14, 2009.
Taiwo, O., "Improvement of Turbo-Alternator Response by the Method of Inequalities." International Journal of Control, 27 (2):305-311, 1978.
Taiwo, O. , "Application of The Method of Inequalities to the Multivariable Control of Binary Distillation Columns." Chem. Eng. Sci., 35 (2): 847-858, 1980.
Vadigepalli, R., Gatzke, E.P. and Doyle III, F.J., "Robust Control of a Multivariable Experimental Four-Tank System." Ind. Eng. Chem. Res., 40:1916-1927, 2001.
Waller, K. V., "Decoupling in Distillation." AIChE J., 20, 592-594, 1974.
Waller, M., Waller, J.B., and Waller, K.V., "Decoupling Revisited." Ind. Eng. Chem. Res. 42:4575-4577, 2003.
Wu, L., Cartes, D., Shih, C., "Web-Based Flow Control of a Three-Tank System." Journal of Systemics, Cybernetics and Informatics, 2(1): 242-251, 2003.
Zakian, V. and Al-Naib, U., "Design of Dynamical and Control Systems by the Method of Inequalities." Proc. IEE, 120 (11):1421-1427, 1973.

APPENDIX

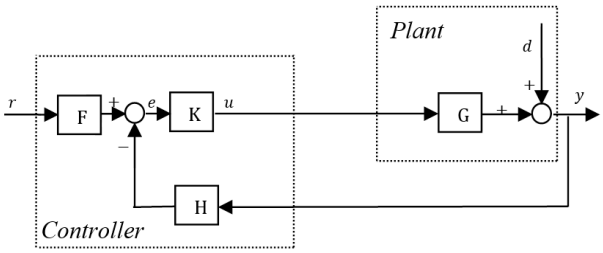

Block diagram describing the structure of a linear model predictive control system

MPC CONTROLLER

$$K = \begin{bmatrix} k_{11} & k_{12} \\ k_{21} & k_{22} \end{bmatrix}$$

$$k_{11} = \frac{s^9 + 17.64s^8 + 144.6 + 710s^6 + 2334s^5 + 5391s^4 + 8808s^3 + 9361s^2 + 6153s + 125.5}{s^9 + 17.83s^8 + 148.9s^7 + 752.3s^6 + 2570s^5 + 6211s^4 + 10640s^3 + 11930s^2 + 8101s + 147.2}$$

$$k_{21} = \frac{0.002317s^8 + 0.03207s^7 + 0.1747s^6 + 0.3497s^5 - 0.3977s^4 - 2.732s^3 - 1.883s^2 + 6.339s + 12.69}{s^9 + 17.83s^8 + 148.9s^7 + 752.3s^6 + 2570s^5 + 6211s^4 + 10640s^3 + 11930s^2 + 8101s + 147.2}$$

$$k_{12} = \frac{0.002348s^8 + 0.0325s^7 + 0.177s^6 + 0.3539s^5 - 0.4059s^4 - 2.778s^3 - 1.925s^2 + 6.405s + 12.85}{s^9 + 17.83s^8 + 148.9s^7 + 752.3s^6 + 2570s^5 + 6211s^4 + 10640s^3 + 11930s^2 + 8101s + 147.2}$$

$$k_{22} = \frac{s^9 + 17.63s^8 + 144.7s^7 + 712s^6 + 2351s^5 + 5467s^4 + 9007s^3 + 9652s^2 + 6355s + 127}{s^9 + 17.83s^8 + 148.9s^7 + 752.3s^6 + 2570s^5 + 6211s^4 + 10640s^3 + 11930s^2 + 8101s + 147.2}$$

$$F = \begin{bmatrix} \frac{1.266s+3.706}{s} & \frac{0.01324s+0.00244}{s} \\ \frac{0.0117s+0.002154}{s} & \frac{1.296s+3.799}{s} \end{bmatrix}, \quad H = \begin{bmatrix} h_{11} & h_{12} \\ h_{21} & h_{22} \end{bmatrix}$$

$$h_{11} = \frac{5.56s^4+174s^3+502.2s^2+47.29s+0.8235}{s^4+6.225s^3+9.758s^2+0.222s}, \qquad h_{21} = \frac{0.003231s^4+1.424s^3+4.466s^2+0.2452s+0.0004787}{s^4+6.225s^3+9.758s^2+0.222s}$$

$$h_{12} = \frac{0.00366s^4+1.443s^3+4.522s^2+0.3178s+0.0005422}{s^4+6.225s^3+9.758s^2+0.222s}, \qquad h_{22} = \frac{5.7s^4+165.6s^3+473s^2+47.54s+0.8443}{s^4+6.225s^3+9.758s^2+0.222s}$$

MIMC CONTROLLER

$$k_{11} = \frac{1.99e15s^8 + 2.75e14s^7 + 1.54e13s^6 + 4.48e11s^5 + 7.17e9s^4 + 6.18e7s^3 + 265624s^2 + 535.2s + 0.4045}{1.538e14s^8 + 1.987e13s^7 + 1.016e12s^6 + 2.638e10s^5 + 3.634e8s^4 + 2.494e6s^3 + 7002s^2 + 6.661s}$$

$$k_{21} = \frac{-1.8e11s^6 - 1.966e10s^5 - 8.08e8s^4 - 1.53e7s^3 - 131149s^2 - 405.6s - 0.4045}{1.538e14s^8 + 1.987e13s^7 + 1.016e12s^6 + 2.638e10s^5 + 3.634e8s^4 + 2.494e6s^3 + 7002s^2 + 6.661s}$$

$$k_{12} = \frac{-1.8e11s^6 - 1.966e10s^5 - 8.08e8s^41.53e7s^3 - 131149s^2 - 405.6s - 0.4045}{1.538e14s^8 + 1.987e13s^7 + 1.016e12s^6 + 2.638e10s^5 + 3.634e8s^4 + 2.494e6s^3 + 7002s^2 + 6.661s}$$

$$k_{22} = \frac{2.048e15s^8 + 3.157e14s^7 + 2e13s^6 + 6.78e11s^5 + 1.31e10s^4 + 1.42e8s^3 + 818511s^2 + 2083s + 1.871}{1.538e14s^8 + 1.987e13s^7 + 1.016e12s^6 + 2.638e10s^5 + 3.634e8s^4 + 2.494e6s^3 + 7002s^2 + 6.661s}$$

SIMPLIFIED DECOUPLER

$$k_{11} = \frac{5.44e19s^{10} + 9.1e18s^9 + 6.44e17s^8 + 2.51e16s^7 + 5.89s^6 + 8.48e12s^5 + 7.4e10s^4 + 3.78e8s^3 + 1.1e6s^2 + 1644s + 1}{3.4e18s^{10} + 5.35e17s^9 + 3.53e16s^8 + 1.27e15s^7 + 2.69e13s^6 + 3.4e11s^5 + 2.47e9s^4 + 9.6e6s^3 + 1.82e4s^2 + 13.27s}$$

$$k_{12} = \frac{-5.83e17s^{10} - 1.16e17s^9 - 10e15s^8 - 4.85e14s^7 - 1.47e13s^6 - 2.85e11s^5 - 3.56e9s^4 - 2.75e7s^3 - 1.2e5s^2 - 264.5s - 0.22}{5e20s^{12} + 1.1e20s^{11} + 1.05e19s^{10} + 5.8e17s^9 + 2.06e16s^8 + 4.86e14s^7 + 7.73e12s^6 + 8.19e10s^5 + 5.55e8s^4 + 2.22e8s^3 + 4528s^2 + 3.56s}$$

$$k_{21} = \frac{-5.44e19s^{10} - 9.1e18s^9 - 6.44e17s^8 - 2.51e16s^7 - 5.9e14s^6 - 8.5e12s^5 - 7.4e10s^4 - 3.78e8s^3 - 1.1e6s^2 - 1644s - 1}{3.76e22s^{12} + 7e21s^{11} + 5.66e20s^{10} + 2.6e19s^9 + 7.39e17s^8 + 1.36e16s^7 + 1.63e14s^6 + 1.24e12s^5 + 5.7e9s^4 + 1.56e7s^3 + 2.25e4s^2 + 13.27s}$$

$$k_{22} = \frac{2.7e18s^{10} + 5.36e17s^9 + 4.61e16s^8 + 2.25e15s^7 + 6.8e13s^6 + 1.32e12s^5 + 1.65e10s^4 + 1.27e8s^3 + 5.6e5s^2 + 1224s + 1}{2.03e17s^{10} + 3.52e16s^9 + 2.59e15s^8 + 1.05e14s^7 + 2.58e12s^6 + 3.88e10s^5 + 3.5e8s^4 + 1.76e6s^3 + 4135s^2 + 3.56s}$$

Full Paper

DETERMINATION OF BULK GRAINS MOISTURE CONTENT IN A SILO USING DISTRIBUTED SENSOR NETWORK

M.O. Onibonoje
Department of Electronic and Electrical Engineering, Obafemi Awolowo University, Ile-Ife, Nigeria.
Tel: +2348069531521

A.M. Jubril
Department of Electronic and Electrical Engineering, Obafemi Awolowo University, Ile-Ife, Nigeria.
Tel: +2348056568457; Email: ajubril@yahoo.fr

O.K. Owolarafe
Department of Agricultural and Environmental Engineering, Obafemi Awolowo University, Ile-Ife, Nigeria.
Tel: +2348056509073

ABSTRACT

This paper presents a solution to the problem of determining the moisture content of bulk grains stored in silos. A distributed sensor network was designed to achieve this. The network consists of sensor nodes and a sink node connected to a Personal Computer (PC) through a USB port. The sensor nodes were calibrated using standard saturated salt solutions.

Data collection, analysis and logging were achieved with Graphical User Interface (GUI) developed using LABVIEW graphical programming software. The distributed system was then evaluated with reference to the standard test values established against the oven-drying method. This study concluded that its approach provides improved flexibility and control in measurement of moisture content of grains over the existing stand alone meters.

Keywords*: Grains, Moisture content, Sensor node, Sink node, GUI, LABVIEW*

1. INTRODUCTION

Storage of grains is an important post-harvesting process in agricultural practice. A safe storage activity must be ensured for the grain produced until it is needed for consumption, multiplication, further processing and commercial purposes. Globally, around 2.4 billion tonnes of grains are produced annually, out of which only 43% are consumed (Jayas *et al.*, 2000). Since grain production is seasonal and consumption is continuous, safe storage must maintain grain quality and quantity. This means that provided the grains are not invaded by insects, mites, rodents, or birds; grains have to be protected from mold infection, heat build up, odour development and microorganisms (Jayas *et al.*, 1995). These infections do develop from unnecessary high moisture content (MC) caused by inadequate drying or moisture rebounds in the stored bulk grains. However, environmental conditions like uneven temperature distribution and humid air flow in the silo (store house) can cause stored grains to develop higher MC, which needs to be adequately measured and controlled.

Measurement of MC of grains stored in silos had previously encountered many problems which include static charges that develop in bulk grains with its accompanying health hazard to the monitoring personnel, and the temperature at different points in the silo is always different thereby rendering the results obtained from instantaneous measurement of moisture content of the grains inaccurate for decision making.

Several approaches and methods had been adopted in determining the MC of grains in silos. These include: oven heating, desiccant, and distillation, microwave spectroscopy, resistance and conductivity, impedance, equilibrium relative humidity, and nuclear magnetic resonance methods. However, there had been observable inherent limitations and problems associated with the methods. These problems include: destructive tendencies in the tested samples, untimely discovery of the infested section of the grains in schedule measurements due to its non-continuous approach, and uneven air flow within the storehouse which makes the localized testing approaches insufficient. Also, if grains are to be held for months, most of these methods are not prudent to continuously or periodically monitor the different portions of the bin, test them for moisture content and examine them for fungal damage. Also, an efficient measurement technique must be cost effective, requiring rapid and accurate evaluation of the moisture content; a test which most of these techniques do not pass.

The application of distributed sensor network in different fields, including agriculture has made it a potential approach with hope of eliminating most of the limitations in the previous methods of MC determination. As discussed by Singh *et al.* (2010), wireless sensor network (WSN) is widely considered as one of the most important technologies for the twenty-first century. A WSN typically consists of a large number of low-cost, low-power, and multi-functional wireless sensor nodes, with sensing, wireless communications and computation capabilities. These sensor nodes communicate over short distance via a wireless medium, and collaborate to accomplish a common task, for example, environment monitoring, military surveillance, and industrial process control. The basic philosophy and advantages behind WSNs is that, while the capability of each sensor node is limited, the aggregate power of the entire network is sufficient for the required mission.

In applying distributed sensor network to solve MC measurement, the indirect equilibrium moisture content method would be adopted. Ray *et al.* (2007) describes this method, using hardwood as a case study, as measuring the relative humidity (RH) in the air space between the target products. The RH in the air surrounding a grain sample at any particular temperature (T) is dependent on the moisture content of the grains. According to Armstrong and Weiting (2007), grain equilibrium moisture content (EMC) prediction is particularly attractive in some applications considering the availability of inexpensive and reliable sensors to measure relative RH and T. Although EMC relationships are grain – type hybrid, or variety specific, and are affected by agronomic conditions, the ease of measuring RH and T with modern sensors makes the use of these relationships attractive for monitoring stored grain. It used SHT75 RH/T sensor with ChungPfost equations to design an instrument for evaluating equilibrium moisture content of

grains. The design adopted wired, localized and instantaneous measurement approach. Chen (2001) determined that a measurement time of 10mins was required for the RH and T sensor he studied to equilibrate to the grain environment for accurate measurement.

Meanwhile, no single equation is general enough to predict the relationship between the EMC of agricultural and food products, and the relative humidity over a wide range of temperature (Brooker *et al*., 1974; Chang *et al*., 1993; Basunia *et al*., 1996; Soysal and Oztekin, 1999; Lucas and Alabadan, 2002; Park *et al*., 2002; Lahsasni *et al*., 2004).

The HendersonThompson (Thompson *et al*., 1968) and ChungPfost equations (Chung and Pfost, 1967; Pfost *et al*., 1976) are satisfactory models for most starchy grains and fibrous materials. The Halsey equation is an adequate model for products having a high oil and protein content (Halsey, 1985). The modified Oswin equation (Chen, 2001) has served as a good model for popcorn, maize cobs, peanut pods and some varieties of maize and wheat. According to Soysal and Oztekin (1999), the GuggenheimAndersondeBoer (GAB) equation is considered the most versatile model for various materials such as inorganic and food products like fruits over a wide range of water activities.

Our study aimed at developing a system for determining MC of bulk grains in a silo using distributed wireless sensor network consisting of sensor nodes and a sink node connected to a PC, and evaluating the measuring system developed by comparing the results with existing systems. Our system made use of the modified Oswin model to express the MC in terms of the RH and T from its sensor nodes.

2. DESIGN AND METHOD

A distributed system of sensor network for MC measurement was developed for bulk grains in a silo. This consists of sensor nodes and a sink node (central hub) being connected to a PC.

2.1. Sensor node

The sensor node contains a programable Temperature/Humidity sensor SHT21 connected to a microcontroller unit (MCU) on a eZ430-RF2500T target board from Texas Instrument. SHT21 is a tiny humidity/temperature sensor made by Sensirion AG, Switzerland. It provides calibrated, linearized signals in digital, true I^2C format. It has a capacitive type humidity sensor and a band gap temperature sensor that produces a stable output even at moderately high humidity levels. SHT21 also contains an amplifier, A/D converter, and one-time programmable (OTP) memory and a digital processing unit. It works at (0 - 100)%RH and (-40 to 125)^oC, but gives a constant relative humidity value between 20 and 80%RH and constant temperature within 20 to 40^oC. It is designed mainly to work within a normal operating range of between (0 - 80)%RH. The sensor has a rated RH accuracy of ±1.8% RH and T accuracy of 0.3^oC. eZ430-RF2500T target board contains the MSP430F2274 microcontroller, CC2500 2.4-GHz wireless transceiver, and radio antenna.

The programming flowchart of the sensor node is as shown in Fig. 1.

The sensor nodes were calibrated using five different saturated salt solutions (NaCl, KCl, $NaNO_3$, K_2CO_3, and K_2SO_4) at temperatures of 5^oC, 10^oC, 15^oC, 20^oC, 25^oC, 30^oC and 35^oC. The RH values of the solutions with corresponding temperature values are compared with the literature values (Greenspan, 1977).

2.2. Sink node

The sink node is made up of eZ430-RF2500T target board, but was connected to the PC through the USB debugging interface. The USB debugging interface enables the eZ430-RF2500T to remotely send and receive data from a PC using the MSP430 Application UART.

All the calibrated sensor nodes are networked to a sink node using a Texas Instrument low-power RF SimpliciTI network protocol. The sensor nodes are programmed to communicate their sampled T and RH to the hub. The sink node communicates all collected data to a Personal Computer (PC) through its available serial port. The flowchart of the network is as shown in Fig. 2.

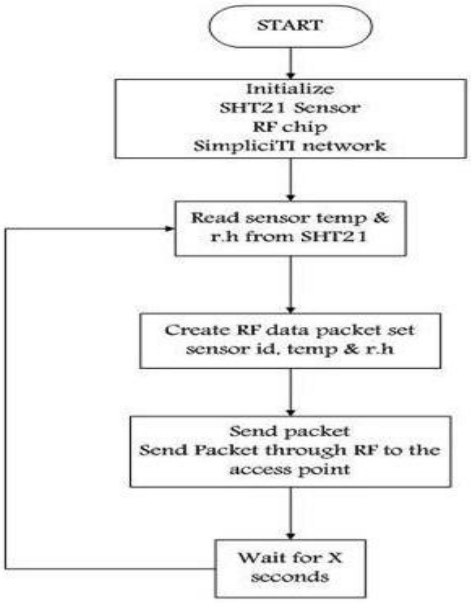

Figure 1: Flowchart of Sensor Node

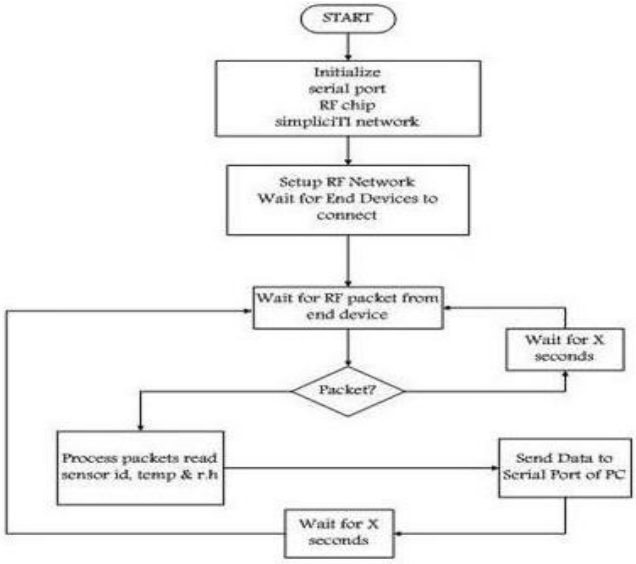

Figure 2: Flowchart of Sensor node – Sink node network

2.3. Graphical User Interface (GUI)

The GUI was developed with LABVIEW graphical programming software. It collects data from the hub, displays, processes and logs it into a file. EMC (dry basis) was computed using the Modified Oswin Model (Equation 1) for shelled corn grain. Modified Oswin coefficients used were from ASAE Standards D245.5 where a = 15.303, b = -0.10184, and c = 3.0358. The programming flowchart of the sink node to the PC is as shown in Fig. 3.

$$M = (a + bT)\left[\frac{R_h}{1-R_h}\right]^{1/c} \quad (1)$$

where: R_h – Relative Humidity (%RH), T – Temperature (^oC), M – Moisture Content (%MC), a, b, and c – constants.

The illustration of the network system is shown in Fig. 4, while the block diagram of the design as well as the implemented sensor node are as shown in Figures 5 and 6 respectively.

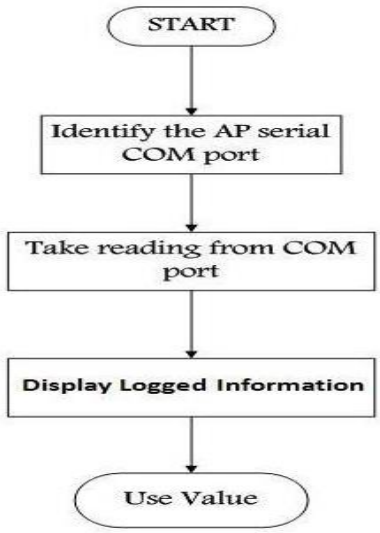

Figure 3: Flowchart of Sink node- Personal Computer (PC)

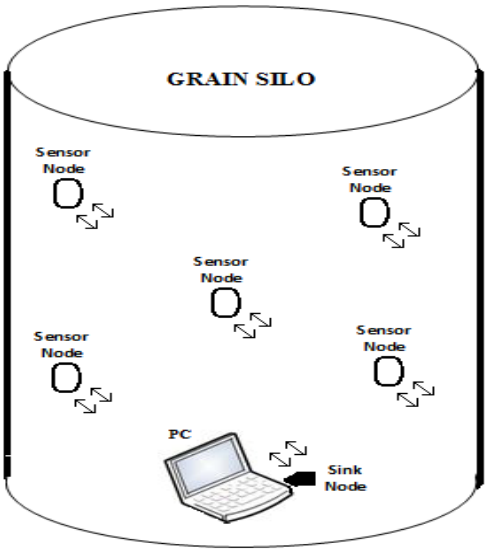

Figure 4: The Distributed System of Sensor Network

3. RESULTS AND DISCUSSION

The results of the calibrated values of the sensor node are as plotted against reference relative humidity values according to Greenspan (1977) in Fig. 7 – Fig. 11.

The results indicate relative agreement with the literature values. For NaCl and $NaNO_3$, the data are in good agreement with the study by Greenspan (1977). For KCl and K_2CO_3, the data fairly agree up to 55% with the Greenspan's study. There is no agreement among the system data and that of Greenspan (1977) for K_2SO_4. This is due to the inability of the SHT21 sensor used in the study to operate in the 90 - 100 %RH range. Overall, the trends shown by our data for these salts are in good agreement with the literature, demonstrating that the method used in this study is suitable for studying the relationship between RH and T, for RH ‹ 90%.

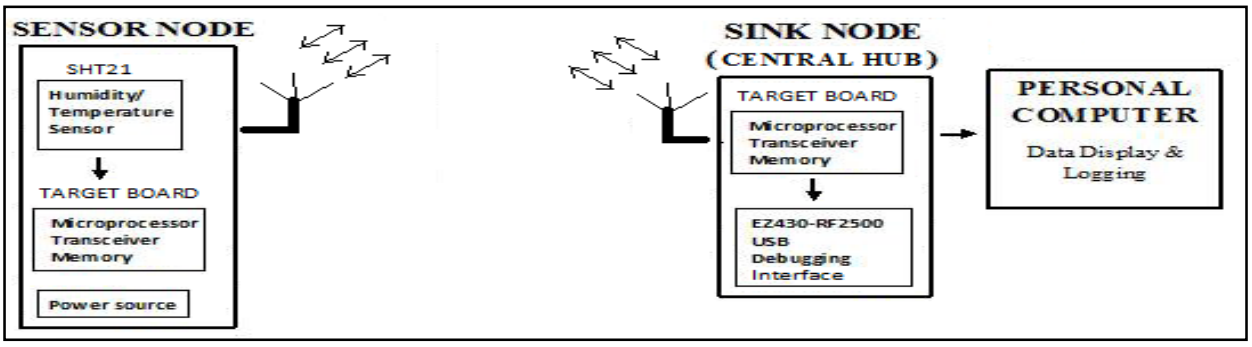

Figure 5: Block Diagram of the Wireless Sensor Network

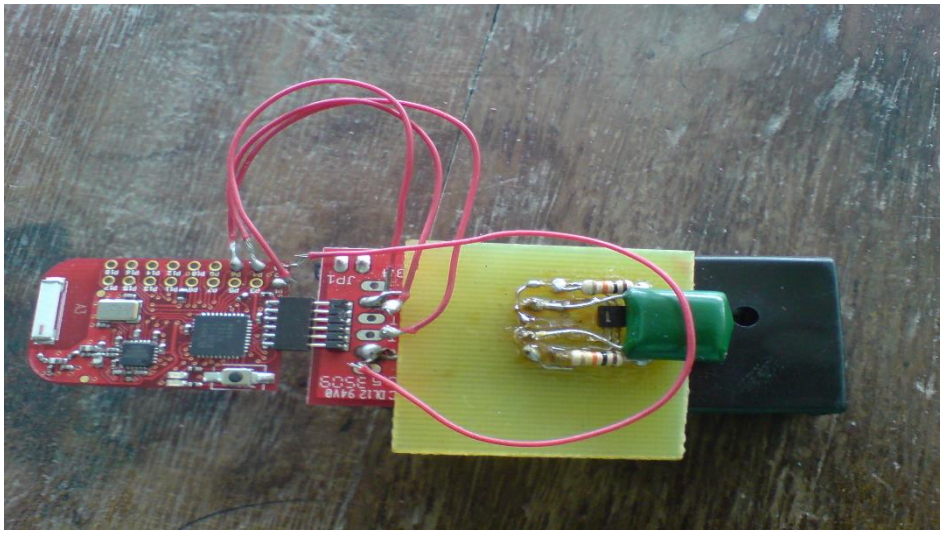

Figure 6: Sensor node

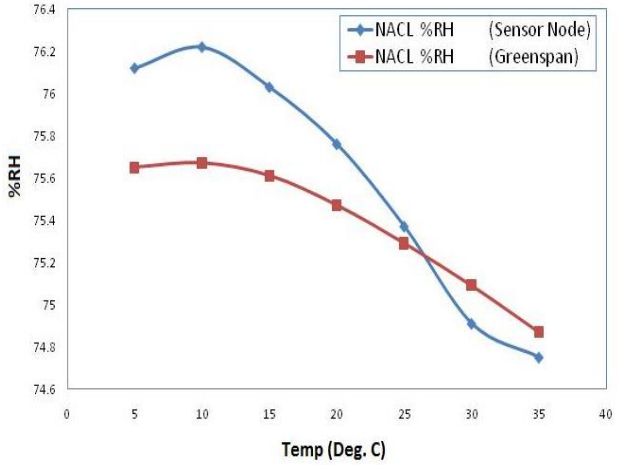

Figure 7: Relative Humidity of NaCl against Temperature

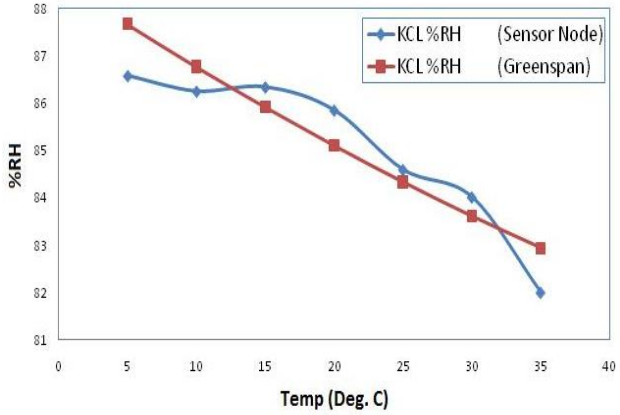

Figure 8: Relative Humidity of KCl against Temperature

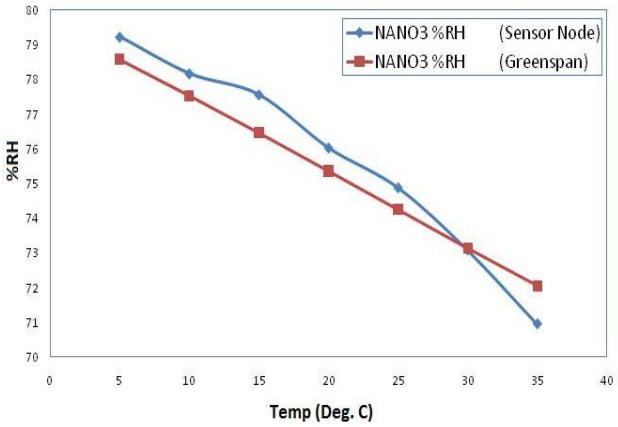

Figure 9: Relative Humidity of NaNO3 against Temperature

On the GUI, the communication port of the sink node connected to the PC is specified in the 'Device Port'. When the system is switched on, the readings of T, RH and MC in each sensor node are as indicated and plotted on the waveform graph. The stream of data is shown on the display desk, while 'MC Threshold' control is used to set the threshold of save storage MC. Whenever the MC › $MC_{Threshold}$ in any of the node, 'ATTENTION' is called for on the display desk and in the particular node as shown in Fig. 12.

The data are then logged into a file with the actual absolute time. The logged result of the system with MC › $MC_{Threshold}$ in node 1 and node 3 unavailable is as shown in Table 1 of the Appendix.

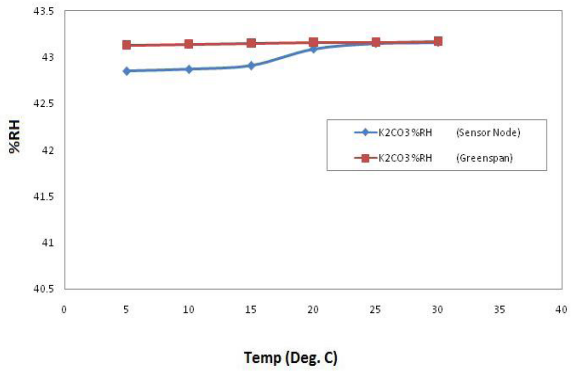

Figure 10: Relative Humidity of K_2CO_3 against Temperature

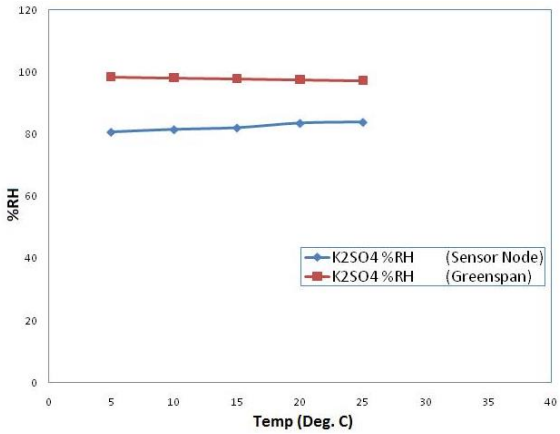

Figure 11: Relative Humidity of K_2SO_4 against Temperature

4. CONCLUSION

A reliable approach in the determination of the moisture content of stored grains had been developed using a distributed system of sensor network. The relative agreement of our calibrated values with the literature values confirms the viability of our method to determine the temperature and relative humidity distribution in a silo.

The advantages of our method include non-destructive approach of the grain samples, continuous measurement and monitoring of the grains, distributed measurement across the strata of the grain bins as against previous localized approach, and remote monitoring of the grain condition which prevent health hazard of the personnel.

The system would not operate effectively for relative humidity greater than 90%, which is an extreme case beyond useful grain storage.

REFERENCES

Armstrong, P. R. and Weiting, M., Design and testing of an instrument to measure equilibrium moisture content of grain. American Society of Agricultural and Biological Engineers. 24(5):617–62, 2008.

ASAE, Moisture relationships of plant-based agricultural products, ASAE Standards D245.5 (44th Edition). American Society of Agricultural Engineers, St. Joseph, MI, 1997.

Basunia, M.A., Abe, T. and Bala, B.K., Application of finite element method for the simulation of temperature distribution during storage of rough rice in cylindrical bin. Agricultural Mechanization in Asia, Africa and Latin America. 27(2):33–40, 1996.

Brooker, D.B., Arkena, F. W. and Hall, C. W., Drying cereal grains. The Avi Publish Co., Connecticut, 1974.

Chang, C.S., Converse, H.H. and Steele, J.L., Modelling of temperature of grain during storage with aeration. Transactions of the ASAE. 36(2):509–519, 1993.

Chen, C., Rapid model to determine the sorption isotherms of peanuts. Journal of Agricultural Engineering Research. 75(2):401–404, 2001.

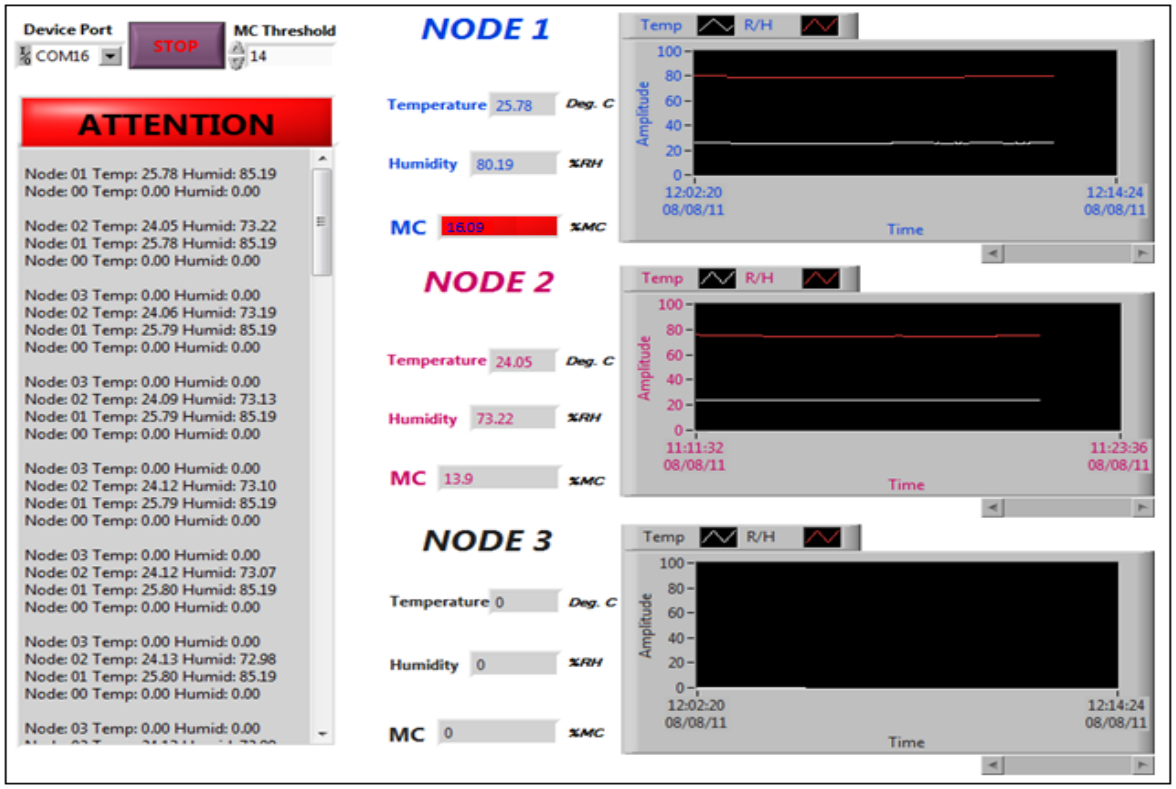

Figure 12: GUI Display during operation

Chung, D.S. and Pfost, H. B., Adsorption and desorption of water vapour by cereal grains and their products part II. Transactions of the ASAE. 10(4):549-551, 1967.

Gillay, B. and Funk, D.B., Effects of moisture distribution on measurement of moisture content of dried corn. Acta Alimentaria. 35 (2):171–181, 2006.

Greenspan, L., Humidity fixed points of binary saturated aqueous solutions. Journal of Research of the National Bureau of Standards A - Physics and Chemistry. 81A(1): 86-96, 1977.

Haigh, A. D., Thompson, F., Gibson, A. A. P., Campbell, G. M. and Fang, C., Complex permittivity of liquid and granular materials using waveguide cells. Subsurface Sensing Technologies and Applications, 2(4):425–434, 2001.

Halsey, G., Physical adsorption on uniform surfaces. The Journal of Chemical Engineering, 16(10):931-937, 1985.

Jayas, D.S., White, N.D.G. and Muir, W.E., Stored-Grain Ecosystems. Marcel Dekker Inc., New York, 1995.

Jayas, D.S., Paliwal, J. and Visen, N.S., Multi-layer neural networks for image analysisof agricultural products. Journal of Agricultural Engineering Research 77:119-128, 2000.

Lahsasni, S., Kouhila M. and Mahrouz M., Adsorption and desorption isotherms and heat of sorption of prickly pear fruit. Energy Conversion and Management, 45(2):249–261, 1985.

Lucas, E.B. and Alabadan, B.A., Simulation of temperature changes during storage of maize in hexagonal wooden bin due to weather variability. Journal of Applied Science and Technology. 2(1):16–32, 2002.

Park, K.J., Vohnikova, Z. and Brod, F. P. R., Evaluation of drying parameters and desorption isotherms of garden mint leaves (Mentha crispa L.). Journal of Food Engineering. 51:193–199, 2002.

Pfost, H. B., Maurer, S. G., Chung, D. S. and Milliken, G. A., Summarising and reporting equilibrium moisture data for grains. American Society of Agricultural Engineers, ASAE Paper No 76–3520, St. Joseph, MI. 1976.

Ray, D., Gattani, N., Castillo, E., and Blankenhorn, P., Identification of the relationship between equilibrium moisture content, dry bulb temperature, and relative humidity using regression analysis. Journal of Wood and Fiber Science. 39(2):299-306, 2007.

Singh, S.K., Singh, M.P. and Singh, D.K., Routing protocols in wireless sensor networks - A survey. International Journal of Computer Science and Engineering Survey. 1(2), 2010.

Soysal, Y. and Oztekin, S., Equilibrium moisture content equations for some medicinal and aromatic plants. Journal of Agricultural Engineering Research. 74(3):317–324, 1999.

Thompson, T.L., Peart, R.M. and Foster, G.H., Mathematical simulation of corn drying. Transactions of the ASAE. 1(4):582–586, 1968.

Full Paper

TECHNICAL POTENTIAL OF BIOMASS ENERGY IN NIGERIA

S.J. Ojolo
Department of Mechanical Engineering, University of Lagos, Akoka, Lagos, Nigeria

J.I. Orisaleye
Department of Mechanical Engineering, Lagos State University, Epe Campus, Lagos, Nigeria
ifeorisaleye@gmail.com

S.O. Ismail
Department of Mechanical Engineering, University of Lagos, Akoka, Lagos, Nigeria

S.M. Abolarin
National Centre for Energy Efficiency & Conservation, University of Lagos, Nigeria

ABSTRACT

The role of energy in the development of a nation cannot be underestimated. The current situation of energy in Nigeria reveals that an energy crisis is pending in the country. However, there is an abundance of renewable energy resources in Nigeria most of which have remained untapped. This paper gives an estimate of the technical potential of biomass energy in Nigeria, the technical potential being the part of the theoretical energy which can be harnessed for energy use. The biomass sources considered are agro-residues, livestock wastes, municipal solid wastes and forest residues. It was discovered that contribution of biomass energy in Nigeria is largely from agro-residues, municipal wastes and livestock wastes while forest residues contribute the least. The energy potential is also expected to continue to grow from about 3.2 EJ in 2010 to about 5.5 EJ in 2020 and may reach about 29.8 EJ in 2050.The estimate compares well with forecasted energy demand and will play a great role in future energy supply. Policy formulations have not favoured the development of biomass technologies for efficient utilization of biomass. There is a need to harness this huge energy potential by employing the various biomass technologies and formulating policies to the effect. There is also a need to enhance the development of the agricultural subsector of the economy where the biomass is generated.

Keywords: *Technical Potential, Biomass, Renewable energy, Energy estimate.*

1. INTRODUCTION

Energy plays a very crucial and important role in the economic, social and political development of a nation. Inadequacy of energy supply limits economic growth, restricts socio-economic activities and adversely affects the quality of life. Electrical energy plays a very important role in the technological and socioeconomic development in Nigeria, as with any nation. However, the demand far outstrips the epileptic supply in Nigeria (Sambo, 2008; Sambo, 2009; Kauffmann, 2005). Petroleum, natural gas, and hydroelectricity are Nigeria's major sources of commercial energy; they are slightly outpaced by the largely non-commercial consumption of fuelwood and charcoal (Osaghae, 2009; RECIPES, 2006). There is also a large quantity of coal which is used majorly in thermal power plants for electricity generation (Olise and Nria-Dappa, 2009). Nigeria also has abundant renewable energy which exists in the forms of solar, oceanic, hydro, wind energy and biomass.

A number of studies have assessed the global and regional potential of bioenergy production with the estimates differing considerably (Smeets et al., 2004, Fischer and Schrattenholzer, 2001). Schmidhuber (2006) differentiates between theoretical and technical potential. Theoretical potential is the total amount of energy produced by photosynthesis and it includes vast amounts of biomass that cannot be harvested because it is too inaccessible or because the cost of harvesting would be too high. Technical potential, however, is that part of the theoretical potential that can be harvested in practice and thus harnessed for practical energy use. Several estimates have shown that the technical potential is a relatively small fraction of the theoretical one.

EIA (2010) provides information about the reserves of crude oil, natural gas and coal used in this section for analysis. Nigeria has depended majorly on her large crude oil reserve which is presently put at 37.2 billion barrels of oil as given by the oil and gas journal. The production of crude oil has also been estimated to be about 2.2 million barrels per day. Most of this is exported while 280 thousand barrels of oil is refined per day for consumption within the country. EIA (2010) reports that according to the oil and gas journal, the natural gas proven reserve is estimated to be about 185 trillion cubic feet. In 2008, Nigeria consumed about 430 billion cubic feet mostly for electricity generation. 140 billion cubic feet was vented, 530 billion cubic feet was flared and about 500 billion cubic feet re-injected for enhanced oil recovery. The gross annual consumption of natural gas is put at 1,600 billion cubic feet. The recoverable coal reserves is estimated to be about 210 million short tons with the production being 9 thousand short tons per annum and consumption being about 12 thousand short tons per annum (EIA, 2010).

On the assumption that new oil or gas reserves are not discovered, it is estimated that the crude oil reserves should run out within the next 50 years and the proven natural gas reserves should run out in about 115 years. Since these have been the major energy sources in Nigeria, major steps need to be taken to explore other energy options which hitherto have been neglected in the country which include solar, nuclear and biomass energies. Technologies for exploiting these forms of energy need to be developed in the short term to guarantee security of energy for the country in the event that the predictions tend towards reality.

This paper aims at developing an estimate for the technical potential of biomass resources in Nigeria with consideration of non edible sources such as agricultural wastes in form of agro-residues and livestock wastes, municipal solid wastes and forest residues.

2. METHODOLOGY FOR ESTIMATION OF POTENTIAL OF BIOMASS ENERGY IN NIGERIA

Biomass considered in this study includes residues from major crop produce (agro-residues), livestock wastes, sawdust and municipal wastes. Data used in the analysis were collected from various sources covering the periods between 2000 and 2010. Simple

relations for the estimation of the biomass potential were developed for each source; and using the data, the results obtained were extrapolated to year 2050. The technical potential was taken to be the total energy derivable from biomass obtained from the various sources.

2.1. Potential of agro-residues

Agro-residues include all crop residues which would have normally been regarded to as waste. These remains have usually been disposed of by burning or by deposition in dump sites if they are not combustible. The estimate was based on the residue quantity and the amount of energy derivable from each. The estimate for agro-residues (crop residues and wastes) was obtained using

$$E_{AR} = \sum E_i r_i$$

where E_{AR} is the energy potential of agro-residues, E_i is the energy content of each residue considered, and r_i is the annual biomass residue. But,

$$r_i = \alpha_i p_i$$

where α_i is the residue to crop ratio of each produce, and p_i is the annual production rate of the crop. Hence,

$$E_{AR} = \sum E_i \alpha_i p_i$$

The residue to crop ratios were obtained from several sources which include Yevich and Logan (2002), Milbrandt (2009) and FAO (2004). The annual crop production was obtained from CBN (2006).

2.2. Potential of livestock waste

Major livestock available in Nigeria include cattle, sheep, goat, poultry and pigs. Livestock produce wastes which have majorly been used as manure. Greater part of the quantity of livestock wastes are however left in heaps without any useful purpose. Livestock wastes can be converted by anaerobic digestion to biogas which can serve as an efficient and clean fuel.

The livestock estimates were obtained using

$$E_{LW} = \sum w_j Y_j E$$

where E_{LW} is the energy potential of livestock wastes, w_j is the quantity of waste from each livestock in kg, Y_j is the biogas yield of each waste, and E is the energy content of biogas. But

$$w_j = q_j w_{aj}$$

where q_j is the quantity of livestock reared annually and w_{aj} is the annual waste produced per head of livestock. Hence,

$$E_{LW} = \sum q_j w_{aj} Y_j E$$

The population of livestock was estimated from the annual growth rate for each livestock from a study by Mbanasor and Nwosu (2003) which stated that the annual growth rate of cattle, sheep, goat, chicken and pigs were 4.17%, 5.8%, 8.5%, 3.9% and 7.6%, respectively.

Biogas has a calorific value of 15.7 to 29.5 MJ/m^3 (Klass, 1998). Milbrandt (2009) gives the amount waste that can be obtained from each livestock and biogas yield from the wastes.

2.3. Potential of forest residues

Nigeria lies in the tropical region which is dominated by a vast land mass covered forest trees. Felling of these trees and processing them to planks yield enormous amount of residue which include bark, sawdust and mill chips. The energy potential is also estimated using

$$E_{FR} = \sum V \rho_b r_n E_n$$

where E_{FR} is the energy potential of forest residues, V is the annual volume capacity, ρ_b is the bulk density of the residue, r_n is the residue to product ratio and E_n is the energy content of each residue.

As a rule of thumb, a log in a sawmill produces 60 to 70% of useful timber as boards, 20 to 30% as wood chips and 10% as sawdust (INRS, 2008). Aruofor (2000) noted that the available forestry statistics in Nigeria are not only deficient in quality and quantity, but are disjointed and their collection suffer long lags. It was estimated, however, that the capacity of sawmills should be about 4,635,800 m^3 by 1997 with the production or capacity utilization should be 2,000,000 m^3. The bulk density of wood chips is about 290 kg/m^3 and that of sawdust is about 400 kg/m^3. The energy content of sawdust is about 15 MJ/kg and that of wood chips is about 14 MJ/kg (FAO, 1986; Klass, 1998).

According to CBN (2006), the increase in the index in forestry production was 5.5%. It was assumed that the demand for forest products increases at the same rate annually.

2.4. Potential of municipal solid wastes

Considering the demographic projection and the impact on wastes generation, the estimate for the energy potential of MSW is estimated using

$$E_{MW} = w_p P E$$

where E_{MW} is the energy potential of municipal solid waste, w_p is the annual municipal waste generation per person, P is the annual population and E is the energy content of municipal solid waste.

The annual generation of municipal solid wastes in Nigeria is about 29.78×10^9 kg; the main constituents being putrescible materials, papers, plastics/rubbers, textiles and metals (Ojolo et al., 2004). Municipal solid wastes have a heating value of 12.7 MJ/dry kg (Klass, 1998). With an estimated population of about 129 million people in 2005 (RECIPES, 2006), the annual generation of MSW per person in Nigeria is, thus, put at 231.3 kg/year/person, that is about 0.63 kg/person/day, based on the 2005 population estimate. The population statistics for Nigeria from the U.S. Census Department (2010) was used for the demographic information.

3. RESULTS AND DISCUSSION

a. Estimate of energy potential for all biomass sources

Table 1 presents the estimate of energy potential of agro-residues in 2005 and the relative contribution of each residue to the potential. The estimate shows that the annual derivable energy obtainable from agro-residues is about 1.924 EJ. The major contributors to the potential are fruit and vegetable wastes, sorghum stalks, maize residues, rice residues and cassava peels which contribute about 60% of the total annual energy potential. Table 2 shows the five-yearly estimate of energy potential of agro-residues which is based on the 6% annual increase of agricultural produce according to CBN (2006). It is assumed that the increases in annual production of agricultural produce and annual generation of agro-residues are equal. The estimate shows that the energy potential in 2020 will be about 4.6 EJ and could rise to about 26.5 EJ in 2050. Table 3 presents the population estimates of livestock in Nigeria between 2005 and 2050 while Table 4 present the energy potential of livestock wastes in Nigeria between the same periods. The energy estimate shows that the energy potential of livestock wastes in 2020 will be about 346.4 PJ and could increase to about 2.24 EJ in 2050. The wastes from cattle and goat contribute the higher part (›75 %) of the annual energy potential while sheep, poultry and pigs together contribute less than 25 %. Table 5 shows the quantity of forest residues produced in Nigeria in 1997 and the energy from each waste. The 5-yearly energy potentials of forest residues for full and utilized capacities from 2005 to 2050 are shown in Table 6 using the increase in forest production index. The results show that the energy potential of forest residues in 2020 at the current utilized capacity will be about 12.3 PJ and could reach about 62 PJ in 2050. At full capacity however, the energy potential of forest residues in 2020 will be about 28.4 PJ and may reach 142 PJ in 2050. Table 7 presents the population estimates, estimated annual municipal solid wastes generation and energy derivable from the wastes. The municipal solid waste, as well as its energy potential, is assumed to increase with increasing population. The energy potential of municipal solid wastes which could be harnessed is about 534.4 PJ in 2020 and may increase to about 987.1 PJ in 2050.

b. Biomass energy potential versus energy demand

A summary of the results is presented in Table 8 which shows that the total potential of biomass in Nigeria as at 2020 will be about 5.5 EJ and has the potential to increase to about 29.8 EJ by 2050. The results show that forest residues contribute the least to the overall annual biomass energy potential. Agro-residues, livestock wastes and municipal solid wastes together contribute over 99% of the overall biomass potential in the country. Agro-residues are the largest single contributor to the overall biomass potential producing over 75% of the total annual energy potential. Energy commission of Nigeria has forecasted the demand of energy in Nigeria from 2000 to 2030 using the Model for Analysis Energy Demand (MAED) and Wien Automatic System Planning (WASP) package (Sambo, 2008). The total energy demand by sector, assuming a 10% Gross Domestic Product growth, is shown in table 9. The total annual energy demand has been extrapolated to 2050 assuming the average growth rate of 8.3%. The total energy demand and the total energy potential of biomass are compared in Fig. 1. The comparison shows that with efficient utilization, energy from biomass in the form of agro-residues, livestock wastes, forest residues and municipal solid wastes have the potential of meeting the energy demand in the short term as seen between 2005 and 2025. Beyond 2025, the energy demand exceeds the bio-energy potential. This may be due to a predicted rapid increase in population or increased industrial activities within the country.

According to Dayo (2007), fuelwood has constituted over 60% of the annual energy consumption between 1990 and 2005. Assuming a continuing trend, the consideration of fuelwood in the estimate of the biomass potential will enhance the possibility of biomass energy to meeting energy demands in Nigeria as shown in Fig. 1. However, the use of fuelwood for energetic purposes is being discouraged in Nigeria to prevent deforestation which has a negative effect on the environment. Hence, to suffice the demand for energy while stepping down energy from fuelwood, there will be a need to exploit energy crops which can be cultivated in both arable and grass-lands. The cultivation of energy crops will increase the bioenergy potential. There may also be the need to exploit greatly other forms of renewable energy such as solar and wind energy, and hydropower.

c. Policy formulation, application and opportunities for bioenergy in Nigeria

Efficient use of biomass must be assured to be able to utilize the better part of the obtainable bioenergy potential. The conversion processes have been classified into direct combustion; thermochemical processes involving carbonisation, pyrolysis and gasification; and biochemical processes involving fermentation and esterification. Currently, most of the biomass resources are utilized by direct combustion mostly in the rural areas in the country. The effeciency of this method of utilization is between 5 and 15% which is rather inefficient. Other means of conversion should be exploited other than the direct combustion.

Table 10 shows the progress of research and application of biomass technologies in Nigeria. The applications at the domestic and industrial levels have been considered. The Table, derived from investigation, shows that the traditional utilization of biomass, requiring direct combustion of the biomass is used domestically. However, industrially, biomass is not being utilized yet. However, products from other forms of bioenergy conversion routes have not been widely used either domestically or industrially. Researchers are working on other forms of biomass technologies and are also trying to adapt them to the Nigerian situation. Some of them are outlined. Ojolo et al. (2004), Ojolo and Orisaleye (2010), Ismail (2010), Bamgboye and Oniya (2004), Abolarin (2011), Ojolo and Bamgboye (2005) and Enweremadu et al. (2008) have researched into thermochemical conversion of biomass. Research activities in biochemical conversion of biomass have been carried out by Abdulkarim and Maikano (2001), Hussaina (2002) Abdulkareem (2005), Okonko et al. (2009) and Adenipekun and Fasidi (2005). Experiments and investigation of technologies on the production of biodiesel has been carried out by Ogbonnaya (2010).

Energy policies have been made in Nigeria in 1993, 1996 and 2003 (ECN, 2003). However, the policies have not seemed to state exactly how to implement and develop the use of bioenergy in the country but has placed more focus on developing and financing conventional energy. Dayo (2008) also holds this position. The implication of this is the slow development rate of renewable energy in the country. Whilst an energy crisis is pending in the country, there is a need to focus on and pool resources, hence policies, to harness the high potential of renewable energy present in the country. Such policies should also cover the development and modernisation of agriculture, investment in infrastructure and development and commercialisation of biomass technologies.

4. CONCLUSIONS

The study has examined the technical potential of biomass energy in Nigeria. The situation of energy in Nigeria shows that an energy crisis is pending in the country as its oil reserves may not last up to half of a century. It has been found in this study that Nigeria has a large resource base of biomass energy which has hitherto been unharnessed. The biomass sources considered are agro-residues, livestock wastes, municipal solid wastes and forest residues. The biomass energy in Nigeria is contributed to largely by agro-residues, municipal wastes and livestock wastes while forest residues contribute the least. The energy potential is also expected to continue to grow from about 3.2 EJ in 2010 to about 5.5 EJ in 2020 and may reach about 29.8 EJ in 2050. The estimates compare well with the forecasted energy demand up to 2025 but beyond 2025, the comparison is better with consideration of fuelwood. Most of the biomass technologies are still at the development stage and are yet to be applied on industrial scale. Policy formulations have not favoured the development of biomass technologies for efficient utilization of biomass. There is a need to harness this huge energy potential by employing the various biomass technologies and formulating policies to the effect. There is also a need to enhance the development of the agricultural subsector of the economy since biomass is agriculturally generated.

REFERENCES

Abdulkareem, A.S., Refining biogas produced from biomass: An alternative to cooking gas, Leonardo journal of sciences 7:1-8, July-December 2005.

Abdulkarim, B.I. and Maikano, H., Refining of biogas produced from biomass (cow dung) by removing H_2S and CO_2, B.Eng. project, Federal University of Technology, Minna, Nigeria, 2001.

Abolarin, S., Design and manufacture of an updraft gasifier, Master of Science Thesis, University of Lagos, Nigeria, 2011.

Adenipekun, C.O. and Fasidi, I.O., Degradation of selected agricultural wastes by *Pleurotus tuber-regium* (Fries.) Singer and *Lentinus subnudus* (Berk)-Nigeria edible mushrooms, Advances in food sciences 27(2):61-64, 2005.

Aruofor, R.O., Review and improvement of data related to wood-products in Nigeria, EC-FAO partnership programme, Food and Agricultural Organisation of the United Nations, Italy, 2000.

Bamgboye, A.I. and Oniya, O.O., Pyroltytic conversion of corncobs to medium grade fuel, FUTA Journal of environment and engineering technology, 12(2): 36-42, 2004.

Central Bank of Nigeria, CBN, Statistical Bulletin, Volume 17, December 2006.

Dayo, F.B., Nigeria Energy Balances: 1990-2005, Technical Paper, Triple "E" Systems Inc., September 2007.

Dayo, F.B., Clean energy investment in Nigeria: The domestic content, International Institute for Sustainable Development, Canada, 2008.

EarthTrends, Energy and resources – Nigeria, EarthTrends country profiles, http://earthtrends.wri.org, 2003.

Energy Commission of Nigeria, ECN, National energy policy, Nigeria, 2003.

Energy Information Administration, EIA, Nigeria Energy Data, Statistics and Analysis - Oil, gas, electricity and coal, Energy Information Administration, www.eia.doe.gov, 2010.
Enweremadu, C.C., Waheed, M.A., Adekunle, A.A. and Adeala, A., Energy potential of brewer's spent grain for breweries in Nigeria, Journal of engineering and applied sciences, 3(2):175-177, 2008.
FAO, Wood gas as engine fuel, FAO forestry paper 72, Food and agricultural organisation of the United Nations, Italy, 1986.
FAO, Unified Bioenergy Terminology (UBET), Wood Energy Programme, Food and Agricultural Organization of the United Nations, December 2004.
Fischer, G. and Schrattenholzer, L., Global bioenergy potentials through 2050, Biomass and Bioenergy 20:151-159, 2001.
Hussaina, H., Refining of biogas produce from biomass (cow dung) by removing H_2S and CO_2, PGD project, Federal University of Technology, Minna, Nigeria, 2002.
Innovative Natural Resource Solutions LLC, INRS, A strategy for increasing the use of woody biomass for energy, National Association of State Foresters, Portland, 2008.
Ismail, S.O., Modelling the kinetics of plastic waste pyrolysis, Master of Science Thesis, University of Lagos, Nigeria, 2010.
Kauffmann, C., Energy and Poverty in Africa, Policy insights No. 8, OECD development centre, www.oecd.org/dev/insights, 2005.
Klass, D.L., Biomass for Renewable Energy, Fuels, and Chemicals, Academic Press, San Diego, CA, 1998.
Mbanasor, J.A. and Nwosu, A.C., Livestock sector in Nigerian economy: policy-direction, Journal of agriculture and food science 1(2):141-147, October 2003.
Milbrandt, A., Assesment of Biomass Resources in Liberia, Technical report, National Renewable Energy Laboratory, USA, April 2009.
Ogbonnaya, M., Extraction of Biodiesel from Jatropha Seeds, MSc Thesis, Department of Mechanical Engineering, University of Lagos, Nigeria, 2010.
Ojiako, I.A. and Olayode, G.O., Analysis of trends of livestock production in Nigeria: 1970-2005, Journal of agriculture and social research 8(1), 2008.
Ojolo, S.J., Bamgboye, A.I., Aiyedun, P.O., and Ogunyemi, A.P., Pyrolysis of shredded plastic waste, Proceedings of the 7th Africa-American International Conference on Manufacturing Technology, Port-Harcourt, Nigeria, 1:412-418, July 11-14, 2004.
Ojolo, S. and Bamgboye, A., Thermochemical conversion of municipal solid waste to produce fuel and reduce waste. Agricultural Engineering International: The CIGR Ejournal, Manuscript EE 05 006, Vol. VII, 2005.
Ojolo, S.J. and Orisaleye J.I., Design and development of a laboratory scale biomass gasifier, Journal of energy and power engineering, 4(8):16-23, 2010.
Okonko, I.O., Ogunnusi, T.A., Fajobi, E.A., Adejoye, O.D. and Ogunjobi, A.A., Utilization of food wastes for sustainable development, EJEAFChe 8(4):120-144, 2009.
Olise, M. and Nria-Dappa, T., Overcoming Nigeria's Energy Crises: Towards effective utilization of associated gases and renewable energy resources in the Niger Delta, Social Action Briefing, No. 2, December 2009.
Okoroigwe, E.C., Oparaku, N.F. and Oparaku, O.E., Harnessing Nigeria's potential for sustainable economic development, National centre for energy research and development, University of Nigeria, 2008.
Osaghae, O.J., Potential biomass based electricity generation in a rural community in Nigeria, Master thesis, Sustainable energy systems, Department of applied physics and mechanical engineering, Lulea University of Technology, 2009.
RECIPES, Country energy information – Nigeria, Developing renewable, www.energyrecipes.org, 2006.
Sambo, A.S. (2008). Matching energy supply with demand in Nigeria, International Association for energy economics (Fourth quarter):32-36, 2008.
Sambo, A.S., Strategic developments in Renewable energy in Nigeria, International association for energy economics (Third quarter):15-19, 2009.
Schmidhuber, J., Impact of an increased biomass use on agricultural markets, prices and food security: A longer-term perspective, International symposium of Notre Europe, Paris, November 27-29, 2006.
Smeets, E., Faaij, A., Lewandoski, I., A quickscan of global bio-energy potentials to 2050 – an analysis of the regional availability of biomass resources for export in relation to underlying factors, Report prepared for NOVEM and Essent, Copernicus Institute – Utrecht University, NWS-E-2004-109, March 2004.
U.S. Census Department, Population Statistics for Nigeria, U.S. Bureau of the Census, International Database, 2010.
Yevich, R. and Logan, J.A., An assessment of biofuels use and burning of agricultural wastes in the developing world, Global Biogeochemical cycles, Massachusetts, USA, 2002.

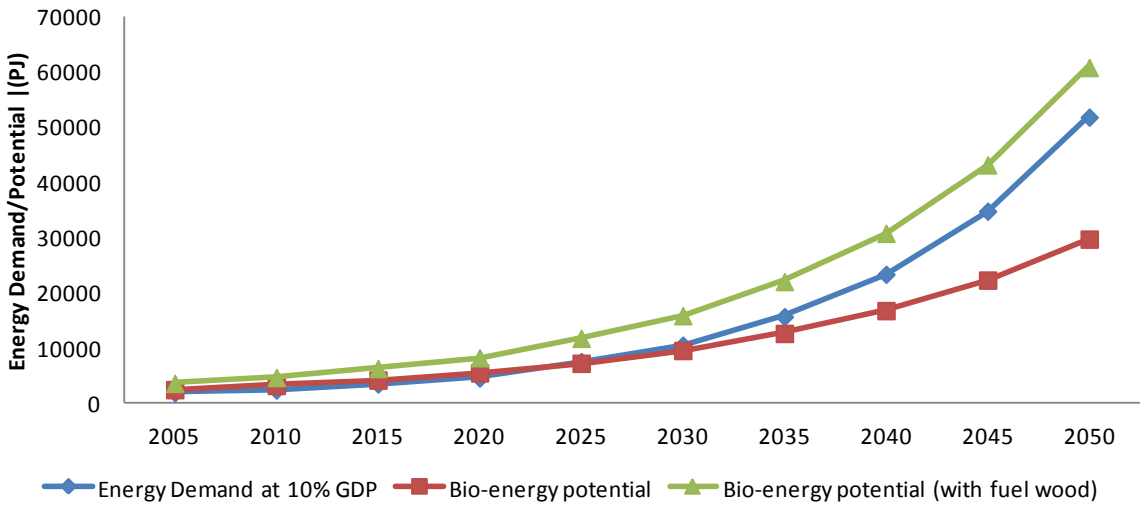

Figure 1: Comparison of Energy Demand at 10% GDP with the Bioenergy potential

Table 1: The estimate for energy potential of Agro-residues obtained in Nigeria in 2005

Agro-residue	Residue to crop ratio range	Assumed residue to crop ratio	Energy content MJ/kg	Annual Crop Production ('000 Tonnes)	Annual residue production ('000 Tonnes)	Annual Energy available (10^{15}J)
Beans	1.58	1.58	12.8	4328.3	6838.7	87.5
Cassava peels	0.4	0.4	16.4	33393.3	13357.3	219.1
Cocoa husks	2	2	17.2	202.6	405.2	7.0
Coconut fibre	1.1	1.1	16.0	216.9	238.6	3.8
Coconut Shells	1.9	1.9	18.0	216.9	412.1	7.4
Coffee husks	0.3 – 1.8	1.2	16.0	230.5	276.6	4.4
Cotton Hulls	0.26	0.26	14.0	536.4	139.5	2.0
Cotton Stalks	3.0 – 5.5	4	16.0	536.4	2145.6	34.3
Fruits and vegetables	2	2	13.1	17866	35732	468.1
Groundnut shells	0.25 – 0.5	0.4	17.4	3350.5	1340.2	23.3
Maize cobs	1.41	1.4	19.5	9503.4	13304.8	259.4
Maize Stalks	0.9 – 4.0	0.8	16.5	9503.4	7602.7	125.4
Palm Empty Fibre Bunch	0.39	0.39	18.1	932.5	363.7	6.6
Palm Fibres	0.2 – 1.1	0.8	11.0	932.5	746.0	8.2
Palm Shells	0.2 – 1.0	0.7	15.0	932.5	652.7	9.8
Plantain	0.25	0.25	17.0	1161.5	290.4	4.9
Potato peels	1.14	1.1	16.4	1528.3	1681.1	27.6
Rice Husks	0.17 – 0.22	0.2	14.6	3713.9	742.8	10.8
Rice Straw	0.8 – 2.5	1.9	11.7	3713.9	7056.4	82.6
Sorghum Stalks	1.5 – 3.7	2.5	18.0	9994.4	24986	449.7
Soyabean	2.1	2.1	16.0	1447.8	3040.4	48.6
Sugar Cane Bagasse	0.05 – 0.2	0.1	8.0	2167	216.7	1.7
Wheat Residue	0.9 – 1.6	1.2	13.9	55.6	66.7	0.9
Yam peels	0.06	0.06	19.4	26700.2	1602.0	31.1
				TOTAL	123238.2	1924.2

Table 2: 5-yearly estimate Energy potential of Agro-Residues

Year	2005	2010	2015	2020	2025	2030	2035	2040	2045	2050
Energy potential of residue (PJ)	1924.2	2575	3445.9	4611.5	6171.17	8258.4	11051.6	14789.6	19791.8	26485.9

Table 3: 5-yearly population estimate of livestock in Nigeria

Livestock	Annual growth rate (%)	Population (Average million heads)									
		2005	2010	2015	2020	2025	2030	2035	2040	2045	2050
Cattle	4.17	20.4	25.0	30.7	37.7	46.2	56.6	69.5	85.2	104.6	128.2
Goat	8.5	27.7	41.7	62.6	94.2	141.6	212.9	320.2	481.4	723.9	1088.5
Sheep	5.8	15.9	21.1	27.9	37.0	49.1	65.1	86.3	114.4	151.6	201.0
Poultry	3.9	132.0	159.8	193.5	234.3	283.7	343.5	415.9	503.6	609.8	738.4
Pig	7.6	8.2	11.8	17.1	24.6	35.5	51.2	73.8	106.5	153.6	221.5

Table 4: 5-yearly estimate for energy potential of livestock wastes in Nigeria

Live-stock	Waste (kg/head/day)	Biogas yield (m^3/kg)	Annual Energy produced (10^{15}J)									
			2005	2010	2015	2020	2025	2030	2035	2040	2045	2050
Cattle	10	0.04	87.9	107.8	132.2	162.2	198.9	244.0	299.3	367.1	450.3	552.4
Goat	2	0.05	29.8	44.8	67.4	101.4	152.5	229.3	344.7	518.4	779.4	1172.0
Sheep	2	0.05	17.1	22.7	30.1	39.9	52.9	70.1	92.9	123.2	163.3	216.5
Poultry	0.1	0.06	8.5	10.3	12.5	15.1	18.3	22.2	26.9	32.5	39.4	47.7
Pig	1.5	0.07	9.3	13.4	19.3	27.8	40.1	57.9	83.5	120.4	173.6	250.4
TOTAL			152.6	199.0	261.5	346.4	462.7	623.4	847.3	1161.6	1606.1	2239.0

Table 5: Energy potential of forest residues in Nigeria (1997)

Forest Residue	Full Capacity			Capacity Utilized		
	Volume (m^3)	Mass ('000 tonnes)	Energy derivable (10^{15} J)	Volume (m^3)	Mass (tonnes)	Energy derivable (10^{15} J)
Sawdust	463,580	185.4	2.7	200,000	80	1.2
Wood Chips	1,390,740	403.3	5.6	600,000	174	2.4
TOTAL			8.3			3.6

Table 6: 5-yearly potential of forest residues at 5.5% increase in production rate (10^{15}J)

	2005	2010	2015	2020	2025	2030	2035	2040	2045	2050
Utilized Capacity	5.5	7.2	9.4	12.3	16.1	21.1	27.5	36.0	47.0	61.5
Full Capacity	12.7	16.6	21.8	28.4	37.2	48.6	63.5	83.0	108.4	141.7

Table 7: Energy potential of Municipal Solid Wastes in Nigeria

	2005	2010	2015	2020	2025	2030	2035	2040	2045	2050
Population Estimate ('000,000)	129	150	165	183	202	226	250	279	306	338
MSW estimate ('000,000 tonnes)	29.7	34.5	37.9	42.1	46.4	52.0	57.5	64.2	70.4	77.7
Energy potential (10^{15} J)	376.7	438.1	481.9	534.4	589.9	660.0	730.1	814.8	893.6	987.1

Table 8: Total Biomass Energy Potential in Nigeria

Biomass resource	2005	2010	2015	2020	2025	2030	2035	2040	2045	2050
Agro-residues	1924.2	2575	3445.9	4611.5	6171.17	8258.4	11051.6	14789.6	19791.8	26485.9
Livestock wastes	152.6	199.0	261.5	346.4	462.7	623.4	847.3	1161.6	1606.1	2239.0
Forest Residue	5.5	7.2	9.4	12.3	16.1	21.1	27.5	36.0	47.0	61.5
Municipal Solid Wastes	376.7	438.1	481.9	534.4	589.9	660.0	730.1	814.8	893.6	987.1
TOTAL (PJ)	2459.0	3219.3	4198.7	5504.6	7239.87	9562.9	12656.5	16802	22338.5	29773.5

Table 9: Total energy demand based on 10% GDP growth rate (mtoe)

Item	2005	2010	2015	2020	2025	2030	Average growth rate (%)
Industry	8.08	12.59	26.03	39.47	92.34	145.21	16.2
Transport	11.7	13.48	16.59	19.7	26.53	33.36	4.7
Household	18.82	22.42	28.01	33.6	33.94	34.27	2.6
Services	6.43	8.38	12.14	15.89	26.95	38	8.7
Total	45.01	56.87	82.77	108.66	179.75	250.84	8.3

Source: Sambo (2008)

Table 10: Progress of Research and Application of Bioenergy as fuel in Nigeria

Conversion route	Research in progress	Domestic Application	Industrial Application
Direct Combustion	✓	✓	×
Gasification	✓	×	×
Pyrolysis	✓	×	×
Anaerobic digestion	✓	×	×
Fermentation	✓	×	×
Biodiesel/Transesterification	✓	×	×

INSTRUCTION TO AUTHORS

Preamble: the manuscripts should be double-spaced and typed on not more than 20 pages of A4 paper. Four copies of the manuscript and originals of diagrams should be submitted. Three referees who have appropriate knowledge of the subject will be appointed for each paper. Our list of reviewers, who are drawn from the international academic and professional engineering community, will be published periodically. Final decisions on papers will be made by the Editorial Board.

The following format is recommended for papers:

Title: The title should be capitalized and be as brief as possible. It should be followed by the author's name(s) and address(es).

Abstract: Each paper should have an abstract, not exceeding about 200 words immediately before the beginning of the paper.

Introduction: This should contain clearly stated objectives, justification for the study and a brief review of literature.

Theoretical development: This should be included where appropriate.

Experimental Procedure: This should state how major measurements were done and degree of accuracy (if any). Sufficient information should be provided to permit repetition of the experimental work.

Results and Discussions: These should be pertinent to the work done and should clearly indicate the degree of reliability of the results.

Conclusions: These should succinctly summarize any important conclusions emerging from the work.

Acknowledgements: (if any)

Notations: Special symbols defined and used in the text should be indicated.

References:

Citing: references in the text should be by the last name and year. E.g. (Ahmed, 1987); Okonkwo et al. (1986); Thomas and Dada (1986).

Listing: This should be in alphabetical order. The recommended format for listing references is as follows: Name(s) and initials of authors, exact title of paper (in quote), the title of the periodical as in World list of Scientific Periodicals 4th Edition (1963-65), vol. (Number):initial and final page numbers, year. Only names actually cited in the text should be listed.

Serial: Okonkwo, E.P., Suru O.O. and Ahmed, T.A., "Properties of farm animal excreta". Ife Journal of Tech. 1(2):274-277, 1987.

Book: Schwarts, R.J., "the complete dictionary of abbreviations" T.Y. Cromwell Co., New York, 1955.

Heading and Sub-Heading: All headings and sub-headings should be numbered. All headings should be written in capital letters and should start at the left margin, while sub-headings should have only the first letter of major words capitalized.

Tables: A table should contain enough information to understand it without reference to the text. Tables are to be numbered in Arabic numerals in ascending numerical order as reference is made to them in the text (e.g. Table 2: Taste panel scores for yam flour). They should be placed at the end of the text and should contain no vertical lines. Captions must be placed at the top.

Figures: Illustrations, whether line drawings, graphs or photographs, should be given a figure number by Arabic numerals in ascending numerical order as reference is first made to them in the text (e.g. Fig. 3). Line drawings should be in Indian ink on tracing paper and only black and white photographs with good contrast are acceptable. Figure captions should be clear, precise and placed below the figure.

Equations: Equations should be distinctly typed or written with subscript or superscripts clearly indicated, preferably using Equation Editors. Avoid powers of "e" and use "exp". Equations should be centered on the line, numbered consecutively by Arabic numerals in parenthesis at the right margin. In the text, such equations should be cited as Equation (1) etc.

Units: S.I. Units should be used.

Page Charges: publication charges are N1500.00 ($15.00) per page.

Reprints: Fifteen reprints will be supplied to authors free of charge. Additional reprints may be ordered when the galley proofs are being returned.

Note: Submission of an article implies that the work has never been published, is not being considered for publication elsewhere, and that the authors are completely responsible for the statements made in their articles.

Ife Journal of Technology
Vol. 21, No. 2, 2012

Contents